Flinders
UNIVERSITY

SHANK ACCELERATION PROXIES FOR GROUND REACTION FORCE IN ATHLETIC MOVEMENTS

A technical summary and validation of models presented within the literature

Master of Engineering (Biomedical)

Thesis

ANDREW VONOW

Supervisors:

DR. DAVID HOBBS

PROF. MARK TAYLOR

DR. KYM WILLIAMS

Submitted to the College of Science and Engineering in partial fulfilment of the requirements for the degree Bachelor of Engineering (Biomedical) (Honours), Master of Engineering (Biomedical)

4th November 2020

Declaration

I certify that this thesis:

1. *does not incorporate without acknowledgment any material previously submitted for a degree or diploma in any university; and*
2. *to the best of my knowledge and belief, does not contain any material previously published or written by another person except where due reference is made in the text.*

Andrew Vonow

4th November 2020

Acknowledgements

Dave, for five years you have coached me and given me opportunities to grow in technical and rehabilitative engineering experience. Your kindness goes before you and I have appreciated it so much. Thank you for your guidance, for taking the journey with me, and especially for all of that this year.

Mark, this thesis was all the better for your technical insight and critical appraisals over the course of the project. It was a privilege being challenged in my critical thinking and project management with you; I will surely hold onto it for many years to come. Thank you for all of your input.

Kym, you have got to be one of the most encouraging blokes I know. Your time, guidance, and reassurance this year have meant so much, and I truly look up to you in this regard. Thank you for that.

Executive Summary

Overuse injuries in elite netball have been reported at rates of up to 23.8 per 1000 hours of game play (Hume and Steele, 2000), with between 66 to 92% of these occurring at the lower limb (Hopper *et al.*, 1995, McManus *et al.*, 2006). Since acceleration and force are linearly dependent, this thesis aimed to determine whether a wearable accelerometer at the lower limb could be used to determine an objective level of impact dose. If so, and if dose could be quantified in terms of risk, the prediction could be used to monitor and prevent overuse injuries.

There were 16 articles identified as having previously studied the relationship between ground reaction force and acceleration. For the 15 locations across the body that these articles used to predict impact force, five different kinds of proxy models had been considered: linear, logarithmic, Fourier, machine learning, and an unknown application. Variables that were most notably identified to affect prediction accuracy were technique, movement, and proxy type. These models were reported to have produced several *very large* ($R^2 > 0.7$) correlations between force and acceleration.

Three of the literature-identified models were validated against a trial dataset collected in a previous generation of this project. Linear and logarithmic models were used to predict force *events* from acceleration, and a kind of machine learning was used to predict the *entire waveform*. The models that considered events correlated 14 different triaxial acceleration waveform events against 6 different force waveform events. The investigation considered accelerations from the thigh, shank, and ankle, with one accelerometer at each position on both legs.

The strongest correlations were *almost perfect* ($R^2 > 0.90$) and were between the integration of vertical force, which is vertical impulse, and the integration of axial acceleration *at the ankle*. Although the shank and thigh also produced, on average, at least *very large* correlations, the ankle was deemed the optimal position for relating these waveforms. There were no events across the linear and logarithmic models that produced correlations that were consistently above $R^2 = 0.36$ (*moderate*). However, the machine learning model predicted the entire waveform with an accuracy of $R^2 = 0.41$, which was considered more favourable than the event-based linear and logarithmic models. As such, the investigation *did not* reproduce the literature-based results.

If it can be shown in the future that impulse can indeed be used as an indicator of impact dose, and if these results can be reproduced, then lower limb acceleration may indeed be used as a proxy for monitoring impact dose and in overuse injury management and prevention.

Table of Contents

List of Tables

List of Figures

Chapter 1. Introduction

1.1. Introduction

This chapter frames the thesis by providing a brief understanding the development of overuse injuries and by identifying the potential for such injuries to be prevented or monitored through the development of a wearable device. The sport of focus within this investigation has been selected as netball.

1.1.1. Injuries

A primary cause of stress fractures in the lower limb is inadequate adaption to repetitive cyclic loading (Brukner and Bennell, 2020). As ground reaction force (GRF) strains the bone, microdamage accumulates in weaker regions, with excess strain leading to fatigue reaction and failure (Brukner and Bennell, 2020). Investigations have been undertaken to consider the contribution of excess fatigue and loading rates to injury development, and to determine how these characteristics can be measured with wearable devices in runners (Kiernan *et al.*, 2018) and team-sports such as Australian football (AFL) (Colby *et al.*, 2014), soccer (Ehrmann *et al.*, 2016), and rugby (Gabbett and Ullah, 2012).

Studies like these have concluded that variables such as system acceleration, movement velocity, and total distance covered during training sessions and gameplay may provide risk indicators for overuse injuries and fatigue. The research is particularly relevant to the injury management of female netballers. As shown in Figure 1, injury proportion by number of *female* hospitalisations in netball and handball has been found to be the highest of all sports (Schneuer et al., 2018). It has been further reported by Netball Australia that *"netball is the activity with the second largest adult female participation rates (89%), behind Pilates (90%)"* (Netball Australia, 2019).

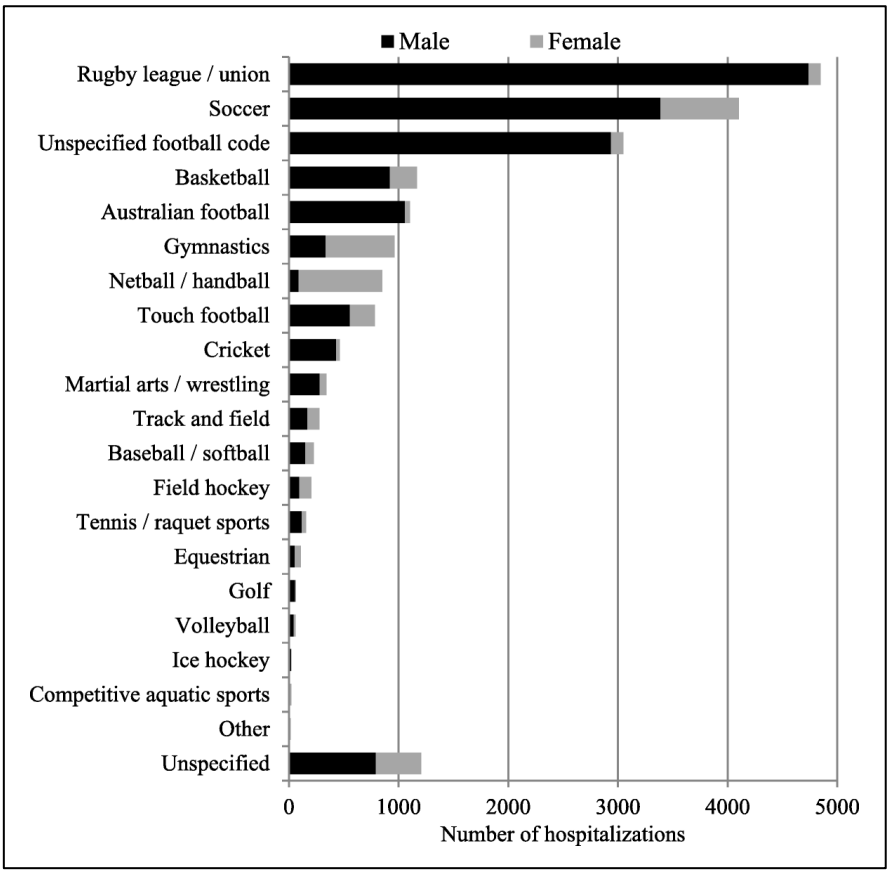

Figure 1: Number of hospitalisations of children in Australian sport between 2005-2013 (Schneuer et al., 2018). Reprinted with permission under CC BY 4.0.

Within netball, the incidence of fatigue and overuse related injuries has been reported in elite players at 9.08 (Best, 2017) and 23.8 (Hume and Steele, 2000) per 1000 hours of game play, and 14 per 1000 hours in non-elite players (McManus *et al.*, 2006).[1] In one study, the incidence rate of injury in elite and non-elite participants over the 5 consecutive years of a 14-week competition was 5.4% (Hopper *et al.*, 1995), and in the 1988 Australian Netball Championships, overuse injuries were sustained by more than 25% of elite participants (Hopper and Elliott, 1993), where it was seen that playing level had little effect on the number of players injured. Interestingly and perhaps unsurprisingly, these injuries are not evenly distributed throughout the body.

In studies that have monitored netball injuries, a proportional 92.6% (Hopper *et al.*, 1995) and 66% (McManus *et al.*, 2006) of injuries are reported as having occurred in the lower limb. When Bissell and Lorentzos (2018) considered a cohort of 37 players, they found that lower limb injuries were prevalent in 75% of players, with an equal prevalence of knee (47.2%) and ankle (47.2%) injuries

[1] Consider that in the case of 23.8 injuries per 1000 hours (1 injury per 42 hours), if an elite player is training at this higher-risk level for 5 hours per week, this could mean experiencing an injury after just over 8 weeks.

across all players. Best (2017) reported that over a third of the total injuries were sustained in the ankle, and Hopper *et al.* (1995) found the proportion to be 84.3%.

Best (2017) found that injuries were more commonly sustained during competition, with 71.2% of all injuries in their study occurring in matches rather than during training. One may consider whether all kinds of high intensity training is therefore hazardous, but although Stevenson *et al.* (2000) related higher damage levels with greater exposure periods in training and match time combined, McManus *et al.* (2006) found that training for four or more hours per week was actually *protective* against injury. Indeed, there seems to be a level of training desirable for strength-training and protection, yet over which injuries do become prevalent (Gabbett and Ullah, 2012).

Hopper *et al.* (1995), considering competitive matches only, reported that only 5% of injuries required medical attention from a health care professional; whereas Stevenson *et al.* (2000), who considered match *and* training time, reported that 20% of injuries required such attention. Best (2017) even found a significant association between match *quarter* and injury occurrence ($p = 0.019$), with peak incidence occurring in the third quarter. As to when incidence increases during a season, Best (2017) found that 57.6% of injuries had occurred in the first half of the season, whereas over a similar period, Bissell and Lorentzos (2018) observed ankle injury prevalence to increase. This may concur with Colby *et al.* (2014), who found that in elite *footballers*, three-weekly cumulative loads were the most indicative of injury risk, rather than a long-term outlook on summation.

These results indicate that injuries are prevalent among elite and non-elite athletes alike, with variable incidence rates among both cohorts. Injuries sustained to netball players are found primarily located in the lower limb, and commonly located at the ankle. Risk is seen to increase within games, seemingly indiscriminately of point throughout the season, with injuries generally increasing with greater exposure periods. However, exposure can also contribute towards strength building and protective benefits, without necessarily increasing risk, meaning that load monitoring may be valuable in both injury prevention and strength-training.

Although the exact benefit of wearable devices in this area is still being determined, it has been observed that *"an increase in peak acceleration might indicate higher loading rates, a reduction in shock absorption quality and a higher impact on the body"* (Reenalda *et al.*, 2016). If this is so, and an accurate relationship between acceleration and impact can be defined, then wearable

accelerometers could be used as tools to record acceleration, and this acceleration could be used as a proxy for impact. Furthermore, if wearable accelerometers can be used to quantify impact dose, then they may be beneficial in overuse injury management, by producing consistent, valid, and accessible methods of impact dose and injury risk.

1.1.2. Considering a Device

Any device that is to be developed for targeting load management and injury prevention in netballers must be grounded not only in the physiological relationship between impact force and acceleration; and in literature-based design recommendations; but also in an understanding of the desires and needs of current athletes. Therefore, an experienced, professional coach of an elite netball team in the Netball SA (South Australia) Premier League was initially consulted for insight on behalf of current athletes. This discussion, the conclusions of which are given below, included two main considerations: injury prevention, and location and attachment.

Injury Prevention

It was explained by the coach that as players fatigue, the prevalence of injuries increases due to heavier landings and less controlled movements. Inefficient recovery rates tend to bring structures to failure, especially when participating in multiple activity sessions per week. As such, an ideal device would provide quantitative, objective reasoning for why a player should not persist in training when persistence may cause them to develop an injury. It would aid in the prevention of future injuries, use previous injury data to indicate risk, and enable players to rate their feelings subjectively. This would include promoting efficient recovery from past injuries and high amounts of activity, informing the decision to rest and recover rather than persist until injury. This would be quantified as a *recovery level* and would be used to inform safe training intensity and variety.

The primary desirable within an interface would be an alert system on increases to injury risk. The device would indicate whether visual observations by coach and player are consistent with the objective data. The interface would be user-friendly and provide only necessary information on performance and injury risk, allowing all involved to focus on training, only needing to consider the data when risk has developed. Ideally, the device would be used during training and matches.

Location and Attachment

The device would be small, developed such that it could be worn according to South Australian and Australian Netball regulations. A suitable location such as the ankle would need to be selected

such that the device is minimally obstructive, easily accessible, and not hazardous during gameplay. As players do not ordinarily wear compression tights, the device could not be placed under tights or sleeves worn over the legs. However, if tights were necessary, then although players might wear them during training, it is less likely that they would wear them during games; although ultimately, the players would wear what is necessary for injury prevention.

Players tend to wear ankle-length socks, but crew socks may be worn when their ankle is strapped. Because injuries are prevalent, most players strap or brace their ankles and knees each game for both prevention *and* treatment, even if they are not currently injured. Players commonly use the *stirrup* and *heel-lock* techniques for strapping ankles, using under-wraps of rigid Elastoplast. The coach explained that similar techniques may be suitable for a new device. Since players do not use leggings or straps except at the ankles and knees, a device that requires strapping in an abnormal position may not be welcomed, allowed, or used by players. As such, although a device may be fitted on mid-shank during trials, it is unlikely that a device placed here would remain when competing. Ideally, the device would be placed medial or lateral to the central axis of the leg; above the ankle, slightly caudal from the medial malleolus or the lateral malleolus; around the sock line, akin to a watch placed on the wrist; this location would likely be acceptable.

The aesthetics of the device are also important, and a device that is not aesthetically appealing would not likely be welcomed, even if it were technically approved. It was also acknowledged that the development of a device in this area may require trial and error, testing for device profiles, usability, and comfort.

Summary

In light of the high prevalence of injuries in elite and non-elite players alike, there remains a need for an accessible method of injury management and prevention. The application of a wearable accelerometer may provide this. Due to the high rate of lower limb injuries, and with the need for a regulation-approved device, a device inferior on the body seems the most suitable, and therefore will be the focus of this investigation. In the chapters that follow, a clear objective for this investigation will be defined, the literature will be reviewed and synthesised, and conclusions will be provided towards the search for an accessible method of lower-limb injury prevention.

1.2. Defining the Thesis Objective

This section states the aim of the thesis and a brief method for undertaking the investigation.

1.2.1. Aim

The aim of this research thesis is to establish an answer to the following question:
Is data collected from wearable accelerometers placed on the lower limb sufficient to model an effective and useful relationship between ground reaction force and acceleration that is generalisable between different subjects, movements, and external conditions?

Divided into five primary research areas, this project will aim to:

1. Determine whether there is a relationship between force and acceleration at the *lower limb*.
2. Determine whether this relationship can be accurately modelled using data collected from *wearable accelerometers*.
3. Determine whether this relationship is *generalisable* between subjects, movements, and external conditions.
4. Determine whether measuring acceleration at the lower limb using wearable accelerometers can provide data that is *useful* for the prevention or monitoring of injuries, fatigue, and rehabilitation.
5. Determine information on the running of a trial such that new data can be collected, and a relationship derived, based on the recommendations and performance of these studies.[2]

1.2.2. Method

This investigation will be conducted in three parts, the methods of which will be further explained throughout the thesis.

- Firstly, a systematic review of current literature regarding the topic will be undertaken, and information synthesised for conclusions towards the research aims (Chapters 2 - 6).
- Secondly, an investigation will be undertaken in which previous data will be analysed based on insights gained from the literature (Chapter 7).
- Finally, a discussion will consider and conclude on the results of the literature review and investigation (Chapter 8-9).

[2] If retrievable, this information will include insight on device development, attachment methods, and data analysis.

Chapter 2. Literature Review

2.1. Methods and Search

This chapter explains the method by which the literature in this thesis was investigated. It explains why certain articles have been included and excluded, and it tabulates the articles that qualified as primary sources.

2.1.1. Terms and Protocol

Articles qualified for this review if they provided an understanding on four key areas: wearable devices, the lower limb, acceleration, and force. As such, the following search term was developed to retrieve articles inclusive of this information:

wearable AND (ankle OR shank OR "lower limb") AND acceler AND force*

This search term was queried in six relevant databases: Medline, Scopus, PubMed, IEEE, ProQuest and Science Direct. Script was written in MATLAB to sort between unique titles within the search results of each database. Across the six databases, 154 individual titles were retrieved, from which 99 articles were unique. Each unique title was reviewed based on title, abstract and potential relevance to the discussion, and 76 articles were selected for further review. From these 76 articles, 5 qualified for the review. An additional 11 articles were also included in the review: 5 were identified within the reference lists of the qualified articles, and 6 were obtained through external sources. This process has been illustrated in Figure 2.

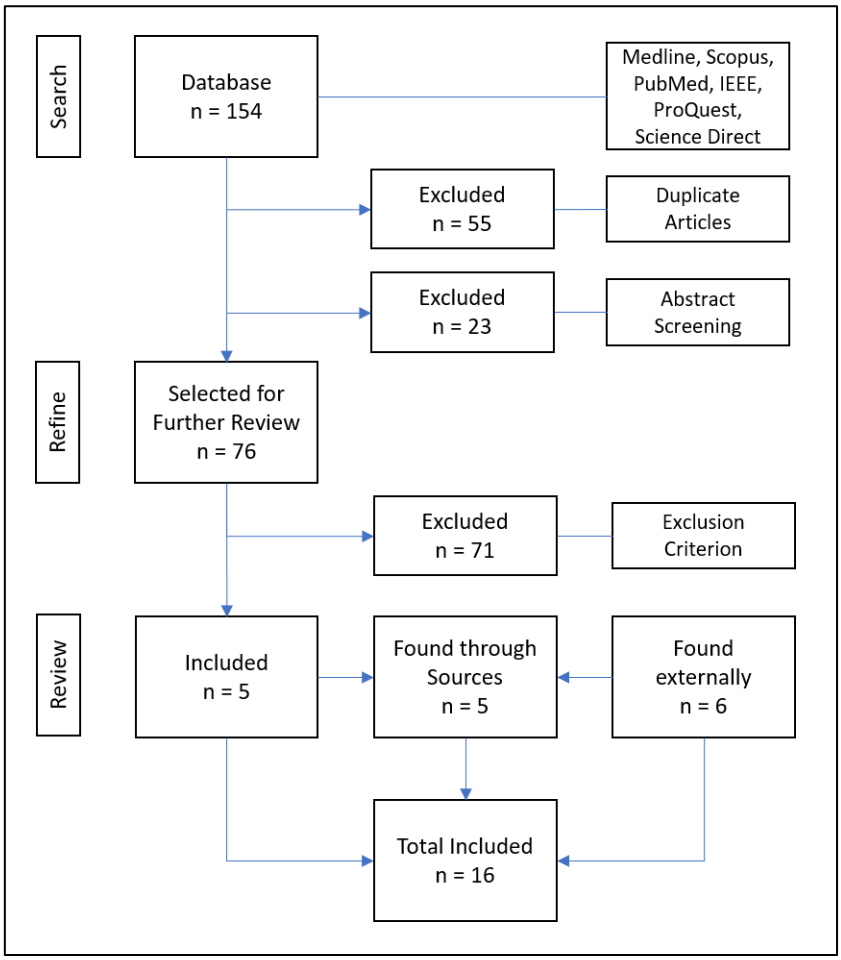

Figure 2: Article Screening Process.

2.1.2. Exclusion Criteria

The following criteria were used during both the *screening* and the *refine* process to exclude articles as primary sources. Articles were excluded if they:

- Did not collect acceleration data using an accelerometer.
    - Articles were included if they measured acceleration but did not specify the device as an *accelerometer*, or if the device used was a multifunction device i.e. if a study used terms such as *inertial measurement unit (IMU).*
- Did not consider the placement of the accelerometer in relation to the lower limb.
    - Articles were included if the accelerometer was *not* placed on the lower limb, but only if they provided insight into the effectiveness of this placement with regards to kinematics of the lower limb.
- Did not use acceleration to predict ground reaction force.
    - Articles were excluded if they used acceleration data to predict power or impulse.
- Were not articles that included a trial.

    - Articles were excluded if they were reviews, discussions, trial proposals or device introductions.
- Were not written in English.

2.1.3. Additional Articles within the Discussion

During the article selection, although articles were excluded, relevant and valuable information to this discussion was noted and included in the synthesis. Of these non-qualifying articles from which information was included, they were predominantly obtained though the original database search. The synthesis also includes articles identified through the references of these articles and from additional external sources.

2.1.4. Information Collected in the Review

Information collected on the qualifying articles has been given in Table 1.

- Articles have been numbered sequentially in Table 1 as $[x]$; these numbers are referred to by infographics within this thesis, and where possible have been hyperlinked accordingly.
- Device placement sites were arbitrarily classified as either the head, neck, trunk, upper leg, or lower leg. Where possible, detailed locations and attachment methods have also been included.
- Articles are classified as having used a kind of inertial measurement unit (IMU). 'IMU' has been used as a broad term for any device that collected acceleration data from the subject. In some cases, gyroscopes, magnetometers, and other sensors were also present within the device.
- Sampling rates and filtering cut-off frequencies have been included where possible. This will be discussed in further detail in the synthesis to follow, but it must be noted that filters between studies varied in kind and order (i.e. 4^{th} order Butterworth etc.); only the cut-off frequencies have been specified within this table.
- *Force Sensor* has been used as a generalised term for whichever force sensor was used in the investigation. It covers *force plate, instrumented treadmill, and pressure-sensing insole.*
- The algorithm models specified do not necessarily explain every process used within each study. They have merely been included in an attempt to describe the fundamental techniques that were used to model the data within each study.
- Algorithm classifications have been classified as *linear, logarithmic, Fourier, non-linear etc.*

The articles within this table will henceforth be referred to as the *qualified articles*.

2.1.5. Qualifying Articles

Table 1: Articles that qualified for the review.

AUTHOR, DATE	ACTIVITY, PARTICIPANTS	DEVICE PLACEMENT	TRACKING TECHNOLOGIES USED	SAMPLING RATE, FILTERING CUT-OFF			ALGORITHM MODEL	CONCLUSIONS
Thesis Index [#]		*In terms of head, trunk, lower leg, and upper leg; and attachment method.*	*Including:* *- Axes Collected* *- Dynamic Range* *- Commercial Device*	*Accelerometer*	*Force Sensor*	*Motion Capture*	*Unless otherwise stated, methods determine force from acceleration, with variables:* $F = force\ (N)$ $m = whole\ body\ mass\ (kg)$ $a = acceleration\ (ms^{-2})$ $t = time\ (s)$	
Callaghan *et al.* (2018) [1]	Cricket (Pace Bowling) n = 11	***Trunk*:** Dorsal between scapulae *Double sided tape, additional strapping tape* ***Lower Leg:*** Left tibia, proximal to knee *Manufacturer-supplied click-in body strap*	**Wearable IMU** - *Triaxial* - *±16g* - *MTw, XSENS Technology* **Force Plate**	***Sampling*** 75 Hz ***Filtering*** **Lower Cut-Off:** 10 Hz **Higher Cut-Off:** 120 Hz	***Sampling*** 975 Hz	-	***Linear, Correlation*** $\boldsymbol{F} = m \times \boldsymbol{a}$ *Further performed one-dimensional statistical parametric mapping of force and acceleration patterns.*	Both the vertical peak force and the vertical impulse as calculated from tibia IMU was significantly different ($p < 0.05$) from the force plate criterion measure: vertical peak force = 2228.43 ± 837.99 N (force plate) vs. 4295.66 ± 1393.41 N (tibia IMU). There was a significant correlation ($p < 0.01$) between vertical peak ($r = 0.832$) and impulse ($r = 0.865$) and force plate criterion measures. Although the absolute and relative reliability of these IMU measurements may be beneficial for load monitoring, the segmental acceleration of cricket pace bowlers did not represent whole body acceleration appropriately.
Charry *et al.* (2013) [2]	Running n = 3	***Lower Leg:*** Left and right shank, midpoint of tibia medial	**Wearable IMU** - *Triaxial* - *±24g* - *ViPerform: accelerometer*	***Sampling*** 100 Hz (x-axis) 20 Hz (y-axis) 20 Hz (z-axis)	***Sampling*** 300 Hz	-	***Linear-Logarithmic, Correlation*** $\boldsymbol{GRF} = a * \log_2(\boldsymbol{acc} + 1) + c$ *where:* $a(m) = 4.66 * m - 76.6$	GRF estimation quality quantified using RMSE. Logarithmic correlation between heel strike acceleration and peak vertical GRF was greater than

		malleolus and knee medial joint line *Adhesive sticker*	*LSM303DLHC from ST Microelectronics – c.f.* Penghai *et al.* (2014) **Force Plate**				$c(m) = 24.98 * m - 566.83$ $acc = maximum\ event\ tibial\ axial\ acceleration$ *Coefficients in equations a(m) and c(m) were calculated empirically based on the mass of the three subjects.*	linear correlation ($R^2 = 0.95\ vs.\ 0.81$); correlation differences were similar in initial peak acceleration, maximum peak acceleration and peak-to-peak acceleration events. Highest correlation for all subjects between GRF and the logarithmic acceleration function occurred at the maximum acceleration peak. Including body mass in algorithm reduced error by 30%. Different runners at similar running speeds had varied results. ViPerform, which uses a single 3D accelerometer, was concluded as viable for force estimations outside the lab.
Davis *et al.* (2018) [3]	Running n = 169	***Lower Leg:*** Left distal medial tibia -	**Wearable IMU** - *Triaxial* **Instrumented Treadmill**	-	-	-	***Correlation*** ***Load rates*** *and* ***accelerations*** *over 8 consecutive steps were averaged and then correlated.*	All correlations were significant, except resultant tibial acceleration with vertical instantaneous load rate in fore-foot strike. All correlations were between 0.37 to 0.82. Peak vertical tibial acceleration was correlated for all strike patterns ($r = 0.72, p < 0.001$). It was concluded that vertical tibial acceleration may be the best surrogate for the load rate of running impact.
Elvin *et al.* (2007) [4]	Jumping n = 6	***Lower Leg:*** Left and right shank, fibula (over fibular head) *Sleeve over knee:*	**Wearable IMU** - *Uniaxial* - *±70g* - *ADXL78, Analog Devices Inc.* **Force Plate**	***Sampling*** 1000 Hz	***Sampling*** 1000 Hz	-	***Correlation*** Acceleration jump data from both legs were averaged and interpolated for a single record. The algebraic mean of the TAA was related to the single GRF output of the force plate.	Across subjects, average r^2 for Peak vertical GRF and Peak TAA was strong and significant ($r^2 = 0.812, p \leq 0.01$); likewise between jump height (force) and jump height (acceleration) ($r^2 = 0.879, p \leq 0.01$). Jump height *did not* correlate with peak

		Drytex Knee Support					Coefficients of determination (r^2) calculated by standard linear least square correlation for: 1. Peak impact vertical **GRF** vs. peak impact **tibial axial acceleration** 2. Jump height (force) vs. jump height (acceleration). 3. Peak impact force vs. jump height (force) 4. Peak impact acceleration vs. jump height (acceleration) Jump Height calculations: $H = gt^2/8$ Where t = total flight time: - In (force) calculation, t = the time between when GRF = 0 (i.e. when the body is not touching the plate). - In (acceleration) calculation, t = the time between when $a = -g$.	impact force ($r^2 = 0.127$) or peak impact acceleration ($r^2 = 0.119$). Errors may be present due to tibia-impact line angle. The dynamics of skin motion with sleeve slipping were discounted due to intra-participant consistency. When the force along the X and Y axes are ignored, a maximum 20% error is observed in the tibial axis GRF.
Guo *et al.* (2017) [5]	Walking n = 9	***Trunk:*** L5 vertebra - ***Neck*** C7 vertebra - ***Head*** Forehead -	**Wearable IMU**s - *Triaxial* - *±6g* - *Opal™, APDM Inc.* **Pressure-Sensing Insoles**	***Sampling*** 128 Hz	***Sampling*** 128 Hz	-	***Non-Linear Model*** *64-term Non-linear AutoRegressive Moving Average with eXogenous input (NARMAX) model obtained to predict vertical GRF of right and left feet:* $\boldsymbol{vGRF} = \sum_{i}^{n} \theta_i \phi_i(\vec{\boldsymbol{a}}_{\boldsymbol{sensor}}(\boldsymbol{k}), \vec{\boldsymbol{a}}_{\boldsymbol{sensor}}(\boldsymbol{k}-\boldsymbol{1}), \dots, \vec{\boldsymbol{a}}_{\boldsymbol{sensor}}(\boldsymbol{k}-\boldsymbol{L}))$ This considers: - Gravity - Time-varying accelerations - Time-varying orientations	Mean error from L5 position for outdoor controlled walking was 3.8%, with cross correlation coefficient of ρ=0.993 (p<0.01). Mean error from L5 position for outdoor free walking was 5.0% with cross correlation coefficient ρ=0.990 (p<0.01). Model prediction errors were minimum in the L5 model compared to C7 and forehead. C7 model had the smallest inter-subject variability and a more stable performance than the other proxy models. However, the performance of the proxy

							- Associated time delays - Decomposition of left and right components of gait signal The data based on individual sensors using an *iterative orthogonal forward regression algorithm*. It models both feet vertical GRF separately from the single accelerometer, based on its membership in the gait cycle.	models was similar in all locations.
Havens *et al.* (2018) [6]	Running n = 14	***Upper Leg:*** Left and right thigh, between lateral epicondyle and greater trochanter ***Lower Leg:*** Left and right shank, between lateral malleolus and lateral epicondyle of femur *Both:* *Nylon elastic band wraps;* under *semi rigid plastic plates;* under *elastic straps* under *duct tape.*	**Wearable IMU** - *Triaxial* - *Opal™, APDM Inc.* **Force Plates** **Motion Capture**	***Sampling*** 128 Hz ***Filtering*** **Higher Cut-Off:** 12 Hz	***Sampling*** 1360 Hz	***Sampling*** 340 Hz	***Correlation*** *Stepwise regressions calculated for between-limb accelerations in the shank and thigh between loading and power.*	Between limb differences in surgical vs non-surgical limbs indicated that greater differences in thigh axial acceleration was related to greater differences in GRF and knee power absorption. Axial acceleration predicted knee power absorption and deficits in surgical limbs were observed. Thigh acceleration correlated more strongly with GRF than tibial acceleration. Relationships were not identified between knee mechanics and shank acceleration. Shank acceleration may not be as useful as thigh acceleration for knee joint power, but each may provide information on knee loading deficits.

Hennig and Lafortune (1991) [7]	Running n = 6	***Lower Leg:*** Tibia, lateral condyle, 3cm below proximal articular surface *Bone-mounted Steinmann traction pins*	**Bone-Mounted IMU** - *Triaxial* - *Entran EGA3-25D* **Force Plates**	***Sampling*** >250 Hz ***Filtering*** **Higher Cut-Off:** 60 Hz	***Sampling*** 1000 Hz	-	***Linear*** *Correlation and regression calculations.* *For:* PPA = ***Peak Positive Acceleration*** $FRP1$ = ***(Peak Vertical Force)****/(Time to first Peak Vertical Force)* PHF *= Peak Horizontal Breaking Force* bw *= Bodyweight* $PPA(g) = a + b * FRP1(bw/s) - c * PHF1(bw)$ <u>Measured Results: $\mathrm{R} = 0.94, \mathrm{R}^2 = 0.88$</u> $a = 0.65, b = 0.105, c = 2.83$ <u>Mean Results: $\mathrm{R} = 0.99, \mathrm{R}^2 = 0.99$</u> $a = 0.99, b = 0.114, c = 3.73$	The rate of loading (time development of force) has a closer relationship to tibial peak accelerations ($r = 0.87$) than vertical force peaks ($r = 0.76$). Peak tibial accelerations may be sufficient for determining GRF data. It was suggested that the mechanics of absorbing impact may differ between individuals, affecting the generalisability of any particular result prediction. Peak horizontal GRF and loading rate under multiple regression could provide a valid estimate of peak tibial acceleration ($r^2 = 0.99$).
Lafortune *et al.* (1995) [8]	Running n = 5	***Lower Leg:*** Right tibia, lateral condyle, 3cm below proximal articular surface *Bone-mounted Steinmann traction pins*	**Bone-Mounted IMU** - *Triaxial* - *Entran EGA3-25D* **Force Plates**	***Sampling*** 1000 Hz ***Filtering*** **Higher Cut-Off:** 100 Hz	***Sampling*** 1000 Hz	-	***Fourier Analysis*** Fast Fourier Transform (FFT) coefficients found for individual results of 4/5 tests, with transfer functions of **acceleration** (A) to **force** (F): $G(\omega) = \frac{A(\omega)}{F(\omega)}$ Individual TAA patterns identified from multiplication of 5th trial F coefficients with $G(\omega)$. Frequency domain TAA converted to time domain via inverse FFT. Correlations used to determine temporal shift, mean square differences, and peak amplitude.	Goodness of fit between measured and predicted TAAs were increased by increasing the number of terms in the individual transfer functions. The best predication was given by terms 0-4 of $G(\omega)$, with a 5-term model producing a mean signed deviation (MSD) of 0.107 to 0.109. Individual subtleties were contributed to by frequencies above 32 Hz and by tuning lower frequency terms. It was suggested that relative to lower frequencies, those between 62.5-100 Hz may be damped by the foot-shank complex, leading to missing features in the

							4/5 participant results combined for a generic transfer function by which 5th participant results then calculated; process repeated for each participant. Finally, a general $G(\omega)$ calculated from all results. Term coefficients within study.	individual functions. However, these functions lacked bias and as such should be externally generalisable under similar conditions.
Meyer *et al.* (2015) [9]	Various Tasks n = 13 *Walking, jogging, running, landings, jump rope, dancing.*	***Upper Leg:*** Right hip -	**Wearable IMU** - *Triaxial* - *±6g* - *ActiGraph GT3X, ActiGraph; (ACT)* - *Triaxial* - *±8g* - *GeneActive, ActiveInsights; (GEN)* **Force Plates**	***Sampling*** 100 Hz	***Sampling*** 2400 Hz	**-**	***Linear*** *Vertical GRFs calculated with:* $\boldsymbol{F} = m \times \boldsymbol{a}$ Acceleration datasets between IMUs were synchronised by matching to the point of highest cross-correlation. Minimum acceleration values were averaged per step and per trial Observed the differences in regression analyses between sex, age, weight, height, and leg length. Considered differences when values which peaked the dynamic range were included or excluded. Considered only values with little variance.	*"Data from ACT and GEN correlated with GRF (r = 0.90 and 0.89, respectively) and between each other (r = 0.98)."* GRF increased significantly from walking to jogging to running (Pearson correlation <0.001) and landing tasks (10-30cm) also produced significantly higher GRF than in walking, jogging, and running tasks (P<0.014). Rope skipping GRF corresponded to GRF from 10cm landing tasks. Both accelerometers significantly and systematically overestimated GRF from their acceleration values. Systematic bias of ACT was 0.46g and GEN 1.39g. Measurement bias was found to increase with higher loadings.
Penghai *et al.* (2014) [10]	Jumping -	***Trunk:*** Posterior, centre of waist -	**Wearable IMU** - *Triaxial* - *±6g* - *LIS3LV02DL STMicroelectronics*	***Sampling*** 640 Hz (down sampled to 400 Hz)	**-**	**-**	***Linear*** *Gyroscope angular output used to determine rate of change, which is used to determine acceleration in the vertical axis.*	As measured by *Myotest*, the results between the IMU and the *HUR* force platform were *weakly correlated*.

			Force Plate	***Filtering*** **Higher Cut-Off:** 30 Hz			*Total Valid Acceleration:* $\boldsymbol{a_{valid}} = a_x \cos(\theta_1)\cos(\theta_2) + a_y \sin(\theta_1) + a_z \sin(\theta_2)$ *Maximum Jumping Force:* $\boldsymbol{JF_{MAX}} = m \cdot MAX\langle A_t \rangle$ *Maximum Explosive Jump Power:* $EP_{MAX} = m \cdot MAX\,\langle a_t \cdot \left(\int_{t-t_0}^{t} a_t dt + V_{t-t_0}\right)\rangle$ *Maximum Height:* $H_{MAX} = t_0 \cdot MAX\,\langle \sum_0^t V_t \rangle$ FIR low-pass filter cut-off was further applied at 30 Hz.	*Numerical correlations were not given.*
Pieper *et al.* (2020) [11]	Walking n = 12	***Lower Leg:*** **Left and right A**nterior tibia, 50% of shank length. -	**Wearable IMU**s - *Triaxial* - *Delsys TRIGNO™* **Instrumented Treadmill** **Motion Capture**	***Sampling*** 1000 Hz	**-** ***Filtering*** **Higher Cut-Off:** 20 Hz	***Sampling*** 100 Hz ***Filtering*** **Higher Cut-Off:** 6 Hz	**Linear** *Correlations between* ***peak shank acceleration*** *(g) and* ***peak anterior GRF*** *(N) in normal gait and in gait inhibited by a leg brace.* y = Peak Anterior GRF (N) x = Peak Shank Acceleration (g) *For un-braced leg:* $Right$: $y = 241.7x + 6.9$ $R^2 = 0.77, P < 0.001$ $Left$: $y = 224.7x + 15.7$ $R^2 = 0.71, P < 0.001$ *For braced leg:* *Right:* $y = 173.4x + 4.8$ $R^2 = 0.31, P = 0.06$	Changes modulated by GRF and power output correlated with proportional changes in acceleration immediately following push-off. Inducing an impairment via a right knee brace caused a systematic and significant reduction in limb propulsion. Braced leg peak shank acceleration did not correlate with peak anterior GRF ($R^2 = 0.31, p = 0.061$). Peak shank acceleration had a consistent temporal delay following toe-off. A unilateral leg-brace impairment does not replicate neuromuscular limitations present following stroke. However, these results may be beneficial for measuring trailing-limb propulsion.

Raper *et al.* (2018) [12]	Running n = 10	***Lower Leg:*** Medial border of tibia[3]	**Wearable IMU**s - *Triaxial* - *ViPerform v5* **Force Plates**	***Sampling*** 100 Hz (x-axis) 20 Hz (y-axis) 20 Hz (z-axis)	***Sampling*** 1000 Hz ***Filtering*** **Higher Cut-Off:** 100 Hz	***Sampling*** 200 Hz	- Analysis performed with manufacturer program *Running Analysis.* Program algorithm strategy method not given.	On testing the absolute reliability of ViPerform, the device was not found to calculate GRF similarly to a force plate measurement. ViPerform was found to have an accuracy of 83.96%. However, it had an intra-class correlation coefficient of 0.877 (95% confidence interval 0.825-0.915) and as such was deemed excellent. It was concluded that the ViPerform calculates GRF consistently but is not accurate to reference Force Plates. As such it may be useful as an arbitrary load unit. The varying sampling rates may cause the ViPerform to be subject to aliasing. Group data is unlikely to assist measurement, and individual baseline measures will be required in future studies.
Simons and Bradshaw (2016) [13]	Hopping-Jumping-Landing Tasks n = 12	***Trunk:*** Upper back, over second thoracic vertebra *Tight-fitting crop top* ***Trunk:*** Lower back, midpoint of superior iliac spines of pelvis	**Wearable IMU**s - *Triaxial* - *Minimaxx S4 GPS-uni* **Force Plates**	***Sampling*** *100 Hz* ***Filtering*** **Higher Cut-Off:** 8, 15, 20, 50 Hz	***Sampling*** 500 Hz, 1000 Hz ***Filtering*** **Higher Cut-Off:** 100 Hz	-	***Correlation*** Peak resultant **acceleration**, peak vertical **GRF**, peak resultant **GRF** correlated. *PRA from the three trials of each task were averaged. GRF was normalised by body weight.*	Significant differences were not found in peak resultant accelerations (PRA) between drop heights of 57.5 cm and 77.5 cm in upper or lower back placement. The strongest GRF-PRA correlation for the hopping task was found with a 15 Hz cut-off at the lower back, and 8 Hz at the upper back, both producing Spearman's rank correlation coefficients (r_s) of $r_s = 0.860$. Significant correlations were only found in the lower back when recorded from 37.5 cm. The

[3] Mounting setup given according to Liikavainio *et al.* (2007).

		Double-sided tape Fixomull stretch tape, tight-fitting leggings, or compression pants						significance of correlations differed according to the cut-off filters applied. Continuous hopping acceleration (filtered at 20 Hz) had a correlation with GRF of $r_s = 0.825$. Overall, PRA was considered a good estimate of impact loading, especially when recorded at the upper back and filtered at 20 Hz. PRA was able to accurately discriminate between landing heights.

Tan *et al.* (2020)
 	
[14]
	Running
	n = 15
		Trunk:
		Upper Back, T5 vertebra
		
		Trunk:
		Pelvis, mid-point between left and right anterior superior iliac spine
		
		Upper Leg:
		Left thigh, mid-point between left anterior superior iliac spine and left femur medial epicondyle
		
		Lower Leg:
		Left shank, one third point between left femur medial epicondyle and
			Wearable IMUs
			- *Triaxial*
			- *MTi-300, Xsens Technologies*
			
			Instrumented Treadmill
			
			Motion Capture
				Sampling
				200 Hz
				
				Filtering
				Higher Cut-Off:
				75 Hz
					Sampling
					1000 Hz
					
					Filtering
					Higher Cut-Off:
					50 Hz
						-
						
						Filtering
						Higher Cut-Off:
						12 Hz
							Convolutional Neural Network (CNN)
							- Foot contacts detection algorithm segmented data into discrete steps
							- Gait cycle input to the CNN model
							  - Acceleration-XYZ
							  - Gyroscope-XYZ
							- Convolution operations performed on data window and kernels
							- Pooling operations extracted the maximum values
							- Features fed into a fully connected network, with:
							  - Two additional auxiliary inputs (swing phase duration and stride duration)
							  - Three hidden dense layers (activation function was a rectified linear unit function)
							  - One output layer (activation function was an identify function)
								Correlations were strong between running conditions, speeds, footwear, strike patterns and step rates ($\rho \geq 0.88$). From single sensors, correlations between input and output (VALR) were: Shank: $\rho = 0.94$; Foot: $\rho = 0.91$; Pelvis: $\rho = 0.76$; Trunk: $\rho = 0.69$; Thigh: $\rho = 0.65$. Although insignificant, there was an increase in correlation as data from multiple sensors was integrated (1 sensor: $\rho = 0.94(0.03)$; 5 sensors: $\rho = 0.96\ (0.02)$). The shank was therefore deemed the optimum location for impact loading. It was said that the foot is also an especially good location since many commercial devices already attach to the foot. A larger and more general population will enable a more accurate vertical average loading rate estimation model.

		left tibia apex of medial malleolus near proximal end of tibia ***Lower Leg:*** Left foot, left second metatarsal *All IMUs attached with straps around the body segment*					- Output variable: vertical average loading rate (of the resultant GRF waveform)	
Tran *et al.* (2012) [15]	Landing-Jumping n = 10	***Neck:*** At the base of the neck. *Manufacturer-provided harness*	**Wearable IMU** - *Triaxial* - *SPI Pro* **Force Plate**	***Sampling*** 100 Hz ***Filtering*** **Higher Cut-Off:** 20 Hz	***Sampling*** 100 Hz	-	***Correlation*** **Vertical GRF** values adjusted by body weight and compared to filtered **accelerations** (raw and smoothed). Bodyweight adjusted c.f. (Simons and Bradshaw, 2016) i.e. they normalised the GRF rather than multiplying acceleration by mass.	On comparing the commercial device to the vertical GRF values measured by the force plates, all bodyweight adjusted peak accelerations were significantly higher than the vertical GRF between landing tasks. ($p < 0.05$). However, moderate correlations of $r = 0.45$ to 0.70 ($p < 0.05$) were found between these variables. Smoothing this data led to reduced variations in the data, (within 10.9-22.2%). Since the level of acceptability was deemed 20%, this device was considered able to quantify impacts consistently, though not from raw data.
Wundersitz *et al.* (2013) [16]	Running n = 17	***Trunk:*** Centre of the upper back, approximately above second	**Wearable IMU** - *Triaxial* - *±8g* - *SPI Pro*	***Sampling*** 100 Hz ***Filtering***	***Sampling*** 100 Hz	-	***Linear, Correlation*** $\boldsymbol{F} = m \times \boldsymbol{a}$	There were weak to moderate correlations ($-0.26 < r < 0.33$) across all cranial-caudal force tasks. There was a strong correlation for $0°$ change of

		thoracic vertebra. *Placed within a mini-backpack, within the manufacturer-supplied harness.*	**Force Plate** **Motion Capture**	**Lower Cut-Off:** **Higher Cut-Off:** 10, 15, 20, 25 Hz				direction ($r = 0.76$) and $45°$ ($r = 0.67$). However, raw accelerometer data significantly overestimated resultant GRF at the force plates ($p < 0.01$). Measurement errors increased with degree of change of direction. However, smoothing data at 10 Hz was found to positively influence the results of the movements performed. There was an indication that smoothed data may provide acceptable agreement for force prediction. Deviation of the IMU from the vertical axis was a major influence on the errors in these results. Absolute errors for single measurements were between 12-24%.

Chapter 3. Modelling Activity Characteristics

Research Aim #1

Determine whether there is a relationship between force and acceleration at the lower limb.

3.1. Recording at the Lower Limb

The qualified articles have examined the relationship between acceleration and ground reaction force across several body segments during movement. If the ideals proposed in Chapter 1 are to be verified, it must be determined whether this relationship can be modelled by data recorded at the lower limb. As such, this chapter will consider three implications made in the literature regarding placement at the lower limb: the locational accuracy of devices placed there, the attenuation and distribution of impact forces throughout the body during movement, and relevant rules and legislation for device placement as defined by Netball Australia and other sports.

3.1.1. Location

Research on wearable sensor systems may be divided into the recognition of daily activities and the accurate measurement of human motion data (Abdelhady *et al.*, 2019). Within these research areas, there is a clear market opportunity for low-cost devices that are able to measure the plantar and ground reaction forces of gait analysis at a high quality (Abdelhady *et al.*, 2019). The design of such wearable systems would allow users to analyse gait and movement kinetics, without needing access to a laboratory (Jacobs and Ferris, 2015). Fulfilling this requires designing these devices accurately both according to the location from which data is recorded and the accuracy of captured metrics provided by each device.

Location Possibilities

Obtaining consistent accuracy has been a major hurdle in studies that have researched the development of accurate wearable technologies, often due to the variance in results between participants and locations (Elvin *et al.*, 2007). To compensate for this, location protocols and recommendations have been widely researched. Studies have considered acceleration in various applications and locations, with many specifically considering its relationship to impact. Accelerometers have been trialled on the feet (Takeda *et al.*, 2009); the tibia (Tenforde *et al.*,

2020); the hip (Meyer *et al.*, 2015); the lower back (Penghai *et al.*, 2014) and upper back (Wundersitz *et al.*, 2013); the neck (Tran *et al.*, 2012); the forehead (Guo *et al.*, 2017); and even in a plastic mouth piece (Lewis *et al.*, 2001). This wide distribution provides the grounds for this discussion on the benefits and difficulties of location. The placements considered in the qualified articles have been illustrated in Figure 3.

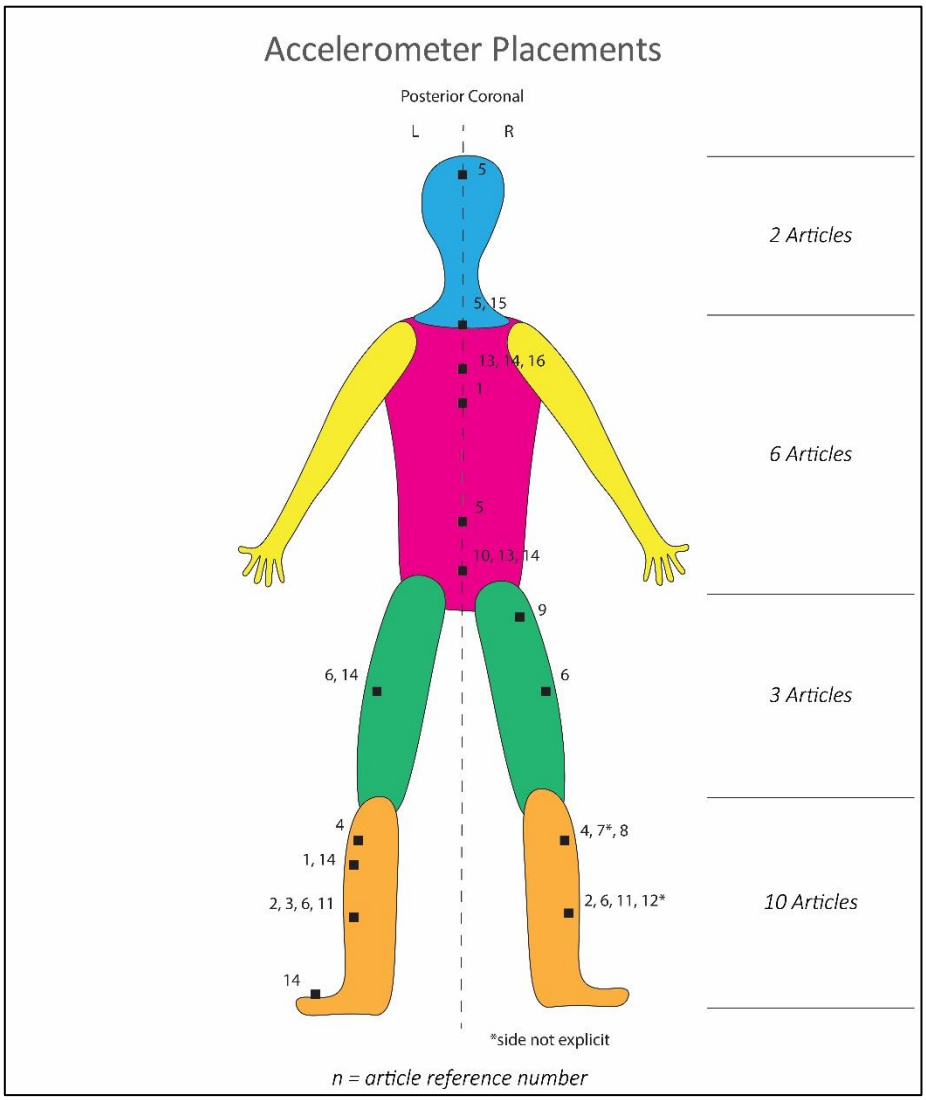

Figure 3: The location of the IMU placements in the qualified articles.

Of the 15 different locations shown in Figure 3, there were 19 IMU placements on the lower half of the body (the lower and upper leg), with 15 specifically on a lower leg. Often in the literature, the lower leg was selected because of the findings of previous studies, or because of placement assumptions. For example, Charry *et al.* (2013) selected the medial tibia on the recommendation of Liikavainio *et al.* (2007), who had reported it an accurate site for recording acceleration. Elvin *et al.* (2007) chose the fibular head since the prominent structure enabled placement repeatability due to the obvious identification of the palpation; and because it was deemed low risk for injury

from falls; and because they had seen it done before (Puyau *et al.*, 2002). Not aware of conclusive evidence for optimal placement, Simons and Bradshaw (2016) assumed that assessing impact loading during jumping and landing tasks would be best represented by the lower back, since this is at the centre of mass. Since the literature review targeted the lower limb, it is unsurprising that most of the IMUs were located here. However, the variance does provide insight into the effects on accuracy between locations.

Rouhani *et al.* (2014) have demonstrated that forces and torques vary significantly across the lower leg, depending on if measured at the shank, hindfoot, forefoot, or toes; and that moments, powers, and forces differ in shape and magnitude between planes. This immediately indicates that three-dimensional effects of segment position and rotation may prove helpful in model development.[4] These effects are objectively seen between placement sites when considering location-based correlations. Tan *et al.* (2020), who tested sensor locations on the body at the trunk, pelvis, thigh, shank, and foot, found that the correlation differed between locations, and was the highest for a single sensor when located on the shank, producing load rate correlation coefficients of $\rho = 0.94$. However, although this may seem optimal for modelling impact due to the high correlation, the shank has been shown to record *lower* acceleration magnitudes than at the foot (Takeda *et al.*, 2009).

Waveform Differences

After performing a frequency decomposition on the acceleration signals at the abdomen, both thighs, shanks and feet during walking, Takeda *et al.* (2009) observed that the signal was greatest in magnitude at the feet, attenuating as it moved away from the point of impact. For example, as shown in Figure 4, they found that there were high frequency, high magnitudes components unique only to the foot.

[4] The contribution of planes and axes of motion will be discussed further in Chapter 3.2.4.

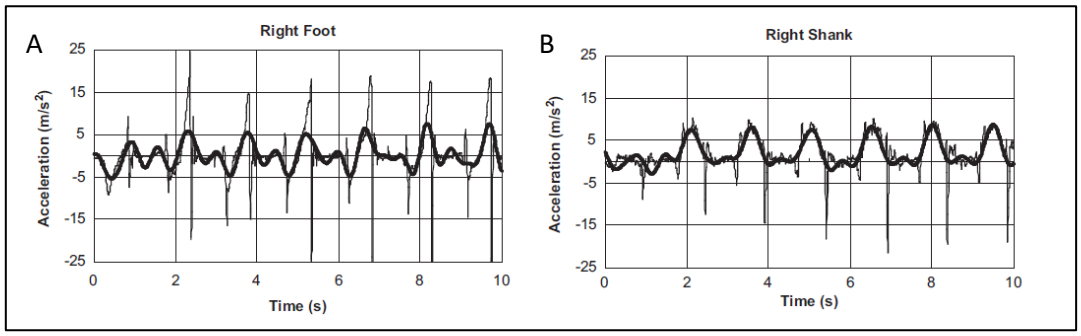

Figure 4: The sum of the primary, secondary, and tertiary acceleration frequency components (bold) of the raw signals of the (A) foot and (B) shank (Takeda et al., 2009). Reprinted with permission from Elsevier.

Since Tan *et al.* (2020) found that the shank was optimal for modelling load rates, but it is here seen that the force magnitude attenuates away from the source of impact, force modelling may depend not primarily upon the acceleration *magnitude*, but on the force-acceleration *waveform similarity*.

And yet, even with the confidence of such studies that consider the shank an optimal representation of ground reaction forces, location may not be the most crucial factor when determining model efficacy. Guo *et al.* (2017) performed a study in which *none* of the locations tested for IMU location were on the lower limb, and this was the study that produced *the highest* correlation accuracy of the qualified articles, with a maximum cross correlation coefficient of $\rho = 0.993$. Nevertheless, this does not invalidate the conclusions of other studies that have considered the practical application of lower limb acceleration, since Guo *et al.* (2017) was one of only two qualified articles to use a machine learning algorithm.[5] Nevertheless, location clearly still affects the relationship. To understand this, the effects of force attenuation and distribution throughout the body must be considered.

3.1.2. Attenuation

Attenuation is particularly important for modelling a relationship in the field of elite sport, since as athletes improve in managing their shock attenuation, the effectiveness of using peak resultant acceleration as a proxy for GRF can also increase (Simons and Bradshaw, 2016). Simons and Bradshaw (2016) determined that the relationship between GRF and torso accelerations is likely to be related, *but not equal*, since the impact force attenuates away from the feet up the trunk. For example, statistically significant differences ($p < 0.01$) have been observed between the trunk and tibia force and impulse measurements (Callaghan *et al.*, 2018).

[5] Different model types will be discussed in Chapter 3.2.1, Linear Models.

Vertical Attenuation

When Meyer *et al.* (2015) placed accelerometers on the hips of children, the acceleration-predicted force both systematically and significantly overestimated GRF, with measurement bias increasing with higher loadings; yet despite this, the accelerometers were deemed reasonably accurate for measuring the impact loading of bone. However, after considering the upper back, Wundersitz *et al.* (2013) asserted that *"accelerometers worn on the upper body… should not be used as an absolute measure of a single foot-strike impact force as they cannot provide acceptable levels of accuracy."*

Higher up again, Tran *et al.* (2012) found that the smoothed data of a commercial IMU at the base of the neck was able to estimate vertical GRF consistently from the bodyweight-adjusted acceleration vectors to within 22%, producing correlations of $r = 0.45$ to 0.70; correlations which could be classified as *moderate* to *very high* (Hopkins, 2006).[6] These results demonstrate that although body placement clearly affects impact prediction accuracy, a limited relationship remains even *after* being attenuated through the entire body.

Expecting an attenuation of force throughout the body, Tran *et al.* (2012) counterintuitively found that the vertical GRF as calculated from the neck was actually *higher* than the force-plate measured vertical GRF. It was suggested that "*there may be dissociation in the theoretically linear relationship between forces and accelerations experienced by the body during impacts, as a result of the segmental nature of human movement"* (Tran *et al.*, 2012). If so, then compensating for this disruption in the transmission of segmental forces would also become a necessary consideration in force modelling. It has been suggested that in the case that higher-than-expected forces are measured from more cranial locations, the errors are largely due to device vibration and can be eliminated by smoothing the data (Wundersitz *et al.*, 2013).[7]

Segmental Attenuation

Pressing deeper into the issue of a segmented approach to kinetics, it is found that forces are even experienced differently within different body segments. Rouhani *et al.* (2014) investigated force approximations with the knowledge that *"shear GRF components are distributed among foot segments in proportion to their vertical GRF."*[8] They found that between the toes, forefoot,

[6] Correlation classifications will be discussed in Chapter 4.
[7] Noise and filtering will be discussed in Chapter 4.
[8] This was determined based on research from Scott and Winter (1993) and MacWilliams *et al.* (2003).

hindfoot, and shank, results differed between both participants *and* segments (Rouhani *et al.*, 2014).

It has also been found that *"rotation of the support upper leg… reduces the vertical acceleration of the hip joint relative to that of the knee joint"* (Bobbert *et al.*, 1992). These findings hold a key implication for the placement of IMUs. If GRF is distributed over each segment, then the reaction force as measured on, for example, the ankle, may give neither the entire force as measured at the foot, nor at the shank, but only a portion or combination of the forces between the two. As such, recording acceleration and approximating impact at specific places on the body will require solving for both inter-segment and intra-segment differences.

A major cause of the attenuation and measurement error within and between body segments may be the presence of subcutaneous fat. To counteract this, Zhang *et al.* (2008) chose to attach their devices to the forehead and the distal anteromedial surface of the tibia, for there is minimal subcutaneous tissue at these locations.[9] Similarly, Marin *et al.* (2020) intentionally did not place the accelerometer at the waist because it would be subject to soft tissue artefact from the wobbling of fat.

Aware of the limitations of recording over soft tissue, Hennig and Lafortune (1991) surgically mounted their accelerometers *directly to the bone* of their participants, completely removing soft tissue movement artefact; they had previously found that axial acceleration peaks were twice as high when measured from a skin-mounted sensor than when directly measured from the bone (Hennig and Lafortune, 1988). Herein lies a difficulty for the modern designer: in order to accurately predict force from acceleration, an accurate model must account for the elimination of movement artefact either in the *mechanical design* or in the *post processing* of the raw acceleration data. However, eliminating movement artefact will not solve every problem: despite removing all movement artefact by mounting to the bone, Hennig and Lafortune (1991) *did not* observe a perfect correlation between acceleration and GRF. Clearly, the mounting method is not the only indicator of a successful relationship.

If the rate of attenuation could be mapped, then perhaps the load at different parts of the body could be determined, but before this can happen, a consistently accurate model at a single location must be identified. Nevertheless, any device must be located where the device can be

[9] However, this study considered the relationship between acceleration and *power*; not force.

attached securely to an inferior location where subcutaneous tissue is minimised, such as on the ankle and anteromedial surface of the tibia (Simons and Bradshaw, 2016).

3.1.3. Rules and Legislation

A final but important consideration regarding this initial discussion on the *placement* of the device regards gaining legislative approval from the sporting organisations in which a device may be used. In a previous study with the same netball team introduced in Chapter 1, the placement of an IMU on the ankle, in a structured non-match environment, was welcomed, and as such may be feasible (Corbo, 2018). The International Netball Federation (2020) specifies in their *Rules of Netball* that during a match, players must wear a registered playing uniform with suitable footwear (5.1.1 (i) a), and that *"players may not wear anything that could endanger themselves or other players"* (5.1.1 (iv)). Explicit prohibitions within this criterion include any adornment or jewellery, except a tape-covered wedding ring (5.1.1 (iv) a), or a tape-covered medical alert bracelet (5.1.1 (iv) b).

Similarly, the International Basketball Federation (2020) (FIBA) specifies in the official basketball rulebook that *"players shall not wear equipment (objects) that may cause injury to other players,"* explicitly prohibiting a variety of soft and hard guards, anything which could cut or cause abrasions, and jewellery (Rule 3, article 4.4.2). Since ankle braces are permitted, it may be that an unobtrusive device could be permissibly developed for this location; however, so as not to be classified as jewellery, it would require further confirmation; as qualified later in the FIBA rulebook, *"any other equipment not specifically mentioned… must be approved by the FIBA Technical Commission"* (Rule 3, article 4.4.5).

Regarding prohibited objects, similar rules apply for volleyball (Fédération Internationale de Volleyball, 2016) (Article 4.5), Australian football (AFL) (Australian Football League, 2019) (Article 9.2) and rugby (World Rugby, 2019) (Regulation 12). Under these rules, it is reasonable to expect that a safe and unobtrusive wearable device above the ankle may not be prohibited. Clearly, before the official use and advertising of any device, these governing bodies should be consulted for confirmation and approval.

3.2. Algorithms

Although several methods exist for collecting data and modelling the relationship between acceleration and GRF, it has been shown that the development of a generalisable algorithm is not straightforward. This section will discuss some of these methods and algorithms more broadly. This

holds relevance to understanding whether acceleration is only valid as an indicative proxy, or whether a definite relationship is possible.

3.2.1. Linear Models

The literature seems to be divided on the effectiveness of different linear and non-linear algorithms, and on using plain correlations or more complicated models, when consider a multivariate of input data. When considering the published, peer-reviewed research on the topic over the past 30 years, there has recently been a spike in interest, with more than half of the identified qualifiable articles being published within the last 5 years, as shown in Figure 5. Over this period, new strategies for modelling the relationship have also been introduced. These strategies have progressed from linear correlations to advanced machine learning and artificial intelligence models. Now more than ever, there is a call to develop algorithms which utilise the improved techniques incorporated in machine learning strategies, and provide an understanding on the relationship development in light of the multivariate of available data (Mahdavian *et al.*, 2019). The relationships identified in these articles will now be discussed.

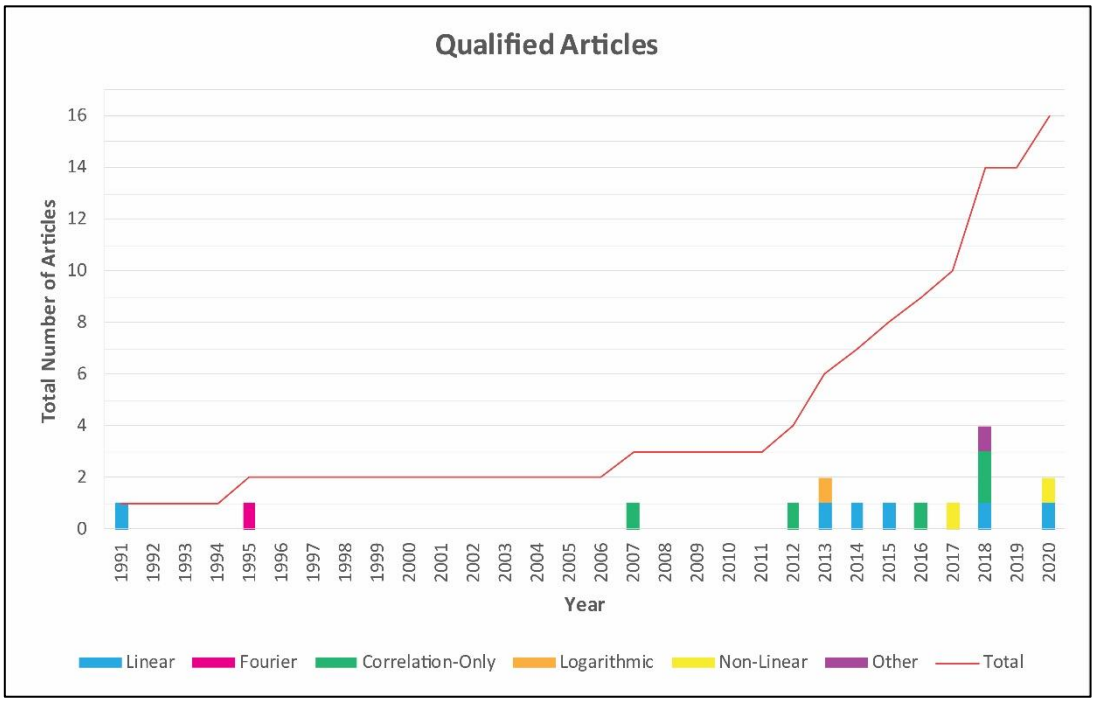

Figure 5: The publishing of the qualified articles and their algorithm models.

Linearity

The aforementioned results have challenged the theory of linearity between acceleration and force within the human body, with difficulties pertaining to attenuation, tissue composition and location-based acceleration waveform differences. However, even the fundamental waveforms of

force and acceleration during gait are not the same, as illustrated by waveforms in Figure 6 from Hennig and Lafortune (1991).[10] It is important to state that although the natural assumption may be to take Newton's Second Law of Motion, $Force = mass \times acceleration$, and relate force to acceleration by a simple product with mass, there are several other factors that must be considered.

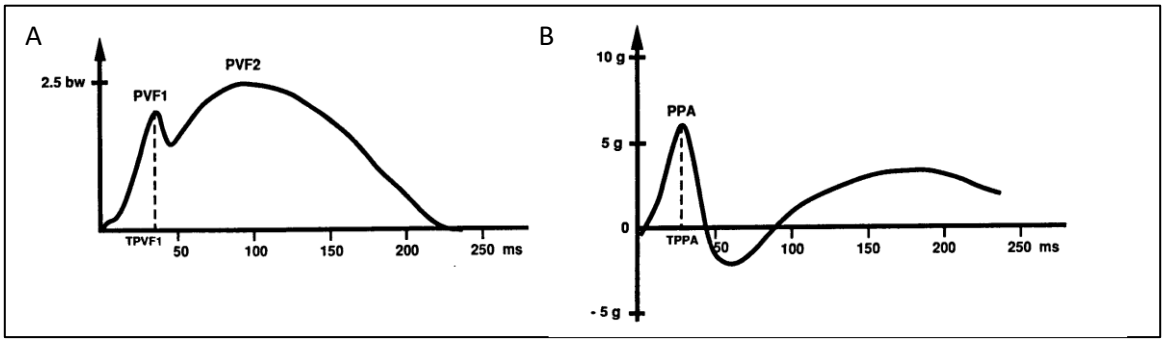

Figure 6: (A) Vertical GRF and (B) tibial axial acceleration, during the stance phase of a cyclic running activity at 4.5 ms^{-1} (Hennig and Lafortune, 1991). Reprinted with permission from Human Kinetics, Inc. via Copyright Clearance Centre Inc.

For example, a lack of linearity was observed several times throughout the literature, with Callaghan *et al.* (2018) finding that peak vertical GRF was significantly different from tibial acceleration ($p < 0.05$), with mean differences of over 2000 N. After using a higher-order cross-correlation *non-linear* model with pressure-sensing insoles, Guo *et al.* (2017) concluded that *"a linear model is not sufficient to describe the relationships between [acceleration and vertical GRF]."*

This may be due to the fact that the timing of the peak force and acceleration events is different, and not necessarily consistent. Bobbert *et al.* (1992) found that the peak vertical force component occurred at 25 ms after touchdown, and decreased to a local minimum at 40 ms before then increasing again i.e. Figure 6 (A), and Hennig and Lafortune (1991) observed peak positive acceleration to occur approximately 5 ms prior to the first peak vertical force ($p < 0.01$).

Now, this is not to say that there is *no* valid linear relationship between acceleration and force; just that this relationship may not always *appear* to be present. In fact, as shown in Table 2, the correlations reported by the studies who explicitly used a linear model could be considered *large*, and at best*, almost perfect*: the minimum correlation with a linear model was from Wundersitz *et al.* (2013) at $r = 0.67$; the highest from Meyer *et al.* (2015) was $r = 0.90$. Direct correlations between acceleration and force were less close: the minimum correlation with a correlation-only

[10] Also see Chapter 3.1.1, Location.

model is from Davis *et al.* (2018) with $r = 0.37$; the highest is from Simons and Bradshaw (2016) with $r = 0.86$ (*very large*).

Table 2: The best correlations obtained within studies that used linear models to relate acceleration with GRF.

Study		Relationship	Best Correlations Attained
[9]	Meyer *et al.* (2015)	Linear	0.89 to 0.90
[1]	Callaghan *et al.* (2018)	Linear	0.832
[7]	Hennig and Lafortune (1991)	Linear	0.76
[16]	Wundersitz *et al.* (2013)	Linear	0.67 to 0.76
[11]	Pieper *et al.* (2020)	Linear	0.71
[10]	Penghai *et al.* (2014)	Linear	*Not given*
[13]	Simons and Bradshaw (2016)	Correlation-Only	0.86
[3]	Davis *et al.* (2018)/Tenforde *et al.* (2020)	Correlation-Only	0.37 to 0.82
[4]	Elvin *et al.* (2007)	Correlation-Only	0.812
[15]	Tran *et al.* (2012)	Correlation-Only	0.45 to 0.7
[6]	Havens *et al.* (2018)	Correlation-Only	*Not given*

This may support the notion that mass is a contributing factor, since the linear correlations (from participant-specific, mass-adjusted models) were higher than the correlations of data which had not been modified by mass. Across these studies, if it is a correct conjecture to suggest that the proportionality between force and mass (following Newton's Second Law) is responsible for the greater range of correlations,[11] then it may be true that the participants involved within these studies also had a wider variance of mass between them.

Further considering linearity, in a study on vertical jumping, Elvin *et al.* (2007) produced a strong and significant linear correlation between peak vertical GRF and peak tibial axial acceleration (TAA) ($r^2 = 0.812$, $p \leq 0.01$), showing that there is still value in pursuing linearity as a factor. On using imperfect linearity to understand waveform characteristics, Lafortune *et al.* (1995) concluded from Pradko *et al.* (1967) that *"some deviation from linearity [in the GRF-TAA relationship] should not cause loss of essential characteristics,"* and Raper *et al.* (2018) has also concluded on the value of imperfect relationships: despite the values predicted by *Running Analysis* being consistently above the actual force, the intra-class consistency deemed the model valuable as a relative indicator.[12] As such, although no single linear approximation has perfectly reconciled the differences between acceleration and GRF, there may still be certain characteristics

[11] The correlation range width for linear relationships is $0.90 - 0.67 = 0.23$; for correlation-only it is $0.86 - 0.37 = 0.49$.

[12] Running analysis was the manufacturer-supplied application used for predicting GRF from the acceleration data of the device.

which can contribute to the development of an efficacious model. However, in the case that a direct linear relationship cannot be established, two things must be considered: non-linear models, and the variables used to predict them.

3.2.2. Non-Linear Models

Logarithmic Predictions

Another strategy used in the literature was a *logarithmic* approximation. In a simple variation on the classic linear approach, Charry *et al.* (2013) estimated the relationship by logarithmically modelling the vertical GRF using mass and acceleration:

$$GRF = a(mass) + b(mass) \times \log_2(acceleration + 1)$$

They found that the logarithmic approach produced a much better approximation of GRF from tibial axial acceleration than their linear model, with correlation coefficients of $R^2 = 0.95$ (*logarithmic*) against $R^2 = 0.81$ (*linear*). Concluding on their results, shown in Figure 7, they observed *"a non-linear nature of the tibial accelerations amplitudes at different running velocities"* (Charry *et al.*, 2013).

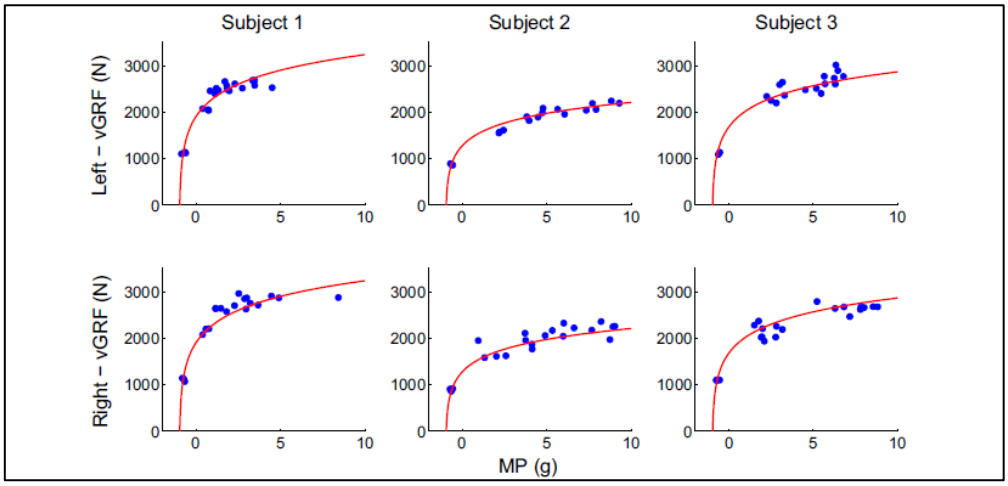

Figure 7: Prediction of GRF using tibial acceleration for three subjects on the left and right shank (Charry et al., 2013). Reprinted with permission from IEEE © 2013 IEEE.

Fourier

The models proposed have not been limited to the time-domain. For example, rather than assuming that the relationship can be modelled linearly by time, Lafortune *et al.* (1995) performed a Fast Fourier Transform on their acceleration data, establishing a Fourier series transfer function by relating acceleration and force in the frequency domain. And, as opposed to each of the other

qualified articles that developed a relationship based on acceleration, they developed this relationship by using *GRF as the independent variable* from which they calculated acceleration.

Their five-term model in the frequency domain produced a high accuracy relationship with a mean signed deviation of $MSD = 0.107\ N$. However, their general transfer functions for all participants lacked the ability to predict underlying mechanisms, explaining impact transmissibility, leading to larger time shifts and mean square differences compared to individual subject-specific functions (Lafortune *et al.*, 1995). They had previously found that acceleration patterns were highly reproducible between steps, meaning that the *cyclic* activities were well suited for analysis in the frequency domain (Lafortune, 1991).

Previous studies have considered the frequency contribution of similar waveforms, where there is a close resemblance between the acceleration and the modulated cyclic waveform built from primary frequencies.[13] However, the difficulty with using frequency-based models is that although approximations can be made, they cannot approximate non-cyclic movement patterns, since by their very nature, cyclic functions require patterns; not movements that lack rhythm. For example, the division of frequencies whilst running will differ from the (relatively) chaotic movements within a court-based game entailing steps, pivots, stops and jumps in random succession.

Udofa *et al.* (2016) predicted force from *optical motion capture* acceleration with sinusoidal functions. However, they suggested that the bell curve of their waveform may have contributed to prediction overshoot. They suggested that although half-sine waves are more often used in biomechanical literature than bell curve functions, half-sine waves introduce systematic errors on "*the leading and trailing edges of the waveform"* (Udofa *et al.*, 2016); and this may prove problematic if considered in the future.

However, consider the scenario that a series of random movements patterns were distinguished from one another. Perhaps, these movements could be individually modelled by using a series of pattern recognition algorithms. In effect, this would be producing a function set that describes a range of potential movements, where the sequence of movements would be described as a discontinuous function. This could even be extended between algorithms: a portion of the signal could be described linearly, a portion logarithmically etc. If this were possible, a device would need to determine the current gait event, then select the correct algorithm, and then perform the corresponding prediction. A rule-based matrix of selection data could be developed, where

[13] See Figure 4.

variables within the gait cycle are identified such that the movement and associated model are also identified, and from there the appropriate model selected.

If different movements were considered within a signal, then *in effect,* the kind of algorithm that is being considered is actually neither a linear nor frequency modulated signal, but now a kind of timeseries or pattern recognition model, such as those used in machine learning and artificial intelligence. Fuzzy logic may be one method of applying this.

Fuzzy Logic

The use of a fuzzy similarity algorithm would allow the comparison of a reference rule-base dataset with data obtained during an investigation (Alaqtash *et al.*, 2010). Acceleration and force data obtained from gait stages would enable identification of the optimal procedure for analysing the data, including the order that algorithms are applied and the kind of algorithms that are used.

Alaqtash *et al.* (2011) used fuzzy relational matrices to determine the level of similarities between *variables* identified within any given gait phase by identifying the mean and standard deviations of rule-based matrix results for all subjects, and the grades of similarity to each phase within the gait cycle. Their matrices provided information on the segment accelerations and their respective similarities.[14] Alaqtash *et al.* (2011) explains the benefits of this method in five points, explaining that fuzzy logic is effective for:

(1) *"reducing the massive data extracted from gait kinetics and kinematics in 3D,*
(2) *[being] easy to interpret and understand,*
(3) *offering insight into non-linear relationships among gait variables,*
(4) *providing quantitative comparison, [and]*
(5) *[having] less complexity and fast processing time, and therefore, offering a possibility for real time applications."*

Using fuzzy logic in an impact prediction algorithm would enable comparing between gait events, the revelation of model efficacy, and the opportunity to define results based on the relative goodness of fit to one another. However, as effective as this may be, such a separation of model

[14] This study did not qualify for the review since it did not predict force from acceleration; it used the forces and accelerations of healthy subjects to determine gait differences in patients impaired by multiple sclerosis.

shapes may be unnecessary if a time-series neural network is selected since these patterns would be internally recognised whilst generating the algorithm.

3.2.3. Machine Learning Models

There are several strategies that utilise machine learning strategies, such as neural networks, random forest models, and support vector machines. Two of the qualified articles used machine learning neural network algorithms, with Guo *et al.* (2017) using a non-linear autoregressive timeseries algorithm and Tan *et al.* (2020) using a convolutional neural network. Both studies reported almost perfect correlations. Both also tested the sensor position in their algorithm correlations, reporting similar values for results from all positions. This may indicate that the algorithm used has a greater influence on the correlation than the placement does, it and goes to show the power of machine learning. However, Guo *et al.* (2017) reported that using a non-linear dynamic method of statistical analysis had its own difficulties, with the neural networks becoming difficult to visualise and analyse.

Neural Networks

Convolutional neural networks were used effectively by Tan *et al.* (2020), with the mean of every correlation above $\rho = 0.9$. They considered four key areas: activity type (*speed*), subject clothing (*footwear*), movement technique (*strike pattern*) and time movement sustained (*step rate*); areas that will be further considered later in this discussion.[15] Tan *et al.* (2020) did not determine their correlations with a direct GRF analysis, but rather determined a vertical average loading rate for their participants from peak tibial acceleration.[16] In their results, the linearly predicted peak acceleration correlation coefficient ($\rho = 0.51$ to 0.75) was much smaller than every correlation coefficient generated with the neural network ($\rho = 0.88$ to 0.95).

These lower linear correlations are much closer to the correlations reported by Pieper *et al.* (2020) ($r = 0.71$ to 0.77), Tran *et al.* (2012) ($r = 0.45$ to 0.70), and Wundersitz *et al.* (2013) ($r = 0.67$ to 0.76), affirming the difficulties associated with linearity and demonstrating the effective use of machine learning algorithms.

One reason that neural networks are beneficial for limiting errors is because of their ability to cope with minor placement deviation (Tan *et al.*, 2020). The placements were chosen by Tan *et al.* (2020) after considering 120 combinations of location and device number for optimal data

[15] Chapter 5, *Applying the Relationship*.
[16] Vertical average loading rate is further considered in Chapter 3.2.4, *Algorithm Variables*.

analysis, determining the 31 best configurations by the smallest normalised root mean square error of each combination. This method, and the kind of CNN model that they used, meant that *"no sensor placement calibration was required for the experimental setup, which could potentially increase the academic and clinical use of the CNN model"* (Tan *et al.*, 2020). However, this kind of analysis is not yet confirmed as generalisable, with Tan *et al.* (2020) concluding that a need remains for wider participant ranges in algorithm development and Guo *et al.* (2017) acknowledging that future research must include more random activities of daily living, rather than single cyclic walking patterns. Guo *et al.* (2017) likewise recommended that wider age groups and participants be selected, including those with pathological gaits, rather than only young, healthy volunteers.

Tan *et al.* (2020) also commented that further analysis could be warranted to determine whether using multiple segments could provide significant information on additional loading impact variables, because their results had showed statistically insignificant differences between using one or more devices.

Machine Learning Model Differences

When Mahdavian *et al.* (2019) compared random forest, neural network and support vector machine models to predict force and torque from *motion capture* data, they found that the entire force and torque waveform could be predicted over the gait cycle, albeit there being no single machine learning model that out-performed every other model in each axis prediction.[17]

Marin *et al.* (2020) performed a comparative analysis, this time considering attachment sites for effect differences on the ability of different devices to distinguish between low to high intensity exercise, and of the devices to assess those differences in light of the metrics and the metabolic equivalence of each task. It used five different algorithms as suggested by other studies for transforming the raw data and relating the results to one another, demonstrating the value of comparing such models with their varied results. These results clearly show that whether modelling with a single, suitable relationship, or with separate relationships, when researching, several different algorithms should be considered.

[17] They found that the random forest model performed best In F_x, F_y, M_y and M_z ($R = 0.89; 0.93; 0.95; 0.89$) and that the neural network performed best in F_z and M_x ($R = 0.97; 0.91$).

3.2.4. Algorithm Variables

Just as there are several methods for data collection, so there are several variables that contribute to its determination. The variables that were raised in the qualified articles have been summarised below in Table 3. This section will consider the contribution and effects of each of these variables to an effective algorithm. There have been several major determinants proposed for modelling force and acceleration. Three of these are suggested by Takeda *et al.* (2009): translational acceleration (from movement), gravitational acceleration (from gravity), and the noise collected by each device.[18]

Table 3: Variables used in the qualified articles for modelling the force-acceleration relationship.

	Variables			
Dependent	***Force***	***Studies***	***Acceleration***	***Studies***
Independent	Acceleration (time)	All	Vertical force	[7]
	Mass (either normalised by mass, or acceleration multiplied by mass)	[1],[2],[9],[10],[13],[15],[16]	Mass	[7]
	Gravity	[4],[5]	Horizontal breaking force	[7]
	Gyroscopic data (segment orientation)	[10],[14]	Time to force event	[7]
	Jump height	[4]		
	Flight time	[4]		
	Frequency components	[6]		
	Gait components (Left vs. Right decomposition)	[5]		
	Gait phases: swing phase duration and stride duration	[14]		

Mass

The force exerted on the body due to gravitational acceleration, affected by mass, is a preliminary factor that must be considered, especially since it has been shown that relationships differ between body segments.[19] In fact, considering mass within these relationships is imperative, since during running, an average error reduction of 30% has been observed in multi-subject calculations after its inclusion (Charry *et al.*, 2013). Clark *et al.* (2017) has shown that the separation of body mass into two regions may contribute to establishing a relationship among runners. These results

[18] The effects of noise are covered in Chapter 4.1.
[19] Chapter 3.1.1, *Location*.

have been further verified by Udofa *et al.* (2016) who expanded the testing to predict peak impact forces across different speeds, with different products of body weight. They considered that $m_1 = 0.08m_b$ represented the stance foot and shank and that $m_2 = 0.92m_b$ represented the remaining mass, and found that this mass division produced higher correlations than mass divisions of $m_1{:}\,m_2 = 1.5\text{-}98.5\%$ and $16\text{-}84\%$.[20]

It is important that these locations are specified within discussions on causal relationships, especially when considering the trajectory of these segments as measured from different positions. When both legs are involved in a combined GRF reading, it may also be necessary to consider how results relate to the algebraic mean of the tibial axial acceleration of each leg, or a breakdown of this depending on technique (Elvin *et al.*, 2007).

Acceleration

It is maintained that gravitational acceleration is a uniaxial acceleration on a body, most freely measured when the body is stationary. Gravitational acceleration was considered by Takeda *et al.* (2009) as the gait pattern which presented the lowest amount of positional error, compared to other decomposition patterns of a full gait analysis. However, when considering gravitational and translational acceleration together, the effects of translational acceleration, combined with gravity, ultimately yield a triaxial acceleration vector under which the body is influenced. Therefore, models may need to account for the acceleration experienced in each of the three axes and consider the benefits of using singular or resultant axes.

The contribution of body segment angle to the overall trajectory must also be considered, since *"centrifugal forces due to angular motion of the tibia have a major influence on the magnitude and shape of tibial acceleration signals"* (Hennig and Lafortune, 1991); and this is further supported by the findings of Havens *et al.* (2018), wherein the *"linear acceleration detected at the thigh and shank was not only a result of the shock from the body colliding with the ground but [also] the rotation of the segments."* As such, translational resultant acceleration is identified as a key variable for consideration, especially in light of how uniaxial accelerometers can be a limitation

[20] When compared against measured waveforms for foot strikes, the 8-92% model ($R^2 = 0.95 \pm 0.04$) predicted measured waveforms better than the 1.5-98.5% ($R^2 = 0.83 \pm 0.16$) and 16-84% ($R^2 = 0.74 \pm 0.21$) models. Although these correlations between force and acceleration were made with data from motion capture devices, the case for mass division still stands, since these results are using translational acceleration characteristics alone.

(Elvin *et al.*, 2007) and that *"tri-axial resultant data are likely more valid than uniaxial data for measuring impact forces"* (Wundersitz *et al.*, 2013).

However, that triaxial acceleration is preferred or even necessary is not to say that *resultant* triaxial data must be used; rather, when single or global axes are selected as axes of reference, results can still be promising. For example, although Meyer *et al.* (2015) found that their algorithm had systematically overestimated the GRF, they still observed correlation of up to $r = 0.90$ by only considering data in the vertical axis. However, they did say that for more variable daily living activities, using only vertical rather than resultant data *"may not be adequate"* (Meyer *et al.*, 2015). Hennig and Lafortune (1991) actually reported the *highest* correlation between force and acceleration when considering *horizontal* breaking force in their calculation. Furthermore, Macadam *et al.* (2017) relayed how Mero (1988) found significant correlations between velocity and horizontal force, and velocity and vertical forces, in block start sprints; also that acceleration correlated with propulsive impulse ($r = -0.66$).[21]

Calculating Acceleration

When using resultant acceleration throughout the review, the common method used among studies for determining resultant acceleration, such as in Simons and Bradshaw (2016), was:

$$a = \sqrt{a_x^2 + a_y^2 + a_z^2}$$

If determining global vertical acceleration, one method is to use the angular *rate* of gyroscopic axis data to determine valid accelerations during movement. With the x-axis aligned with the spine, angular changes in coronal and sagittal body movements were calculated by Penghai *et al.* (2014); and since the only movements were vertical jumps, transverse (z-y plane) rotational data was excluded and in this plane considered *"substantially constant."* As such, the angular rate of the x-z plane (sagittal) was θ_1, the y-x axis was θ_1, and the valid vertical acceleration was given by:

$$a_{valid} = a_x \cos\theta_1 \cos\theta_2 + a_y \sin\theta_1 + a_z \sin\theta_2$$

This equation determined the vector along a single *axis* independent from any device (*the global vertical*), and as such, although only a single axis was considered, a triaxial accelerometer was required. If choosing a particular axis to monitor data in without this calculation, an important

[21] Macadam *et al.* (2017) also relayed that similar findings in both track and field, and team sport athletes, had been found by Hunter *et al.* (2005).

factor is maintaining device alignment, since deviation from each axis causes deviation in results if not properly reconciled (Rouhani *et al.*, 2014). This highlights the need for either repeatable placement position, or the need for a generalisable function that, after an initial calibration, uses triaxial vectors from any position.

It is interesting that despite 15 of 16 studies using triaxial IMUs to record acceleration data, as shown in Figure 8, many of these only considered acceleration in a single axis: either in the vertical axis, which was then related to the vertical GRF, or along the tibial axis, rather than a resultant magnitude.[22] In a study on change-of-direction movements, Wundersitz *et al.* (2013) observed that the cranial-caudal axis had poor agreement with the global vertical axis, since the cranial-caudal axis would become misaligned during motion. When comparing the results between axial measurements in different angle change-of-direction movements, they found that the maximum uniaxial correlations were $r = 0.39$, and the maximum triaxial correlations were $r = 0.76$ (Wundersitz *et al.*, 2013). They also acknowledged that a limitation of locating an IMU on the upper body is that it must be able to compensate for postural movements due to the deviation from posture from the true vertical axis.

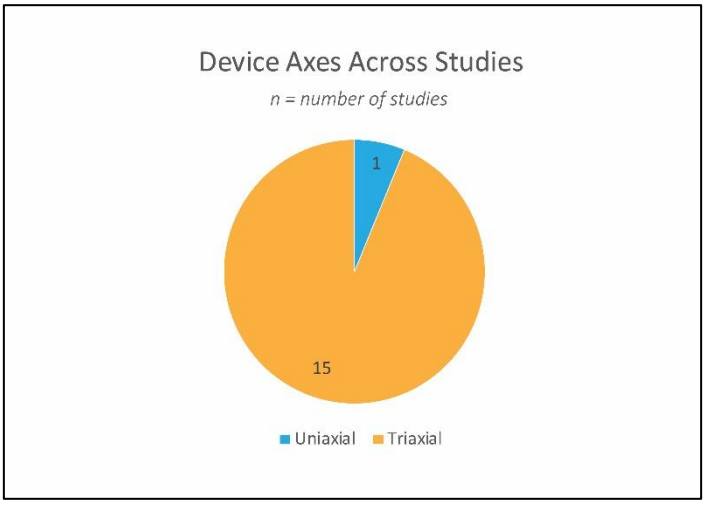

Figure 8: Portion of studies that used triaxial vs. uniaxial devices.

Force

A second set of three factors that may contribute to the model have been suggested by Hunter *et al.* (2005). It may be noted that these are *similar* to those aforementioned from Takeda *et al.* (2009), with the difference being in what may be perceived as the *mass adjusted* effects of

[22] Chapter 2.1.5, *Qualifying Articles*.

acceleration; they are: GRF (relative to the *translational* acceleration), gravitational force (relative to the *gravitational* acceleration), and wind resistance.[23] Force will here be considered.[24]

The gold standard measurement for impact load is ground reaction force, which is often measured by triaxial force plates (Simons and Bradshaw, 2016). Just as with acceleration, different force axes may be of interest, depending on which exact force-acceleration model is being considered. It has been found that "*shank orientation and resultant GRF vector are similar at heel strike"* (Lafortune *et al.*, 1995), and that acknowledging the effects of orientation is particularly important, since *"ignoring the F_x and F_y components [of the 3D tibial accelerations] causes a maximum error of 20% in the tibial axis GRF"* (Elvin *et al.*, 2007). As was mentioned above, Wundersitz *et al.* (2013) attributed errors to a misalignment of the crania-caudal axis to the global vertical axis of the force plate. Strictly speaking, Callaghan *et al.* (2018) has defined vertical peak force as the *"maximum force or force signature measured in the vertical direction,"* and the braking peak force as the *"maximum force or force signature measured in the posterior direction."*

These components can be further mapped on body segments. Similar to how the global vertical acceleration was calculated from the triaxial gyroscopic output, an *axial* force can be calculated by decomposing the triaxial force plate components. The following formula is one method that was used in the qualifying articles to determine the GRF component along the *tibial axis* from the reaction force vector (Elvin *et al.*, 2007, Zatsiorsky and Zaciorskij, 2002):

$$F_{TA} = F_x(\sin\alpha\cos\beta) + F_z(\sin\alpha\sin\beta\sin\gamma + \cos\alpha\cos\gamma) + F_y(\sin\alpha\sin\beta\cos\gamma - \cos\alpha\sin\gamma)$$

$$F_{TA} = GRF\ component\ along\ tibia\ axis$$

$$F_z = vertical\ GRF;\ F_x = posterior\ GRF;\ F_y = medial\ GRF$$

$$\alpha = \angle tibia\ to\ vertical\ (sagittal);\ \gamma = \angle tibia\ to\ vertical\ (frontal);\ \beta = \angle tibia\ to\ vertical\ (horizontal)$$

If angles are not correctly accounted for, then the directional forces may not be correctly considered. Arami *et al.* (2014) found that IMU-based estimates of knee flexion angles lacked the precision to monitor knee kinematics, but that precision could be improved with anisotropic

[23] Of course, Hunter's wind resistance is not directly related to Takeda's third variable of *noise*, but it is interesting in that both definitions contain a third, external variable such as this. The distinction may have been because Hunter *et al.* (2005) considered acceleration in *sprinting* and Takeda *et al.* (2009) in *walking*.
[24] Wind resistance is an *external* factor which is only experienced in *some* circumstances; therefore, it is necessary to understand and confirm the presence of a general relationship in a contained environment before accounting from random variables such as wind. Such external conditions will be further considered in Chapter 5.2.2, *Differences by External Condition.*

magnetoresistive sensors in a fusion framework. Since *"the angle of the tibia relative to the ground at initial contact is dependent on hip and knee angles during this phase of gait, and is thought to vary between an angle of 20◦ and 40◦ depending on speed"* (Raper *et al.*, 2018), these considerations must be made when comparing IMU data to force plate data, rectifying the directions of measurement when relevant. Indeed, the appropriation of this research into predictive models may provide crucial information to the development of high loading forces, with Tran *et al.* (2012) relaying from Lafortune *et al.* (1996) that "*in response to more severe running impacts, knee contact angle…"* has been found to increase, so as to *"…improve shock attenuation through the lower limb."*

Waveform Features

Most studies that considered a relationship between acceleration and GRF only compared peak accelerations, but this may not necessarily be the most effective method of understanding impact. A few studies, like Lafortune *et al.* (1995), Guo *et al.* (2017), and Callaghan *et al.* (2018), considered modelling the entire waveform, but because of the variability of non-cyclic movements, it may not be possible to make a simple relationship that describes every waveform.[25] This has implications for the way that the sampled datapoints are inserted into any chosen model, since *"if a model takes each sample independently as the input, it will not be able to extract non-linear relationships between different samples, and it will be more sensitive to the noise of each sample"* (Tan *et al.*, 2020). However, as has been shown, when considering a timeseries of points, rather than a point-to-point analysis, algorithms are indeed able to determine the entire waveform.[26]

As such, any relationship must first consider the kind of feature that it aiming to predict – peak, or entire waveform – since this will affect the kinds of variables chosen to be input into the data. It may even be that there are other specific variables that can be taken from the acceleration or force waveform which can contribute to the effective design of a model relating acceleration and GRF. The following tables (Table 4 and Table 5) expand on the variables that constituted 'acceleration' and 'force' in Table 3 by showing what previous studies have used for modelling a

[25] Chapter 3.2.1, Exploring Non-Linearity.
[26] Chapter 3.2.1, Machine Learning Algorithms.

relationship between acceleration and force. Several of these variables will be validated later in this investigation.[27]

Table 4: Variables taken from the force waveform to use in modelling the acceleration-force relationship.

Force Waveform	
Variables	**Studies**
Vertical GRF	[13] Simons and Bradshaw (2016)
Resultant GRF	[13] Simons and Bradshaw (2016)
Vertical average load rate (VALR)	[3] Davis *et al.* (2018)
Vertical instantaneous load rate (VILR)	[3] Davis *et al.* (2018)
Resultant instantaneous load rates (RILR)	[3] Davis *et al.* (2018)
First peak vertical force (PVF1)	[7] Hennig and Lafortune (1991)
Time to first vertical force peak (TPVF1)	[7] Hennig and Lafortune (1991)
Force rate to first peak force (PVF1/TPVF1)	[7] Hennig and Lafortune (1991)
Second peak vertical force (PVF2)	[7] Hennig and Lafortune (1991)
Peak horizontal braking force	[7] Hennig and Lafortune (1991)
Time to peak horizontal braking force (TPVF2)	[7] Hennig and Lafortune (1991)
Jump height[28]	[4] Elvin *et al.* (2007)

Table 5: Variables taken from the acceleration waveform to use in modelling the acceleration-force relationship.

Acceleration Waveform	
Variables	**Studies**
Peak vertical accelerations (VTA)	[3] Davis *et al.* (2018)
Resultant tibial accelerations (RTA)	[3] Davis *et al.* (2018)
TAA heel-strike	[2] Charry *et al.* (2013)
TAA initial peak acceleration	[2] Charry *et al.* (2013)
TAA Peak-to-peak	[2] Charry *et al.* (2013)
Time to peak axial acceleration	[7] Hennig and Lafortune (1991)
Jump height[29]	[4] Elvin *et al.* (2007)

Table 6: Additional variables considered in the qualifying articles.

Variables	**Studies**
Force: Horizontal impulse	Hunter *et al.* (2005)
Force: Vertical impulse	Hunter *et al.* (2005)
Acceleration: Power	[10] Penghai *et al.* (2014)

[27] The studies cited here are not exhaustive of where these variables have been used; some variables were investigated in several of the qualified articles. As such, these are only example studies of where these variables have been used. This list is not exhaustive of the features of the respective waveforms, but only indicates that these variables were investigated in these studies.

[28] In this study, jump height was estimated from both force and acceleration. If there was a relationship between force and the estimated height, and acceleration and the estimated height, then this could have provided evidence for a strong relationship between force and acceleration via this estimated height calculation. Alas, the correlations between force and height, and acceleration and height, were found to be weak.

[29] See note 28.

Time-Dependence

There are other factors that can be considered, especially if kinematics of jumping movements or time-series patterns for the development of algorithms is desired (Elvin *et al.*, 2007, Guo *et al.*, 2017). VALR has been defined as *"the average slope between 20% and 80% of the most linear part of the [force] curve in the region between foot strike and the [point of interest],"* with the point of interest defined as *"the point just prior to the slope reducing by* $15BW/s$*"* (Futrell *et al.*, 2020). They further defined VILR to be "*the peak slope within the region between 20% and 100% of the [force] curve between foot strike and [the] POI."* These are further illustrated in Figure 9.

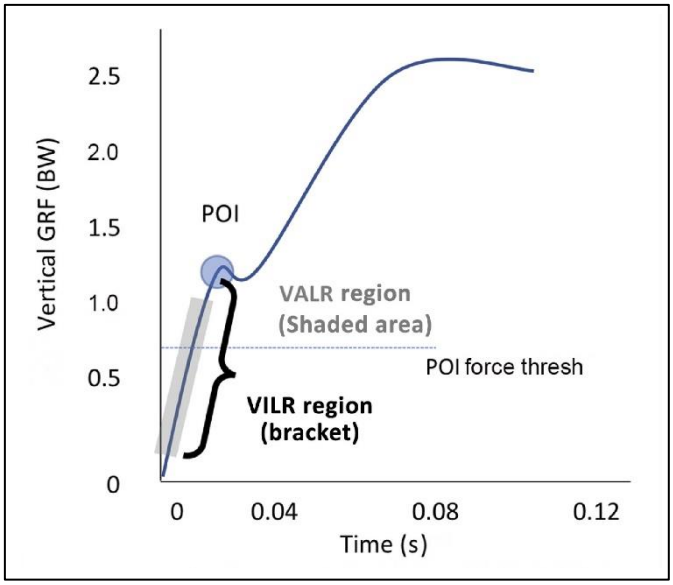

Figure 9: Calculating load rates in the vicinity of the first local maximum (Futrell et al.*, 2020). Reprinted with permission under CC BY-NC-ND 4.0.*

VALR was used by Tan *et al.* (2020) to obtain a correlation of $r = 0.94$ with GRF, following this result with the conclusion that *"it is possible to train a more general and accurate VALR estimation model using a larger data set consisting of a broader population."* When Davis *et al.* (2018) calculated the difference between load rate indicators, they found that vertical tibial acceleration had a stronger correlation with VALR, VILR and RILR than resultant tibial acceleration, and found that correlations were similar between these load rates. So too, when Hennig and Lafortune (1991) explored the potential contributors to force, they concluded that the rate of loading (that is, the time development of force), has a closer relationship to tibial peak acceleration ($r = 0.87$) than the peak of the vertical force ($r = 0.76$).

It has even been shown that force can be determined based on the timing and motion of gait events, without using wearable accelerometers to calculate the acceleration, with Clark *et al.*

(2017) determining that the vertical GRF-time waveform pattern could be explained by contact time, aerial time, and acceleration. In a similar way, Udofa *et al.* (2016) has suggested that contact time, aerial time, and lower limb acceleration are determinable by wearable accelerometers using specific models. Within the acceleration curve, *"the derivative of the acceleration, or jerk, appears to provide consistent characteristics for touchdown and toe-off that would allow for the detection of contact and aerial times via signal processing" (Udofa et al., 2016)*.

Another method for determining flight time was used by Elvin *et al.* (2007), who counted the time after the accelerometer reads $-g$, which is when only gravitational acceleration is being considered, and finishes when the sensor is just greater than $-g$ (Elvin *et al.*, 2007). Flight time has also been suggested as a variable which can be used for determining jump height, finding that jump height as calculated from flight time gave better concurrent validity and repeatability than when calculated from maximal vertical velocity (Rantalainen *et al.*, 2018). However, jump height was considered as a variable for relating to acceleration and force, but with only minor correlations by Elvin *et al.* (2007), and not deemed a valid estimate for drawing these variables together.

If there are relationships between the derivates of any of these curves, then the original values could be determined by integrating the derivatives. Or, rather than differentiation, in the case that there is a relationship between the *integration* of the force and acceleration curves, then vice-versa. This would become a relationship between acceleration and energy; the integration of force gives impulse, which demonstrates the change in momentum of an object. Callaghan *et al.* (2018) has defined vertical impulse as *"the area under the vertical force or force signature-time curve,"* and braking impulse as *"the area under the anterior/posterior force or force signature-time curve," and* Hunter *et al.* (2005) has demonstrated this by calculating the horizontal and vertical impulse, which could be written as:[30]

$$I_H = \int_{t_1}^{t_2} GRF_H$$

$$I_V = \int_{t_1}^{t_2} GRF_V - \int_{t_1}^{t_2} GRF_{Bodyweight}$$

[30] These formulae were not explicitly stated within the study; they have been written as interpreted from the study methods.

Power

It may be that power could be used within the impact dose relationship, since the joint power curve, when integrated, gives energy absorption (Zhang *et al.*, 2008); this may contribute to an understanding of fatigue.[31] A transfer function between power and acceleration could be determined by finding the shock reduction from a power spectral density function (Zhang *et al.*, 2008). The relationship between acceleration and power is not linear, so Jiang *et al.* (2019) used random forest machine learning algorithm to attain power from acceleration, finding that the model was almost perfect.[32] However, it was suggested that there is large variability of power generated between individuals under the same testing conditions (Jiang *et al.*, 2019). If not using a machine learning algorithm, maximum explosive jumping power could be calculated as given by Penghai *et al.* (2014):

$$EP_{MAX} = m \cdot MAX \langle a_t \cdot \left(\int_{t-t_0}^{t} a_t dt + V_{t-t_0} \right) \rangle$$

Rantalainen *et al.* (2018) has stated that *"jump height and power are closely related,"* and they found that jump power, as estimated from a wearable accelerometer with the centre of mass known, provided similar results to the force plate. However, in an earlier article, Winter (2005) has emphasised that *"efforts to explain jumping in the context of power are at best misguided and a distraction and at worst a misrepresentation of the mechanical constructs involved."* In light of these different conclusions on power, for the sake of investigating the *primary* model contributors, the investigation will not proceed in this area of analysis.

[31] This is a conjecture. Fatigue will be considered further in *Chapter 5.2.1, Pathophysiological Application of Predictive Models.*

[32] Results had an intra-subject accuracy of $R = 0.98$. The obtained random forest model underestimated ankle joint power peak amplitude, though peak power occurrence was correctly detected with negligible delay in intra and inter subject testing.

Chapter 4. Collecting, Refining and Classifying Data

Research Aim #2

Determine whether this relationship can be accurately modelled using data collected from wearable accelerometers.

4.1. Collecting Reliable Data

Prior to the implementation of any of the aforementioned algorithms, strategies for data collection and refinement must be established. These involve selecting devices for data capture, determining attachment methods, and configuring the dynamic range and sampling rate of each device. As specified in the introduction, a wearable accelerometer will be considered sufficient if it is able to produce a relationship between acceleration and force without requiring information from other devices. Following data collection, the recorded data must be refined to remove noise and device inaccuracies. As such, this section will also consider the filtering of data and error reduction, and an objective scale of result classification. As specified in the introduction, a wearable accelerometer will be considered effective if it produces a relationship with an acceptable amount of error.

4.1.1. Wearable Devices

The case for collecting data using wearable devices lies in the conclusion that collecting kinematics from wearable devices provide the highest practicality for data retrieval of GRF measurements, as opposed to laboratory-based force-plates (Mundt et al., 2020). Wireless and lightweight sensors are ideal for field measurements (Elvin *et al.*, 2007), and enable athletic loading to be measured over long distance training environments with real-time visualisation (Abdelhady *et al.*, 2019, Raper *et al.*, 2018). However, their reduced accuracy means that development must be directed towards long-term reliability (Shahabpoor and Pavic, 2017), with the crucial need for consistent accuracy. It has been suggested that accuracy can be increased with multiple devices, where data is combined to estimate lower-limb kinematics (Jiang *et al.*, 2019); however, it has also been suggested that more data complicates the analysis (Guo *et al.*, 2017). These kinds of issues, including device attachment methods, will be discussed here. A summary of the devices that were used in the qualified articles is shown in Table 7.

Table 7: Technologies utilised by the qualified articles.

Variable	Technologies	Number of Studies	Studies
Acceleration	Wearable IMU	13	[1],[2],[3],[4],[5],[6],[9],[10],[11],[12],[13],[15],[16]
	Bone-Mounted IMU	2	[7],[8]
Force	Force Plate	12	[1],[2],[4],[6],[7],[8],[9],[10],[12],[13],[15],[16]
	Instrumented Treadmill	2	[3],[11]
	Pressure-Sensing Insole	1	[5]
Movement	Motion Capture	4	[6],[11],[12],[16]

Using Multiple Sensors

Studies that compared single devices to multiple devices will first be considered. In a study that measured kinematics from six devices on a single participant, and compared the differences between combinations, Zeca *et al.* (2018) found that the best estimation for centre of pressure could be obtained when the model incorporated measurement data from six devices with a prediction error of 2.5% (anterior-posterior) and 7.1% (medial-lateral). From the left ankle alone, it was 2.7% and 7.6% respectively.[33] These results would indicate that when considering centre of pressure, a single device may be sufficient, since the improvement was only slight, and this is more practically accessible outside of a laboratory. Furthermore, depending on the accuracy required, the improvement may not even be substantial enough to *justify* using more than a single device. This seems consistent with the force-acceleration results obtained by Tan *et al.* (2020): after considering 31 placement combinations of five IMUs, the correlation from multiple sites was $\rho = 0.96$, and the single-device lower-shank measurement was $\rho = 0.94$; this improvement was not statistically different (Tan *et al.*, 2020).

After determining that angular velocities did not majorly improve force prediction accuracy, Guo *et al.* (2017) explained that *"using less information will reduce the complicity of the model and increase the model's robustness"* (Guo *et al.*, 2017). However, they did agree that angular velocities are important for predicting centre of pressure, showing that sensors must be carefully chosen for the desired information. *"Effective technological solutions should be well-matched to the clinical need at hand but no more sophisticated and complex than needed to promote widespread adoption and feasibility"* (Pieper *et al.*, 2020). Further examples that have validated single-device performance in force estimation outside of laboratory-based environments include Charry *et al.* (2013) with *ViPerform*, and Guo *et al.* (2017) with *Opal*. However, when Meyer *et al.* (2015) compared the *ActiGraph GT3X* and *GeneActive* devices, they found that both devices

[33] Errors from the left ankle were lower than the right ankle and fifth lumbar vertebra.

significantly and systematically overestimated GRF when their raw data was linearly approximated, as shown in Figure 10.

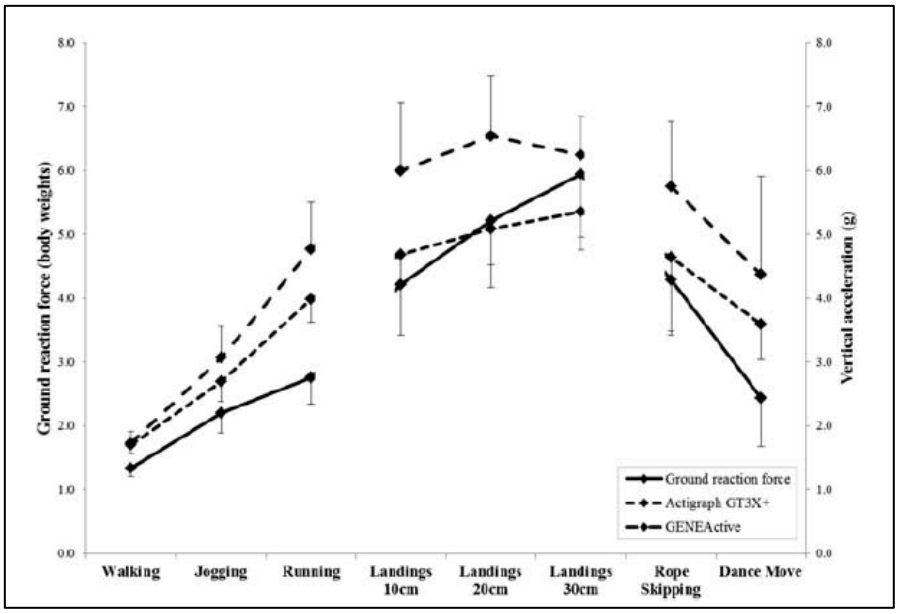

Figure 10: GRF and vertical peak accelerations using commercial accelerometers, in $\mu \pm \sigma$ (Meyer et al., 2015). Reprinted with permission from Taylor & Francis.

Whichever devices are chosen, advances in technology for basing training regimes and data applications must be evaluated for device reliability. In contrast to the conclusion from Charry *et al.* (2013), Raper *et al.* (2018) reported that the ViPerform did *not* perform accurately to its claim.[34] If a decision is ever made for custom development, the product limitations must be clear and accurate, lest they be disproved, especially when offered for injury management (Raper *et al.*, 2018).

In custom designs, the kinds of sensors imbedded within any device should be chosen carefully. These designs could also consider including additional sensors, since gyroscopes and magnetometers have been found to "*reduce orientation, offset, and integration errors of the lower limb vertical acceleration parameters"* (Udofa *et al.*, 2016). However, devices ought not include unnecessary hardware, and the hardware included should be chosen intentionally.[35] Although not covered here, methods have been proposed for developing wearable devices and ground reaction force sensors, and should be investigated prior to their deployment (Clark *et al.*, 2017). Several

[34] These statistics are further discussed in Chapter 4.2.3, *Classifying Statistics.*
[35] For example, the inclusion of force-sensitive resistors may lead to noisy and inaccurate data (Mahdavian *et al.*, 2019).

important aspects of device design were raised within the literature. Some of these, including attachment method, dynamic ranges, and sampling rates, will now be considered.

Attachment Method

Wearable device attachment methods are broad and ingenious, but should never be chosen arbitrarily, since inadequate securing of devices is a primary source of error due to vibrations and unrelated accelerations (Udofa *et al.*, 2016). As explained in Chapter 3, errors may be present in the data due to higher levels of subcutaneous fat causing movement artefact in the accelerometer and must be limited. The kinds of attachment methods that were specified in the literature have been summarised in Table 8, with colours identifying similar methods.

Table 8: Attachment locations used in the qualified articles.

[#]	Location	Attachment Method
[1]	**Trunk**	Double sided tape, additional strapping tape.
	Lower Leg	Manufacturer-supplied click-in body strap.
[2]	**Lower Leg**	Adhesive sticker.
[3]	**Lower Leg**	-
[4]	**Lower Leg**	Sleeve over knee; Drytex Knee Support.
[5]	**Trunk**	-
	Neck	-
	Head	-
[6]	**Upper Leg**	Nylon elastic band wraps under semi rigid plastic plates under elastic straps under duct tape.
	Lower Leg	Nylon elastic band wraps under semi rigid plastic plates under elastic straps under duct tape.
[7]	**Lower Leg**	Bone-mounted Steinmann traction pins.
[8]	**Lower Leg**	Bone-mounted Steinmann traction pins.
[9]	**Upper Leg**	-
[10]	**Trunk**	-
[11]	**Lower Leg**	-
[12]	**Lower Leg**	-
[13]	**Trunk**	Tight-fitting crop top.
	Trunk	Double-sided tape Fixomull stretch tape, tight-fitting leggings, or compression pants.
[14]	**Trunk**	Straps around the body segment.
	Upper Leg	Straps around the body segment.
	Lower Leg	Straps around the body segment.
[15]	**Neck**	Manufacturer-provided harness.
[16]	**Trunk**	Placed within a mini-backpack, within the manufacturer-supplied harness.

The primary aim in attachment design must be to reduce movement artefact whilst retaining a secure and comfortable fit, and the inclusion of orientation data from different sensors requires that they be correctly aligned with the physiological axis that they claim to represent. The extreme

in the removal of movement artefact, which is by the time-consuming process of surgically mounting accelerometers to the bone, as done by Hennig and Lafortune (1991) and Lafortune *et al.* (1995), is clearly not viable as a generalised solution, meaning that some compromise must be identified between compensating for residual movement and minimising it.

To this end, many solutions have been attempted: Reenalda *et al.* (2016) used double sided adhesive skin tape and foot clips laced onto the shoes; Zhang *et al.* (2008) used *Velcro* straps; Simons and Bradshaw (2016) used tight clothing such as crop tops, leggings and compression pants. Sleeves have also been suggested as beneficial, with the participants of one study reporting not having felt the sensor nodes on the sleeve (Elvin *et al.*, 2007). None of these solutions were reported as having caused many problems for the users or within the data, and yet most studies did not provide comment on the magnitude of any slipping or movement artefact which may have been produced. Elvin *et al.* (2007) justified not visiting this problem by assuming that any slipping present was at least consistent for individuals, though perhaps different *between* individuals. Rather than attaching the device onto a person, studies have also designed shoes within in-built force sensors; however, insoles can be inconvenient, costly and uncomfortable for daily living, and can be easily damaged with long-term pressure (Abdelhady *et al.*, 2019).[36]

As mentioned, if developed for a particular sport, its design must accord with game regulations. Designs must be comfortable and welcomed by players, and must consider aesthetics, ease-of-use, durability, and safety. In light of the present discussion, it seems that minimising movement artefact from the device, whilst still retaining user comfort, is the most pressing design problem. Although power will not be discussed further within this report, wireless design also necessarily entails the inclusion of a power source, and as such this must be appropriately designed for (Corbo, 2018, Talukder, 2020). Memory requirements could be overcome by using devices that transmit data from the device immediately following capture: studies capturing force and limb movement have previously used transmission frequencies ranging from 5 to 750 Hz (Abdelhady *et al.*, 2019).

[36] However, research has been undertaken to use pressure insoles for monitoring instability (Noshadi *et al.*, 2013) and postural identification (Sazonov *et al.*, 2011), with varied results.

4.1.2. Technological Specifications

Dynamic Ranges

When considering the specifications of the accelerometer to use within any design, an important consideration is the *dynamic range* of the device. Given as a product of gravitational acceleration (g), this is the sensitivity range through which the accelerometer can record acceleration without peaking. The accelerometers used by Meyer *et al.* (2015) did not have suitable dynamic ranges, with values peaking at 6 g and 8 g and invalidating portions of their data. Clearly, dynamic ranges must be carefully chosen. Clark *et al.* (2014) has recorded that when running at 3.5 to 10.5 ms^{-1}, lower limb velocity at touchdown is ordinarily between 0.8 to 3.1 ms^{-1}, and the time for that velocity to reduce to 0 ms^{-1} is ordinarily 0.070 to 0.025 s. Udofa *et al.* (2016) identified from this that the accelerometer range during such movements is 1.2 to 12.7 g, concluding that accelerometers with a dynamic range of ± 16 g are therefore suitable for measurement. However, the quality of the chosen sensor is also a factor, even if the device has a high dynamic range: when using a uniaxial accelerometer with a dynamic range of ± 70 g, Elvin *et al.* (2007) found that the range response was only linear up to ± 50 g. The dynamic ranges of the devices used in the qualified articles are shown in Table 9.

Table 9: Dynamic ranges of the devices used in the qualified articles.

Study	Dynamic Range (g)	Axes
[1] Callaghan *et al.* (2018)	± 16	Triaxial
[2] Charry *et al.* (2013)	± 24	Triaxial
[4] Elvin *et al.* (2007)	± 70	Uniaxial
[5] Penghai *et al.* (2014)	± 6	Triaxial
[9] Meyer *et al.* (2015)	± 6, 8	Triaxial
[10] Guo *et al.* (2017)	± 6	Triaxial
[16] Wundersitz *et al.* (2013)	± 8	Triaxial

Sampling Rates

In addition to determining an appropriate dynamic range, sampling rates must also be chosen carefully. The rate must be sufficiently high so as not to cause aliasing, but not so high that device storage capacity becomes insufficient and the battery is drained (Raper *et al.*, 2018). Adequate sampling rates for *force* may be considered in light of how *"maximum impact forces occur typically within a 20-ms time window"* (Elvin *et al.*, 2007). This would imply that that, for example, 100 Hz is likely insufficient, since it would only capture two frames per peak; and unless the peak occurred at the precise time of sampling, the peak is unlikely to be recorded:

$$\text{Sampling rate} = 100\ Hz = \frac{100\ frames}{1000\ ms} = \frac{2\ frames}{20\ ms}$$

It has further been stated that even 240 Hz (< 5 *frames/event*), which is the common camera frame rate used in biomechanical testing, would miss important features of the impact curve (Elvin *et al.*, 2007). Acting on this, Elvin *et al.* (2007) sampled at 1000 Hz. To minimise required storage and battery life, and since they only required primary gait *events*, rather than entire waveforms, they only stored the *maximum* and *minimum* values within each 60 ms time window. However, contrary to this, Guo *et al.* (2017) sampled their force values at 128 Hz, justifying this in that since they had identified that their targeted frequencies were below 10 Hz, "*a sample frequency greater than 64 Hz was deemed high enough to characterise the main frequency spectral."* This is not consistent with Elvin *et al.* (2007), since 10 Hz would indicate a peak within 100 ms; however, Guo *et al.* (2017) did not indicate what the *main* frequency was that they were considering, and as such this may not be the same peak that was identified by Elvin *et al.* (2007).

Considering the acceleration sampling rates, the sufficiency of 100 Hz to capture data at faster running speeds has been deemed inconclusive, with further research required (Charry *et al.*, 2013). Meyer *et al.* (2015) had stated that the sampling rate must be at least double the speed of the fastest movement, and their work could be considered as the desired *further research*, for they also sampled acceleration at 100 Hz, and with correlations of $r = 0.89$ to 0.90, concluded 100 Hz to be *reasonably accurate* for determining GRF. This more recently obtained accuracy could indicate that there were errors elsewhere in the study from Charry *et al.* (2013), but if not, then the fact that a 100 Hz filter has been found inconsistent in its ability to measure acceleration should indicate that a higher rate is necessary.

Furthermore, it should be noted that high correlations do not necessarily mean that complete events were indeed captured, but only that the data which was obtained *from* these sampling rates correlated well. As mentioned from previous studies, to identify the required frequencies, those targeted could be identified with a power-frequency analysis and isolated from this. If this strategy is taken, it must be noted that *"to properly eliminate effects of noise without aliasing, the sampling rate must be above twice the highest significant noise frequency"* (Antonsson and Mann, 1985). If lower sampling rates *must* be used, then resampling data from lower frequencies is also an option (Zhang *et al.*, 2008). A summary of the sampling rates used in the qualified articles is shown in Figure 11.

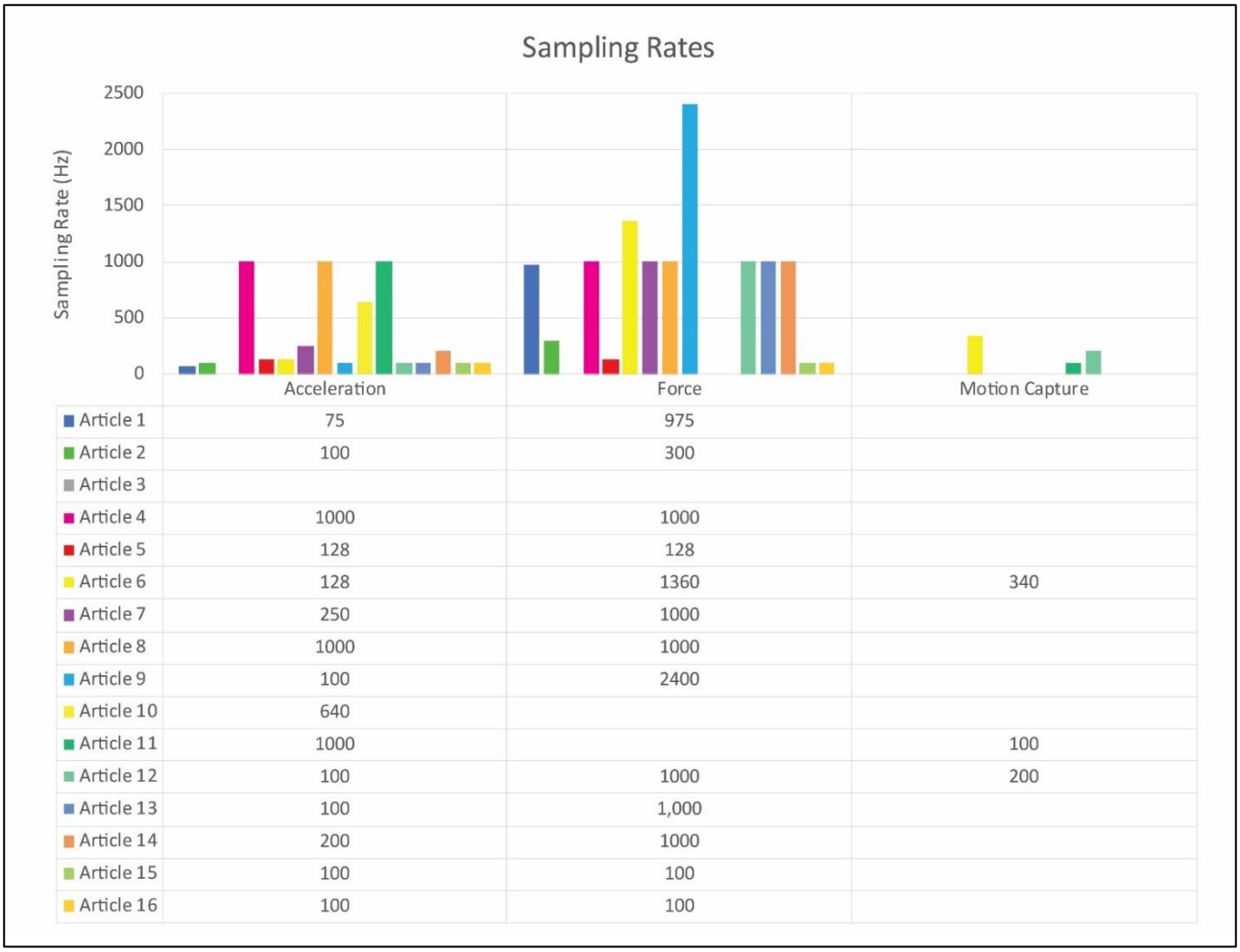

	Acceleration	Force	Motion Capture
Article 1	75	975	
Article 2	100	300	
Article 3			
Article 4	1000	1000	
Article 5	128	128	
Article 6	128	1360	340
Article 7	250	1000	
Article 8	1000	1000	
Article 9	100	2400	
Article 10	640		
Article 11	1000		100
Article 12	100	1000	200
Article 13	100	1,000	
Article 14	200	1000	
Article 15	100	100	
Article 16	100	100	

Figure 11: The sampling rates used across the qualified articles.

A final note on the topic of sampling rates is that when sampling with multiple instruments, data must be synchronised so that time-equivalent samples are correctly compared. There are several methods by which this can be achieved. Penghai *et al.* (2014) used an additional processor to synchronise the accelerometer and the gyroscope, timestamping their data before saving. Elvin *et al.* (2007) connected their devices to an external device that transmitted an electronic pulse and was disconnected prior to completing their trial. In post-processing, Meyer *et al.* (2015) found the highest cross-correlation coefficient for the primary acceleration events of two accelerometers and used this frame as a reference point from which to analyse.

4.1.3. Data Refinement

Filtering

Applying appropriate sampling rates is particularly important when facing the risk that analysis may depend on characteristics that are masked within noise. However, the presence of noise and targeted frequencies may not necessarily be consistent between studies, and as such the

recommended filters may not be directly transferable. Although these rates may be different between studies and applications, understanding the spectrums and filters used in other studies may indicate areas of the spectrum for further consideration in future design planning, and as such their methods shall be considered. Within this, one must consider that whilst the eliminating noise is important, there may be particular frequencies that are helpful for modelling the respective parameters.[37] Different kinds of movements and landings contain different frequency makeups: *"the appropriate cut-off frequency depends on the frequency content of the signal, which in turn depends on the type of task performed*" (Simons and Bradshaw, 2016). As shown earlier, primary frequencies within the signal may be sufficient to model the waveform of a runner.

Using a frequency histogram, Penghai *et al.* (2014) determined that in their *jumping* trial, targeted frequencies at the *trunk* were between 0 to 30 Hz, and they as such used a lowpass filter at 30 Hz. Zhang *et al.* (2008) observed that in drop landings, within the 100 ms after initial foot contact, the first and second peak power of *tibial* accelerations was between 21 to 50 Hz. In a *running* trial, Lafortune *et al.* (1995) found that frequencies in the *lower leg* were *greater* than 30 Hz. In an earlier study, Hennig and Lafortune (1991) observed that *"a power spectrum analysis of the force and acceleration signals revealed that more than 99% of the signal's power was below 60 Hz,"* leading them to use a 60 Hz lowpass filter. They later found that 98% of this content was below 100 Hz (Lafortune *et al.*, 1995). However, contrary to this, Antonsson and Mann (1985) found that in *walking*, 99% was contained under 15 Hz. These results clearly differ between activities and locations, but it seems that there is a consistent gait signal content below 100 Hz.

Correlation strength has been found to differ between use of different filters. When comparing locations across the back, Simons and Bradshaw (2016) found that a 20 Hz filter on the upper back produced the overall best correlations between PRA and GRF. Wundersitz *et al.* (2013) found that for the most appropriate indirect measure of peak GRF, 8 to 10 Hz was best for walking and running tasks, suggesting that *resultant* acceleration data be smoothed with a 10 Hz filter.[38] In a later study, they again found that these filters significantly reduced errors between raw and actual acceleration data (Wundersitz *et al.*, 2015). Rantalainen *et al.* (2018) also considered the effects of filtering acceleration data from the upper back, with low-pass cut-offs between 6 Hz to 20 Hz.

[37] Chapter 3.1, *Recording at the Lower Limb*.

[38] It is important to note that this was a smoothing of the *resultant* acceleration data; not the uniaxial data.

However, they found that filtering had very limited effect on acceleration error and chose to therefore apply *no* filter.

Error Reduction

Another consideration for force recording is that a recording threshold may need to be determined, above which the input data is deemed valid. Jiang *et al.* (2019) considered the gait cycle to have started when force was above 0 N; Hennig and Lafortune (1991) considered foot contact as above 5 N; Guo *et al.* (2017) above 10 N; Pieper *et al.* (2020) above 20 N. Havens *et al.* (2018) considered peak vertical GRF to occur at the first peak following 30 N of contact. The inclusion of these thresholds can reduce errors: Udofa *et al.* (2016) attributed their over-prediction of force to having not incorporated a 40 N contact-identification threshold. They further showed how this can impact impulse predictions, saying that the "*inclusion of the threshold setting at the beginning and end points of the impulse curve function with preservation of the mathematical area under the curve would lower the peak value."* They said that ultimately, the main error was more likely due to the lack of a threshold than the shape of their sine function.

Accelerometers, gyroscopes and magnetometers can provide information on orientation for gait analysis in space without motion capture systems (Mundt *et al.*, 2020). However, this is not without limitation, since accelerometers and gyroscopes are susceptible to drift and noise that can cause error accumulation in multi-step analyses; this is also a problem when testing over long periods (Tao *et al.*, 2007). Magnetometers *"…are highly susceptible to local disturbances in the magnetic field"* (Mundt *et al.*, 2020). Systematic biases have been found in commercial accelerometers of between 0.46 g and 1.39 g, with biases increasing with higher loadings (Meyer *et al.*, 2015). The sensitivity of accelerometers to linear accelerations, and the drift and inclination direction of gyroscopes, have been raised as concerns in sensor design (Abdelhady *et al.*, 2019). It has been suggested that accelerometer bias may corrected by establishing a regression model (Meyer *et al.*, 2015). Gyroscope drift may be correctable by resetting the system after each gait cycle and by highpass filtering (Tong and Granat, 1999). Takeda *et al.* (2009) applied a highpass filter to the raw angular velocity data to remove noise prior to integrating their data for determining joint angles, minimising drift error from raw integration.

4.1.4. Result Validation

Whether or not these relationships can be determined consistently, validity must be determined objectively. As such, the performance of these algorithms and which methods should be chosen

for data analysis must be set. This review does not aim to address methods for statistical analysis in sports medicine and exercise science,[39] but it will consider some noteworthy tools used in previous studies. Studies have used tools such as direct correlations, *Bland-Altman* plots (Raper *et al.*, 2018) and one-dimensional statistical parametric mapping (Callaghan *et al.*, 2018) to compare acceleration and force data.

Methods of comparative analysis include determining the closeness of a prediction model by testing it with the data of a participant from whom the model was not trained. When Lafortune *et al.* (1995) tested their Fourier waveform models, they developed individual-participant models and multiple-participant models, testing these against the participant(s) who had not been included. They found that where the individualised algorithms produced mean standard deviations of $MSD = 0.11$ to 1.10 across the five participants, the generalised algorithm, which was developed from four and tested against the fifth, led to *larger* deviations of $MSD = 0.26$ to 1.26. Tan *et al.* (2020) similarly developed a 14-participant model, testing against the 15th participant.

Guo *et al.* (2017), rather than dividing their data by participants, halved the data of all participants and tested their model with the remaining 50% of the dataset. Both Tan *et al.* (2020) and Guo *et al.* (2017) obtained almost perfect results ($r > 0.90$) with their machine-learning-based models, showing that a generalised algorithm could be successfully implemented. In a slightly different context,[40] Mahdavian *et al.* (2019) considered several different machine learning strategies where, along with speed and angular velocities, they included the weight and height of 108 participants as inputs to train the algorithm. When testing against two participants, their results demonstrated strong correlations ($R = 0.89$ to 0.97) in the forces and moments of all three axes.

When considering acceptable rates of accuracy, Tran *et al.* (2012) set the limit of acceptability to 20%, justifying this by explaining that *"though it is acknowledged that CV values above 10% are rejected in other fields of research, it has been proposed that this analytical goal is often selected as an arbitrary limit for acceptable variability."* Raper *et al.* (2018) used a relative measure to determine the validity of *ViPerform*, stating that a single calculated stride value would be deemed invalid *"if its value was outside a 20% range of the preceding and following strides,"* having calculated this by *"dividing the number of error-free [strides]… by the number of overall strides.*"

[39] This information can be reviewed in Hopkins *et al.* (2009) and Bernards *et al.* (2017).
[40] Mahdavian *et al.* (2019) did not primarily investigate acceleration in their models, but also included walking speed and several angular features; the article was excluded because this project primarily investigated the feasibility of acceleration *alone*.

They found that the device attained an overall accuracy of 83.6% and therefore concluded that the device did *not* accurately measure GRF. However, they also concluded that the device could still be used as a reliable measurement system for a *relative, comparative* load measurement. Jiang *et al.* (2019), who when estimating ankle power was able to attain an inter-subject regression accuracy of NRMSE of 2.37%, which was consistent with the results of Wouda *et al.* (2018), deemed this an acceptable and good result.

Classification

Hopkins (2006) has provided a scale for the classification of correlation coefficients, which has been further used in other studies such as Callaghan *et al.* (2018) and Simons and Bradshaw (2016). When the latter used it, they explained that "c*orrelations classified as 'very high' or 'almost perfect' would indicate that [peak resultant acceleration] provides a good estimate of impact loading."* These categories from Hopkins (2006) are what have been, and will continue to be, assigned to results presented within this thesis, and they have been given in Table 10. This evaluation scheme has been chosen following its use in these previous studies, and its relevance to this field of research: for which the scale was intended and designed (Hopkins, 2006).

Table 10: Classification of correlation coefficients in sport-biomechanics as according to Hopkins (2006). Reprinted with permission from William Hopkins.

Correlation Coefficient	***Descriptor***
0.0-0.1	*Trivial, very small, insubstantial, tiny, practically zero*
0.1-0.3	*Small, low, minor*
0.3-0.5	*Moderate, medium*
0.5-0.7	*Large, high, major*
0.7-0.9	*Very large, very high, huge*
0.9-1.0	*Nearly, practically, or almost: perfect, distinct, infinite*

Informed by this scale, the highest correlations presented within each of the qualified articles is presented in Table 11. These represent what the *final* results were, following the refining of their algorithms and the analysing of their data with the methods originally described in Table 1 on the qualified articles. Of the qualified articles that reported correlations, four reported correlations above 0.9, which as seen, can be deemed *almost perfect*, with all remaining articles producing a *very large* relationship. It must be noted that the correlations among the qualified articles were not determined using identical methods (i.e. some used direct regression coefficients; others Pearson correlation coefficients etc.), and as such these correlations should only be taken indicatively regarding inter-study differences.

Table 11: The best correlations between acceleration and GRF as presented within each of the qualified articles.

Classification	Study	Best Correlation	Classification	Study	Best Correlation
Almost Perfect	[5]	0.993	**Very Good**	[12]	0.877
	[2]	0.95		[13]	0.86
	[14]	0.94		[1]	0.832
	[9]	0.9		[3]	0.82*
				[4]	0.812
				[7]	0.76
				[16]	0.76*
				[11]	0.71
Not Reported	[6], [8], [10]			[15]	0.7*
**this article also presented only moderate correlations*					

Chapter 5. Applying the Relationship

Research Aim #3

Determine whether this relationship is generalisable between subjects, movements, and external conditions.

Research Aim #4

Determine whether measuring acceleration at the lower limb using wearable accelerometers can provide data that is useful for the prevention or monitoring of injuries, fatigue, and rehabilitation.

5.1. Difficulties in Model Generalisation

In the previous chapters, it has been shown that an identifiable relationship between acceleration exists within the body, and it can be determined at the lower leg. However, these models clearly differ between the kind of movements that are trialled. As such, in this section, the effects of movement and technique will be considered. Following this, effects on the relationship of several inter-personal differences will be considered, including physical ability, movement, and external conditions.

5.1.1. Activity Differences

There were a variety of activities for which the trials in the qualified articles were conducted. These have been presented according to activity type in Figure 12, with activities being grouped based on similar movements. If a wholistic, efficacious model is to be developed for a generalised population, the effects of different movements on these models must be understood and, if necessary, changes implemented into the algorithms accordingly.

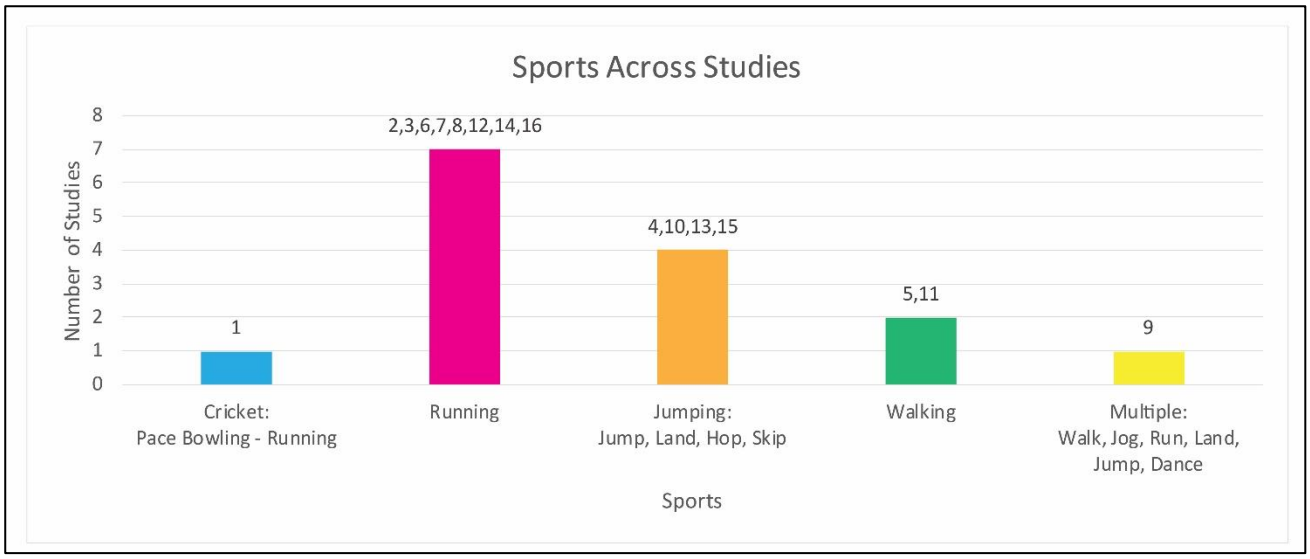

Figure 12: Sports used in the qualified articles. Activities have been grouped according to similarity.[41]

When considering these activities in light of the correlation results that have been presented, the highest three correlations (0.94 to 0.99) were produced in trials where participants had either walked or ran. However, to immediately say therefore that these activities are the best for determining any relationship may not be accurate, since the fourth highest correlation (0.9) was produced in the only study that pooled results from a *variety* of activities (Meyer *et al.*, 2015). In fact, whereas the *highest* result was observed in a study that considered walking (Guo *et al.*, 2017), the *second lowest* of the results came from the *other* study that considered walking (0.7) (Pieper *et al.*, 2020). In light of the previous discussion, perhaps the kind of *modelling* used was the primary reason these studies produced different results. For example, Guo *et al.* (2017) considered machine learning, whereas Pieper *et al.* (2020) considered direct linear correlations.

However, studies which have focussed on walking alone have been critiqued in the literature, with the claim that *"investigating only walking leads to overestimation of sensor accuracy due to the fact that the passive dynamics of walking lead to stereotypical patterns that are easier to predict"* (Jacobs and Ferris, 2015). As such, the present accuracy of these studies should not be considered as generalisable for all activities. Every article that considered jumping produced correlations of less than 0.9, which may indicate that the ground reaction force waveform during jumping is less conformed to a single pattern; or at least not as easily predicted from. Nevertheless, even these correlations would still be classified as *very large*, and as such should not be disregarded; for,

[41] Although pace bowling could be considered running, due to the unique nature of the plantar action of the foot and the rotation of the trunk during a delivery (Callaghan *et al.*, 2018), the running-movement from Article [1] has been kept separate.

besides modelling algorithms, there may be physiological factors which are much more indicative of any such relationship. The differences present between individuals in movement performance will be further considered in the following section.

Trial Design

The importance, and also a clear a limitation, of cyclic-only studies is seen in that *"studies on wearable sensors that only investigate overground and treadmill walking do not deal with the amount of variability that happens in daily life"* (Jacobs and Ferris, 2015). Having noticed this, Meyer *et al.* (2015) attempted to develop a force prediction model from the accelerations of various activities, including one step each from each trial of six different kinds of activities. Despite their accelerometers holding systematic bias, they obtained linear correlations of 0.90. The trials included within this study are shown in Figure 13. This would confirm the conclusion that the investigation of non-stereotypical tasks can lead to more accurate assessments with these kinds of technologies. Jacobs and Ferris (2015) have further explained that *"not including swing phase data in estimation also reduces variability in the data set because it assumes that non-linear transition between stance and swing is predicted perfectly despite sensor noise."*

Table II. Description of the different tasks.

Task	Description	Number of performed trials
Walking	Walking at 3 $km \cdot h^{-1}$	7 trials
Jogging	Jogging at 6 $km \cdot h^{-1}$	7 trials
Running	Running at 10 $km \cdot h^{-1}$	7 trials
Landings 10 cm	Landings from a 10-cm box	2 series with 5 jumps
Landings 20 cm	Landings from a 20-cm box	2 series with 5 jumps
Landings 30 cm	Landings from a 30-cm box	2 series with 5 jumps
Dance move	Breakdance move	2–3 series with 5 moves
Rope skipping	Free rope skipping	2–3 series with 10 skips

Figure 13: The activities trialled within the study from Meyer et al. (2015). Reprinted with Permission from Taylor & Francis.

Netball

Within this discussion on the movement-based effects of force modelling, as has been mentioned, the end purpose of any device must be considered within the trials for which it is designed. The context of this thesis is an investigation into the movements within the team sport *netball*, and as such the eminent movements performed by players during a netball match should be of primary concern within the future development of this project. Netball Australia (2016) has explained the

key skills and movements involved in the footwork of players during a game. Summarised below, these movements include stance, coordination, footwork, and balance:

- The ***two-foot landing*** controls the hip and knee, where during landing, the knee and toes are kept aligned, and the knee is kept slightly bent. Younger players may step forward with one point to maintain balance when lacking core strength required to maintain the stance.
- The ***one-foot landing*** depends on the player's leading direction: leading in the right results in the player landing on their right foot; leading to the left results in landing on the left. Players keep their body weight over the outside foot, with shoulders evenly distributed over the foot; the second foot is planted quickly following this. The player must bend at the hips, knees, and ankles to cushion their landing.
- ***Take-off*** involves starting with smaller steps and strides, quickly moving to larger steps. When leading to the right foot, a player should take off with the right foot; when leading to the left, they take off with the left foot.
- The ***two-foot jump*** involves bending slightly at the hips, knees, and ankles with the weight of the player distributed over knees and toes. The player steps into take-off with the left-right or right-left step pattern and uses both arms to reach and extend upwards. Players land on both feet and cushion their landing by bending at the knees, hips, and ankles. Younger players may be instructed to keep their feet shoulder width apart.
- The ***one-foot leap*** involves players, when running at an angle to the thrower, bend at the hips, knees, and ankles, and run with their weight forward over the toes, pushing off from the take-off foot. The player lands on their outside foot, cushioning by bending at the hips, knees, and ankles.
- A ***pivot (outside turn)*** continues natural body movement after a player has received the ball at full stretch, pivoting on the landing foot. Their weight is brought over the landing foot before turning on the ball of the foot and pushing off with the other foot.

Several of these movements are further specified within *9.6 Footwork of* the netball rule book *(International Netball Federation, 2020).*

5.1.2. Personal Factors

Technique

Factoring intra-personal characteristics into this study on kinetics, it has been identified that *"the ability to accelerate can be effected by an individual's sprinting technique, force production*

capability, and the ability to apply that force in the horizontal direction" (Macadam et al., 2017). In light of such ability-effected differences, it is expected that understanding these differences in technique would be a primary concern in the development of any kinetically driven model. However, apart from foot-strike patterns, which will be considered below, none of the qualified articles specifically targeted understanding the differences of technique when developing the force-acceleration relationship. Trial inclusion criteria within the studies included being elite or sub-elite triathletes (Raper *et al.*, 2018),[42] adults with regular participation in competitive sport (Wundersitz *et al.*, 2013),[43] and moderately active children (Meyer *et al.*, 2015).[44] All studies excluded people with recent injuries, except Havens *et al.* (2018), who recruited only participants that had undergone ACL reconstructive surgery within six months prior to the trial. Since results from elite participants may not necessarily be true also for amateur participants, this may be an important research area in future study.

Davis *et al.* (2018) studied the differences between strike patterns across 169 participants. They found that vertical average loading rate had larger correlations with vertical tibial acceleration in runners with front-foot-strike (FFS) ($r = 0.82$) than rear-foot-strike (RFS) ($r = 0.66$). Summarising several sources in the literature, Futrell *et al.* (2020) found that *"the load rates associated with a habitual FFS pattern are approximately 35%–45% lower than that of a habitual RFS pattern. Transition to an FFS pattern has been associated with a 35%–65% reduction in vertical load rates."* Following up on this, they furthermore found that this transition reduces load rates more than altering the cadence of a runner (Futrell *et al.*, 2020). Although cadence does not typically change foot strike technique (Futrell *et al.*, 2020), research has shown that when running, increasing cadence by 8.6% can reduce average vertical load rates by 18.6% (Willy *et al.*, 2016).

In addition to technique, natural movement can also cause errors, with high trunk rotation of the accelerometer during the moment of recording being found to skew results (Callaghan *et al.*, 2018). Wundersitz *et al.* (2013) has also observed that during running, as the severity of the change of direction increases, the correlation between the acceleration and GRF decreases: their prediction variance from change-of-direction tasks (24%) was double that of straight line running (12%). This may have been in part due to the presence of a technology bias, since Meyer *et al.* (2015) had found that measurement bias was found to increase with higher loadings; that is, with

[42] Elite and sub-elite was defined as anyone "*who trains regularly with a coach and has a specific training/competition aim"* (Raper *et al.*, 2018).
[43] Defined as one or more events per week.
[44] Defined as less than three hours of weekly exercise outside regular school activities.

higher loadings, the degree of overestimation of the accelerometers against the force plate increased. These errors and movement-varying measurements surely present a case for the inclusion of multiple movements within any trial development, since any device developed must be equipped to compensate for the wide range of movements that can be expected in any situation.

Impairment

However, physical differences between participants are not only limited to the size, mass, or strength of a person, but also extends to their physical ability; technique is influenced not only by skill and prior training, but also by impairment. In a comparison of healthy patients with those impaired by multiple-sclerosis, Alaqtash *et al.* (2011) established a reference rule-base from unimpaired subjects, from which to compare the gait force and acceleration to those with MS.[45] The fuzzy-algorithm comparison identified distinctions in gait waveforms between patient sets. For example, the contact force of MS patients was flat with a single peak, with patients having a significantly longer stance phase.

There was only a moderate similarity within the loading response gait phase between patient sets, with force similarities of 0.634 (Y-axis) and 0.659 (Z-axis). Grades of similarity between swing phases were particularly low, with an average phase similarity of 0.179 (initial swing), 0.008 (mid-swing), and 0.289 (terminal swing). These differences were attributed to the abnormal muscle activities within the tibialis anterior, quadriceps and gluteus medius of MS patients, further observing that *"the acceleration curves of the thigh and the hip… [demonstrated low] accelerations for MS compared to healthy subjects throughout most of the gait phases"* (Alaqtash *et al.*, 2011). There was a sharp increased acceleration at the initial contact phase of the MS gait cycle, and insufficient foot clearance during initial swing phase, which will further complicate distinctions in identifying waveform events and in using these to predict force based on a generalised model.

5.1.3. External Factors

Footwear and Landing Surfaces

Within the development of these algorithms and testing procedures, one must consider not only inter- and intra-personal differences, but also *where* each activity has been conducted. For example, with regards to outdoor sprinting, wind resistance is a crucial factor to consider,

[45] Alaqtash *et al.* (2011) did not predict force from acceleration, but only compared the gait parameters between impaired and unimpaired subjects.

especially with such conditions being conducive to fatigue (Hunter *et al.*, 2005). These fatigue-induced effects on running mechanics must be measured in external settings, rather than only the laboratory, since *"in order to get insight into the specific challenges runners face outside the laboratory in real world, measurements need to be performed outside the laboratory in a setting as specific as possible"* (Reenalda *et al.*, 2016). Although external tests may not be possible in initial development stages when force plate-based validation is necessary, this kind of trial may be completed by using pressure insoles.

Rouhani *et al.* (2014) was able to use pressure insoles for estimating gait dynamics by first calibrating their pressure insoles with laboratory force plates, and then developing a pressure distribution map based on those initial measurements. This calibrated insole pressure map was used to estimate force and torque outside the laboratory, obtaining a coefficient of multiple correlations above 0.90. If high accuracy can be obtained consistently, then technology such as this could be used to validate external accelerometer-based force predictions.

Incorporating the differences of external factors into the development of a prediction model may also be important for its reproducibility since landing surfaces and shoe stiffnesses have been found to influence landing impact dynamics. When comparing the effect of shoe compliancy on impact kinetics, Bruce *et al.* (2019) found that greater shoe compliance resulted in lower peak resultant tibial acceleration ($p = 0.005$), but that peak vertical GRF was not different between landing surfaces and shoe types ($p \geq 0.056$). However, when considering soft and stiff landing surfaces, Devita and Skelly (1992) obtained the results in Figure 14. They found that although the temporal features of the waveform were similar between surfaces, landing on a stiff surface had a 23% larger impulse than on a soft surface.

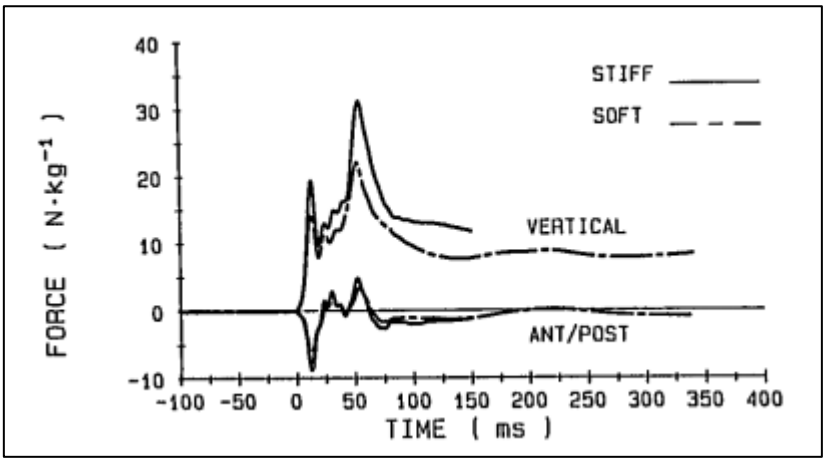

Figure 14: Comparison of ground reaction force between soft and stiff surfaces (Devita and Skelly, 1992). Reprinted with permission from Wolters Kluwer Health, Inc.

Tan *et al.* (2020) considered different kinds of footwear, foot strike patterns, step rate, and running speeds, and they found that their convolutional neural network did not generate significantly different results.[46] They did find that wearing minimalistic footwear had a higher correlation coefficient (0.95) than standard footwear (0.88), which may indicate that standard footwear absorbed more of the force upon impact. Furthermore, peak positive acceleration has been reported to reduce by between 11-20% between different shoes (Crowell and Davis, 2011). Future studies may benefit from including information on shoe compliance when predicting impact. However, it has been said recently that evidence for the effect of landing surfaces and shoe stiffness on jump landing dynamics remains limited (Bruce *et al.*, 2019), and as such, this may require further investigation.

5.2. Injuries

In the research aims, it was stated that a wearable accelerometer will be considered useful if it is able to provide information that can be used in the prevention or monitoring of injuries, fatigue, and rehabilitation. This section will, broadly speaking, seek to establish how some of the information within this thesis may contribute to an understanding of injury prevention and management in sport, and the immediate applications of the methods and results that have been presented within the literature.

[46] The results from Tan *et al.* (2020) can be seen in Chapter 3.2.3, *Table 3*. Study details: **footwear**: standard running shoes (Revolution 4, Nike) and minimalist shoes (V-RUN, Vibram Corp); **foot strike patterns**: FFS, MFS and RFS; **step rate**: baseline rate, 90% and 110%; **running speed**: $2.4ms^{-1}$ and $2.8ms^{-1}$.

5.2.1. Pathophysiological Application of Predictive Models

Having discussed some of the main factors implicating the generalisation of these relationships, this discussion will finally consider some practical applications for these models. Although the relationships between physical loading and bone health have previously been scarce (Meyer *et al.*, 2015), primary considerations for future development must include factors which inform disposition to injury, ways they can be reduced after proper analysis, and how this information can be applied to effective management and prevention of athletic overuse injuries. Clearly, this is a bigger field than can be comprehensively covered within one section of this thesis, and as such this section will aim to provide an introductory understanding to these concepts.

This investigation regarding netball becomes particularly urgent when considering the high rates of female participation with regards to the fact that *"females are exposed to greater knee abduction moments than males"* (Dan et al., 2019). But of course, impact is not only necessary for monitoring in netball. For example, the high injury rates in gymnastics have been thought to be associated with the accumulation of impact loads (Simons and Bradshaw, 2016). Nor is it limited to modelling according to gender; though the differences in body structure do result in different impact dynamics (Dan et al., 2019).

Since wearable accelerometers can providing information on dose-response patterns regarding the bone health of both adults and children (Meyer *et al.*, 2015), there is a broad population who will benefit from accurate developments following this investigation. And, further demonstrating the wide applicability of wearable device driven research, it has even been reported that *"a decrease in ankle and knee power...,"* which may be determinable from wearable accelerometers, *"results in shorter step length in the elderly;"* and that ankle joint power can be used to characterise gait deficits and develop protocols for rehabilitating walking ability (Jiang *et al.*, 2019).

However, a primary concern is that current technologies available for assessing gait pathologies are not widely accessible. For example, instrumented treadmills and motion capture technologies, though extremely useful for performing gold-standard research on pathologies and patient monitoring, are often inaccessible to the general population due to their high expense. The development of wearable sensors make these tracking abilities much more accessible (Pieper *et al.*, 2020). Uses of wearable IMUs include detecting gait phases, monitoring activities of daily living and representing and classifying gait data (Alaqtash *et al.*, 2011).

IMUs can be used to differentiate between walking, running, and jumping locomotion, and to distinguish between different intensities (Lee *et al.*, 2015). Meyer *et al.* (2015) has commented that *"accelerometers are perfectly suited to measure impact loading of bone,"* and Pieper *et al.* (2020) has stated that when using shank acceleration to study the effects of knee bracing and its significance for aiding in the rehabilitation of those with trailing limb propulsion, *"shank acceleration may effectively distinguish intrasubject variations over time, for example due to functional decline or clinical rehabilitation."* Indeed, using low cost, simple sensors may allow the identification of abnormal gait patterns such that falls can be prevented in the older population, prolonging the time with which they can retain independent mobility (Mundt *et al.*, 2020).

Load Accumulation

Using wearable devices to predict impact dose will enable an objective quantification of loading, rather than relying on subjective *ratings of perceived exertion.* The effects of ACL reconstruction, which alter a client's lower extremity mechanics, are seen weeks and years after surgery (Havens *et al.*, 2018), which makes long-term, subjective assessments consistent. This objective rate is what is of primary interest in this study, since *"the aetiology of overuse injuries appears to be related to both the impact and peak forces the limbs experience during each loading cycle"* (Udofa *et al.*, 2016). Accelerometers have previously been used in representing *player load* by measuring accumulated impact forces over time (Wundersitz *et al.*, 2013). Alternatively, Tan *et al.* (2020) considered the possibility for loading *rate* to contribute to these models. They concluded that machine-learning-based vertical average loading rate *"could enable runners to more accurately assess impact loading rates and potentially provide insights into running-related injury risk and prevention"* (Tan et al., 2020).

Clearly, the development of any objective analysis for injury risk will require a consistently accurate risk function that uses kinetics to predict overuse injury. Bailey *et al.* (2018), who considered the modelling of risk in light of the shorter duration high impact loading from military injuries, developed an injury risk function based on the results of axial loading to post-mortem human legs. In their conclusions, they estimated that there was *"50% risk of injury for a leg exposed to 13 Ns of impulse at peak force and 8.07 kN of force for force durations less than and greater than half the natural period of the leg, respectively"* (Bailey et al., 2018).

Similar to how Bailey *et al.* (2018) quantified risk in terms of impulse, Winter (2005) has explained that *"integration of the force–time history [i.e. impulse] can be used to provide a velocity–time*

profile of the body's center of mass and so provide a basis for calculations of the products of force and velocity." Taking this backwards, if integration of the *acceleration* waveform could be used to estimate impulse (the integration of the force waveform), then perhaps a risk factor could be given based on integration of acceleration alone, without needing to focus on event-to-event predictive force modelling. If developed for the purpose of predicting overuse injury risk, these functions will enable a translation of repetitive axial loading into a demonstration of injury prediction.

The kind of short term risk analysis that Bailey *et al.* (2018) has presented may even be indicative of the short-term, high impacts experienced during athletic sports. However, further research into objective quantities of player load must first be made more widely accessible, since when lacking this, previous research has turned to acceleration-based arbitrary loading units to measure player load (Bailey *et al.*, 2017),[47] which do not necessarily translate into known quantities.

This understanding of player loading may not be limited only to injury prediction and prevention but may also extend to using this technology for protective purposes (Gabbett and Ullah, 2012). Indeed, *"although excessive training loads may increase intrinsic injury risk, insufficient loads may achieve the same outcome, with a certain level of load (in-between an underload and overload) likely to be protective for injury"* (Colby et al., 2014). Providing players with a minimum loading dose is even *necessary* for bone and musculoskeletal tissue health, but must be carefully administered, lest higher loads lead to overuse injuries (Udofa *et al.*, 2016).

This research is particularly important when considering team sports, where this training *"reflects a balance between the minimum training load required to elicit an improvement in fitness and the maximum training load tolerable before sustaining marked increases in injury rates"* (Gabbett and Ullah, 2012). Although more could be said on the benefits of protective loading levels, the discussion will now briefly turn to three other pathophysiological benefits that impact modelling from wearable device-collected kinematics may provide: landing, fatigue, and limb propulsion.

Landing and Fatigue

Although Elvin *et al.* (2007) found that jump height did *not* correlate with peak acceleration or peak force, their initial proposition that jump height may be *"an important predictor of ground reaction force and overuse knee injury,"* is yet to be disproved. However, if this is so, then the

[47] Bailey *et al.* (2017) is not the same author as Bailey *et al.* (2018).

variables must be related. The idea of impact dose for injury prevention and shock attenuation without considering ground reaction forces may not be suitable, since this study seems to suggest that shock reduction does not significantly improve with elevated mechanical demands (Zhang *et al.*, 2008). In fact, landing height has been found to have no significant effect on acceleration during impact (Zhang *et al.*, 2008), which may justify the earlier proposition that jumping events are more difficult to estimate force from acceleration than running events are.[48] More recently, Gokeler *et al.* (2017) has demonstrated how accelerometers can be used as rehabilitative assessments before returning to activities post ACL reconstruction by assessing jump height and power.

Coventry *et al.* (2006) found that following a jumping protocol, their ten participants were fatigued, but without significant shock attenuation throughout their body, and Simons and Bradshaw (2016) summarised these effects by explaining that fatigue results in increased GRF without substantially changing the acceleration. This complicates the acceleration-force relationship by implicitly affirming that there are other factors that can lead to increased forces. However, Reenalda *et al.* (2016) has reported that fatigue can *increase* peak acceleration, and that *"an increase in peak acceleration might indicate higher loading rates, a reduction in shock absorption quality and a higher impact on the body."* They further explained that changes in running technique over long periods of physical activity may not necessarily be due to fatigue, but may rather be due to the body adapting its technique to cope with the high impact stresses on the body (Reenalda *et al.*, 2016).

This is consistent with Coventry *et al.* (2006), who has also explained that the body can maintain shock absorption over longer periods of physical exercise by altering its kinematics. This research seems to indicate that although force, acceleration, and fatigue are interrelated, fatigue may not be the best indicator of risk, since bodily changes in response to fatigue are apparently not consistent. However, in netball matches, Best (2017) found a significant association between match *quarter* and injury occurrence ($p = 0.019$), with peak incidence occurring in the third quarter, where it is expected that fatigue would be intensifying. This seems to be a necessary area of future research.

[48] Chapter 5.1.1, *Differences by Movement.*

Limb Propulsion

This relationship could also be used for monitoring and predicting the pathologies of trailing limb propulsion. Pieper *et al.* (2020) tracked the propulsive force output of healthy participants before and after inhibiting their movement with a leg brace by diminishing the right limb propulsion of their participants by simulating a leg impairment similar to that following stroke. Although they found that the unilateral leg-brace impairment did not replicate the neuromuscular limitations present following stroke, they found that the knee brace caused a *systematic* and *significant* reduction in limb propulsion: they observed a reduction of the *very large* correlations in the uninhibited leg ($R^2 = 0.77$) to *very small* correlations in the inhibited leg ($R^2 = 0.31$). This research indicates that propulsive inhibitions could be detectable through accurate gait propulsion and loading predictions. Such propulsive distinctions have also been trialled by Browne and Franz (2019), who found that one could monitor the modulation of trailing limb propulsion by tracking the angular velocities about the ankle.

The technology could be used to monitor technique, looking in advance for signs of oncoming injury. Lee *et al.* (2015) has found that acceleration and angular velocity can contribute to distinguishing between intensity levels, and in particular that angular velocity *"can be used to distinguish between locomotion modes at the same intensity level."* Although angular velocity is not dependent on force, this does demonstrate that wearable accelerometers are able to provide information on gait characteristics for the purpose of pathological monitoring. More directly, Dan *et al.* (2019) has proposed that using acceleration-predicted ground reaction force, can indeed enable devices to screen for asymmetrical gait differences between individuals. Of course, propulsive behaviours are only one aspect of understanding technique modulation post-injury, but it can be seen that there is potential for broad application of this kind of technology by monitoring parameters associated with gait impairments.

Chapter 6. Future Research Areas

As recommended within the literature.

Research Aim #5

Determine information on the running of a trial such that new data can be collected, and a relationship derived, based on the recommendations and performance of these studies.

6.1. Research Implications

Having presented the previous works within the literature, a summary of the future research areas that were recommended in the qualified articles will be given. These recommendations will be used to design a validation trial, wherein the literature-based conclusions and the data of a previous trial will be revaluated in light of the strategies discussed. The summaries within this chapter are only the primary areas for future research that were raised in the qualified articles and are not exhaustive for areas of literature-warranted future research. It may be noted that some of the raised research areas have already been briefly covered within the review; these are included for the purpose of relaying the primary areas that were raised within the articles as future needs.

6.1.1. Recommendations

Future research should determine optimal placement sites for wearable accelerometers, accounting for the reasons of each and considering strengths of using information from multiple locations (Havens *et al.*, 2018, Pieper *et al.*, 2020, Tan *et al.*, 2020, Tran *et al.*, 2012, Wundersitz *et al.*, 2013). It should aim to understand the degree to which movement artefact and soft tissue attenuation at each position affect results (Callaghan *et al.*, 2018, Havens *et al.*, 2018). Attachment methods should be designed for securing against this movement artefact between people, limiting device vibration and movement (Tran *et al.*, 2012, Wundersitz *et al.*, 2013). Interpersonal differences in landing and movement technique should be accounted for, especially with regards to how technique may change over time (Simons and Bradshaw, 2016). This may involve further understanding the contribution of joint angles to peak forces, accelerations, and impact attenuation (Elvin *et al.*, 2007, Simons and Bradshaw, 2016, Tran *et al.*, 2012).

Signals may need to be corrected for gravity and the effects of contact angle when calculating the vertical force componentry (Hennig and Lafortune, 1991). Naturally, this may contribute towards

the need for modelling the shock attenuation of lower limb kinematics and how it affects force and power (Lafortune et al., 1995). This may involve including considerations for landing surfaces (Simons and Bradshaw, 2016) and footwear (Tan et al., 2020).

Further research is required to confirm logarithmic force-acceleration model correlations (Charry et al., 2013). All models should be validated for accurate prediction and for activities of daily living, particularly those which have been designed with machine learning (Guo *et al.*, 2017, Lafortune *et al.*, 1995). Force approximation models should be mapped to specific gait events, and specifically should determine whether the maximum projection of the relationship occurs at mid-stance, when the leg is geometrically perpendicular to the ground (Charry et al., 2013). The development of these models that relate GRF with PRA should include factoring in the effects of body weight, and may mean developing personalised algorithms (Raper *et al.*, 2018, Simons and Bradshaw, 2016).

This research will need to confirm whether vertical tibial acceleration is indeed the best surrogate for load rate in runners (Davis et al., 2018), and contribute to further understanding the value of segment acceleration in the athletic movements of a wider variety of sports, including for pace bowling performance (Callaghan *et al.*, 2018, Elvin *et al.*, 2007) and for machine learning developments (Tan et al., 2020). Running load impairment predictors should be identified for application with knee joint injuries and in rehabilitation protocols like ACL reconstruction (Elvin *et al.*, 2007, Havens *et al.*, 2018). These predictors should consider a method of determining lower extremity loads in pre- and post-intervention programs (Raper et al., 2018). Especially regarding monitoring to pre-injury load levels, consideration should be made for whether prediction models can be used as relative measurements of load (Raper et al., 2018).

Future research may include the development of technology that identifies gait events outside of the laboratory (Pieper et al., 2020), with models that simultaneously estimate average, instantaneous and peak impact load rates (Tan et al., 2020). This software should be further applied to wider sporting applications and for regular consumer activities, with provisions for determining leap ability and explosive power (Penghai et al., 2014). The necessity for device calibration must be established, and additional technologies such as motion capture analysis should be used for measuring and validating predicted kinematics (Callaghan *et al.*, 2018, Wundersitz *et al.*, 2013). Devices should be made so as not to interfere with body movement (Hennig and Lafortune, 1991).

Future device development should use triaxial accelerometers as opposed to a single axial so that multiaxial correlations can be made (Elvin et al., 2007). Dynamic ranges should be selected such that gravitational accelerations during movement do not extend the limitations of the device (Meyer et al., 2015). Methods for synchronising motion capture data with device sensors may need to be considered if additional validation technologies will be considered (Havens et al., 2018). Frequency analysis should be performed by spectral and wavelet analysis so that high frequency signal components can be detected and accounted for, especially with regards to eliminating noise whist retaining signals and in frequency-dependent waveform prediction models (Lafortune *et al.*, 1995, Wundersitz *et al.*, 2013).

These acceleration frequency components should also be considered for how they differ between locations like the upper back (Simons and Bradshaw, 2016). Low frequency studies should also be performed: it needs to be determined whether acceleration cut off frequencies between 20 to 50 Hz are more effective than at 20 Hz (Simons and Bradshaw, 2016). Furthermore, the conclusion needs to be validated that peak resultant acceleration *filtering which maximises* correlations is more important than identifying direct force-acceleration agreements (Simons and Bradshaw, 2016). It must also be determined whether a regression model can negate internal device biases (Meyer et al., 2015), and validation is required for any device that claims to make accurate predictions (Raper et al., 2018).

Finally, regarding trial design for the testing of these models, future trials should include a wider variety of sport-related movements than only jumping and landing, including testing for several running speed variations and their validity during change of direction tasks (Charry *et al.*, 2013, Raper *et al.*, 2018, Tran *et al.*, 2012). Trials should be designed for more participants (Charry *et al.*, 2013, Tan *et al.*, 2020), and the results of previous trials should be extrapolated to larger populations with elite athletes (Elvin et al., 2007). Trials that have developed models for participants with previous impairments should be tested for generalisability to non-injured populations (Havens et al., 2018). Trials should also consider varied age groups and participants with *pathological* gaits, rather than only young, healthy volunteers (Guo *et al.*, 2017, Pieper *et al.*, 2020). Trials should make considerations for broader populations and with equal gender distributions (Meyer et al., 2015). The clinical utilisation of devices like ViPerform should be designed to measure average movements across multiple strides, rather than calculating points for individual strides to obtain higher accuracy (Raper et al., 2018).

6.1.2. Investigation Proposal

Since there remains a need for determining these acceleration-force relationships, it is more expedient to re-evaluate data from two years ago in light of the presented algorithms, rather than designing a new investigation. The investigation to follow will investigate several of the areas recommended above, and it will primarily focus on considering device location. It will consider acceleration proxies for peak forces, load rates, and impulse, simultaneously estimating these variables. Relevant frequencies will be determined based on a power analysis, and noise will be eliminated where possible. The effect of using different filters on correlation accuracy will also be considered. It will consider linear, logarithmic, and machine learning proxy models. It will consider body weight and personalised algorithms, and model generalisation between participants. A comprehensive method will be presented in Chapter 7.

Chapter 7. Investigation

7.1. Investigation Outline

Corbo (2018) began this project by undertaking a preliminary trial to consider the initial validity of the acceleration-force relationship. Participants performed repetitions of up to nine different activities to simulate the kinds of movements experienced in a netball match. The highest correlations obtained using linear correlations were $R^2 = 0.64$, between the integration of vertical force and axial acceleration (Corbo, 2018). In this chapter, the data that was collected in this trial will be re-evaluated in light of the findings gained from the literature to determine whether higher correlations can be obtained.

7.1.1. Background

In the previous study, four participants were instructed to complete nine sets of activities akin to the movements performed in netball. The instructions that were given to participants have been summarised in Table 12. In total, there were 111 individual movements completed by the four participants, but participants did not necessarily complete the same number of repetitions of each movement. In some movements, both legs of a participant may have been in contact with the force plates, so where possible, data from both legs was recorded. Across both legs across the 111 trials, there were 135 valid recordings.

Table 12: Instructions given to participants for completion within the study.

Activity	Instruction
Walk	From a start line, walk towards and over the force plates.
Jog	From a start line, run with *mild* effort over the force plates.
Run	From a start line, run with *medium* effort over the force plates.
Sprint	From a start line, run with *maximal* effort over the force plates.
Cut	Sprint towards the force plates. Strike a plate with the dominant foot, then change running direction 45°, following through on the contralateral foot.
Step-Down	Passively step down from a platform of x mm height.
Jump	Begin by standing with both feet on a single force plate. Using a bilateral arm swing, jump from a standing position with maximum effort.
Run-On	Receive a thrown ball whilst running towards the force plates. Jump into the catch, landing with the contralateral leg on a force plate. Continue running past the force plates.
Two-Foot Land	Sprint towards the force plates. Jump off of one foot and land on two feet, landing with at least one foot on the force plates.

A trial was deemed valid if an entire foot landed within a force plate. The trials had been previously visually sighted on *VICON* to confirm to confirm validity. If a foot landed *across* multiple force plates, the total movement kinetic was derived by summing the output of each relevant

plate. To confirm this validity, trials were further sighted by comparing the acceleration and force waveform: trials were valid if the recorded movement was distinguishable from times of non-contact. Trials were considered invalid if they did not contain a complete waveform, or where there was no clear distinguishable movement. All trials that were marked invalid were excluded from this analysis. Valid trials are summarised in Table 13.

Table 13: Valid trials, according to movement type, participant, foot, and force plate.

	Participant 1		**Participant 2**		**Participant 3**		**Participant 4**	
	$m_1 = 63.2291\ kg$		$m_2 = 72.6537\ kg$		$m_3 = 73.9738\ kg$		$m_4 = 82.0994\ kg$	
	Female		Male		Female		Male	
Movement	**Foot**	**Force Plate**	**Foot**	**Force Plate**	**Foot**	**Force Plate**	**Foot**	**Force Plate**
Walk	R	4	R	3	R	3	L	1
	L	1	R	3	L, R	2, 3	L	1
			R	3	R	4		
Jog	L	2	R	3 & 4	R	4	R	1 & 2
	L, R	2, 3	R	3	L	1 & 2	L	1
	L	1 & 2	R	3	L	2	L	1 & 2
Run	L	2	L	1 & 2	L	1	L	1 & 2
	L	2	L	2	L	1	L	1 & 2
			L	2			L	1 & 2
Sprint	L	2	L	1 & 2	L	1 & 2	L	2
	L	2	L	1 & 2	L	1 & 2	L	2
			L	1 & 2	L	1	L	2
Cut	R	3	R	3	R	3	L	2
	R	3	R	3	R	3	L	2
	R	3 & 4	R	3	R	3		
440mm Step-Down	R, L	2, 1			R	3		
	R, L	2, 1			R	3		
	R, L	2, 1			R	3		
450mm Step-Down							R	3
							R	3
							R	3
460mm Step-Down			L	3				
			L	3				
			L	3				
600mm Step-Down							R	3
							R	3
							R	3
660mm Step-Down	R, L	2, 1	L	3				
	R, L	2, 1	L	3				
	R, L	2, 1	L	3				
Jump	L, R	1, 2	L, R	1, 2	L, R	1, 2	R	4
	L, R	1, 2	L	1 & 3	L, R	1, 2	R	4
			L, R	1, 2	L, R	1, 2	R	4
Run-On	R	4 & 3	L	2	R	4	L, R	2, 3
	R	4	L	2	R	4	L, R	2, 3
					R	4	L, R	2, 3

					R	4		
Two-Foot Land	L, R	1 & 2, 4	R	3 & 4	L, R	1 & 2, 3 & 4	L	1
	R, L	4, 2 & 1	R	4	R	3	L	1
	R, L	4, 2 & 1	L, R	1 & 2, 4	R	4	L	1
			L, R	2, 4	R	3 & 4		

Data Capture

In the trial, four *AMTI* OR6-7 Multi Component force plates measuring 464 mm (width) by 508 mm (length) were sampled at 2000 Hz, with axis orientations as illustrated in Figure 15. These were used in conjunction with *VICON* motion capture markers. The arrangement of the force plates and their utilisation with *VICON* in determining the validity of trials is shown below in Figure 15.

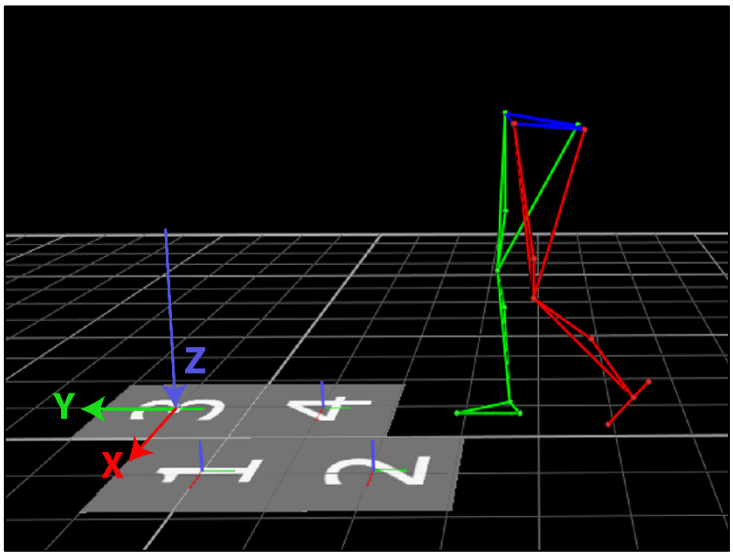

Figure 15: Force plate and motion capture utilisation.

Six *TRIGNO*^{TM} Wireless System PM-W01 EMG devices were utilised, inside each of which was an integrated triaxial accelerometer. These sensors were attached to the anterior medial thigh, the anterior medial shank, and the ankle lateral malleolus.[49] The accelerometers had a software-selectable dynamic range of ± 1.5 g, ± 4 g, ± 6 g, and ± 9 g. The device in this investigation recorded with a dynamic range of ± 9 g. The device had a DC bandwidth of 50 ± 5 Hz, 20 dB/sec, and a sampling rate of 148.1 Hz. The six devices, and their attachment positions and axis orientations, are shown in Figure 16.

[49] Participant 1 had an additional four sensors placed on the medial ankle and heel of each leg. However, for consistency with the other participants, these have been excluded from further analysis.

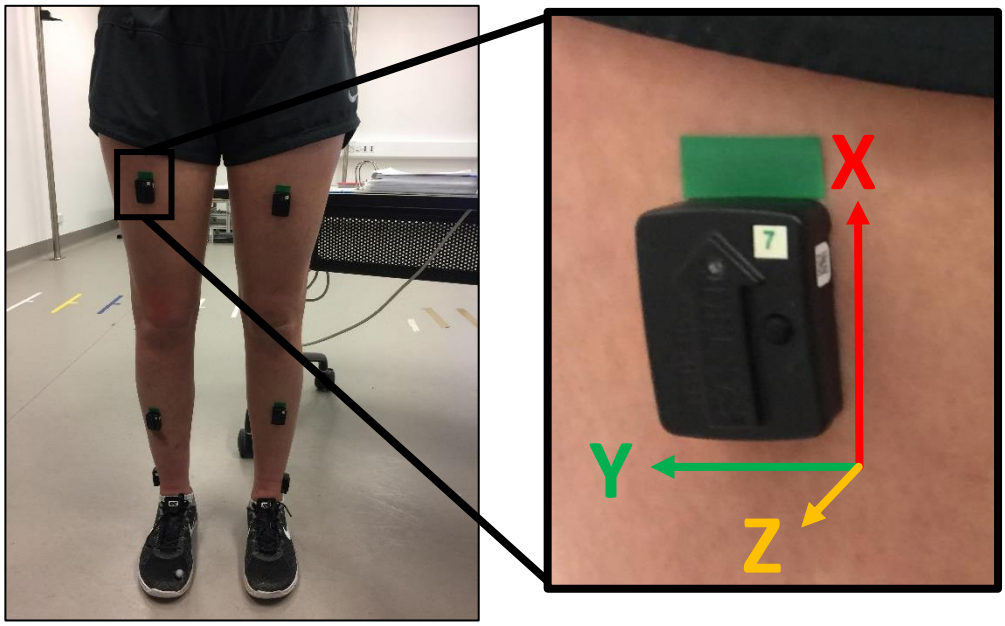

Figure 16: The location and orientation of the six trial devices.

Due to their contralateral placement, the Y- and Z-axis of the devices at the ankle are in opposite directions. To rectify this, a global Y- and Z-axis was defined according to the depiction in Figure 16.

- the *positive* Z-axis of the right ankle accorded with the global *positive* Y-axis, and *negative* Y with the global *positive* Z
- the *negative* Z-axis of the left ankle accorded with the global *positive* Y-axis, and the *positive* Y-axis with the global *positive* Z-axis.

All future references to ankle device axes regard the *global* axes. The positive X-axis of every device shared the same positive global axis and needed no rectification. Within this thesis, *axial* acceleration refers to the acceleration measured along the X-axis of each device.

7.1.2. Investigation Method

This investigation will aim to further explore the research aims in light of the reviewed literature. As the available data did not include pathophysiological information on the participants, **Research Aim 4** (*useful for injury prevention and monitoring*) is untestable within this data analysis, and so will remain literature based. So also, **Research Aim 3.C** (*generalisable according to external conditions*), is untestable within this dataset since the trial was performed within a single, contained environment. **Research Aim 5** (*information on trial design*) is only literature based. As such, this analysis will investigate **Research Aims 1-3**, which are on the sufficiency of data from a wearable device to model a subject- and movement-generalised relationship. The analysis will be

undertaken in two phases, both of which have been designed with these aims in mind. The analysis was completed in *MATLAB R2020a*.

Phase 1: Linear Modelling

Event-to-event correlations will be conducted between the waveforms of each trial, across all locations and participants.

Before modelling these relationships, noise filters will be applied to the raw kinematic data. Models will consider both direct linear correlations and mass-scaled linear correlations. Following this, a 20 Hz filter will furthermore be applied over the acceleration data, in accordance with the literature-based recommendations,[50] to determine the influence of frequency on the acquired waveforms. Following this, cohort-developed correlations will be validated with a leave-one-out cross-validation experiment. In this, the acceleration data of three participants will be used to develop a model that is used to predict the force of the fourth participant; and vice versa, for each participant.

Phase 2: Non-Linear Modelling

Following the linear modelling of Phase 1, the data will be re-evaluated according to a logarithmic approach presented in the literature. Rather than determining a new model, the literature model will be validated with the data of each participant. The correlation coefficients (R^2) and the root mean squared errors ($RMSE$) of the logarithmic results will be compared to the linear results of Phase 1.

Finally, a non-linear timeseries machine learning model will be developed for the prediction of the entire force waveform based on the input acceleration data. The model will be trained with the data of three participants and validated with the data of the fourth; this will be completed for each leave-one-out participant combination. The results of the machine learning model will be compared with the results of the preceding logarithmic and linear investigation.

[50] Chapter 6, *Future Research Areas*.

Excluded Models

In addition to the above non-linear models, the literature also presented both a machine learning *event-to-event* model and a Fast Fourier Transform *waveform* model. These have been excluded from the investigation for the following reasons.

Event-to-Event Modelling: Machine Learning

- It was reasoned that event-to-event based machine learning was not necessary, so long as the *entire* force waveform could be predicted. If the entire waveform can be predicted, then any event *within* the waveform can simply be extracted from the prediction, making individual predictions unnecessary.

Waveform Modelling: Fourier Transforms

- Since Fourier prediction depends heavily upon waveform characteristics in the frequency domain, extended prediction requires cyclic activity, which was not available for this investigation.[51] Similar activities could be stitched together, but this would not enable a validation of the literature-presented algorithm; it would only approximate the data; and would not represent truly cyclic behaviour.
- Furthermore, this prediction method was only used by one study; and this study sought to obtain *acceleration from force*; not force from acceleration. Although this could be explored here, it is divergent from the primary aim of this investigation, and therefore will not be pursued.

7.1.3. Hypothesis

The following hypotheses are based on the research aims, informed by the literature, and with regards to both Phase 1 and Phase 2. It is hypothesised that:

1. There is a *very large* relationship ($\mathrm{R}^2 = 0.7$ to 0.9) between force and acceleration at the lower limb, with the shank being optimal for developing this model.[52]
2. The shank is the most effective position for modelling this relationship.

[51] Of course, single activities can be effectively analysed and reconstructed via a Fast Fourier Transform, but the model for a single activity will certainly not be globally applicable; and even the variability between similar movements is significant enough to produce errors.

[52] This hypothesised statistic: a) is consistent with the most common correlations seen in the literature, and b) will be testing for one class higher than the previous findings of Corbo (2018) (who found $R^2 = 0.64$). It effectively states that that old data, with newer models, can obtain higher results.

3. Generalised models are the most effective when they incorporate subject-specific characteristics.
4. The correlations after filtering the data with a 20 Hz filter will be higher than when the data is only filtered for noise.[53]
5. Logarithmic modelling predicts force more accurately than linear modelling.
6. Machine learning modelling predicts force more accurately than logarithmic and linear modelling.

7.2. Data Preparation

Prior to the analysis, two preliminary procedures had to occur. A filter had to be designed for both the force and acceleration data to remove noise from each raw dataset. Following this, the waveform events that were to be compared had to be extracted from each trial.

7.2.1. Raw Data Filtering

The first kind of raw filtering that was introduced was 40 N force threshold, which was applied over the entire force dataset to eliminate the presence of raw fluctuation in the force plates, as shown in Figure 17. Although this fluctuation was generally around 20 N, there were times that the fluctuation oscillated to 35 N, and as such the 40 N threshold was selected.

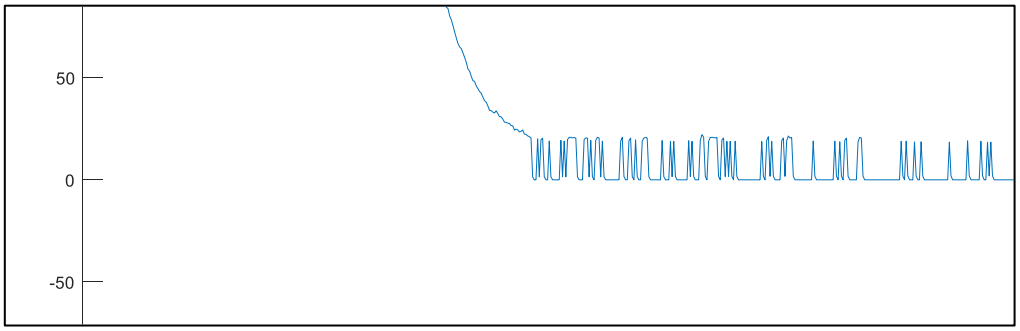

Figure 17: Force plate noise fluctuation (N).

Although a single filter may have been sufficient to remove the above noise, the introduction of a low magnitude force threshold was consistent with several articles in the literature,[54] and it was also used to define the start and end time of any particular activity; it was considered that an activity had occurred when the force spiked above 40 N.

[53] This is based on the findings of Simons and Bradshaw (2016) (Chapter 4.1.3 and 6.1.1).
[54] Chapter 4.1.3, *Data Refinement*.

Following the introduction of this threshold, it was necessary that additional filters be designed for the force and acceleration data to smooth the remaining noise. The force plates were observed to carry minor noise and since the accelerometers had been *linearly* up-sampled to 2000 Hz from 148.1 Hz, they were rugged signals (Figure 18).[55]

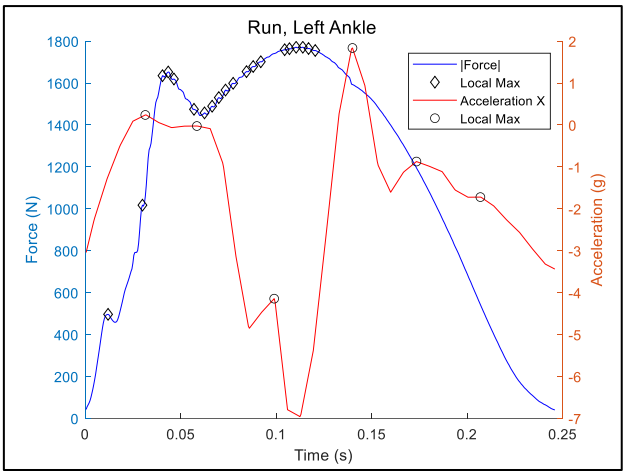

Figure 18: Raw resultant force and axial acceleration data of Participant 2. Local maximums indicate the presence of noise.

Force Filter Design

In determining an appropriate filter design, it was considered that, as per the Nyquist sampling criterion, the highest frequency obtainable in the data without aliasing would be half its sampling rate. Even though acceleration was up-sampled to it, the datasets of both force and acceleration were recorded at 2000 Hz, meaning that this frequency is 1000 Hz.

$$f_{NQ} = \frac{f_s}{2} = \frac{2000\ Hz}{2} = 1000\ Hz$$

As such, it is immediately known that the desired frequencies are all under 1000 Hz. The power spectra for both signals up to this frequency is shown in Figure 19.

[55] This filter investigation considers resultant force and axial acceleration, for these were two of the predominant signals investigated in the literature. Although the signal of each axis may be susceptible to different amounts of noise due to directional motion artefact, it will be assumed following this investigation that the filters designed are applicable to all three axes, and as such, that it is not necessary to determine further axis-specific filters.

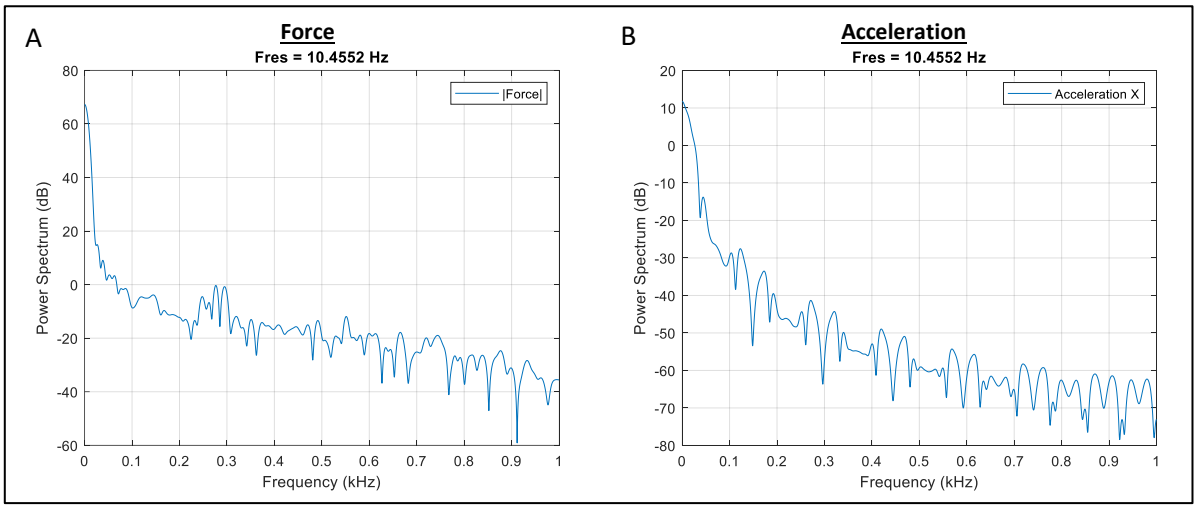

Figure 19: Raw data power spectra of (A) resultant force and (B) axial acceleration.

As seen, the primary frequencies for both signals are within the first 100 Hz, with a power range of over 50 dB. As such, it may be reasonable to immediately design a lowpass filter to accommodate this range alone. However, before accomplishing this, it is helpful to confirm the location of the noise that was present in Figure 18. In the force data, there were approximately 8.5 high frequency oscillations within $t = 0.05$ to $t = 0.8$ seconds, suggesting an oscillation frequency of $286Hz$. This is shown in Figure 20.

$$\text{Oscillation interval: } \Delta \approx \frac{0.03s}{8.5} = 0.0035s$$

$$\text{Oscillation frequency: } f_0 = \frac{1}{\Delta} = \frac{1}{0.0035s} = 286Hz$$

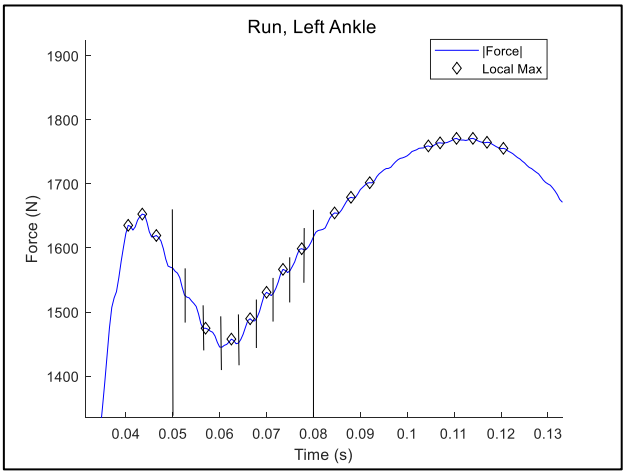

Figure 20: An analysis of noise in the raw resultant force data of a trial from Participant 2.

On inspection of the power spectrum in Figure 19, this high-frequency, high-power component is clearly identified to occur at either 276.7 Hz or 295.0 Hz (Figure 21). Likely, both have contributed

to the observed noise, and as such, any lowpass filter with a sharp attenuation at a pole before this would adequately remove both frequencies. However, when considering the maximum power in the spectrum, it is identified that all frequencies greater that approximately 90 Hz are at least 70 dB less than the frequency of maximum power in this signal. As such, the cut-off frequency was selected to be 100 Hz, which was consistent with Raper *et al.* (2018) and Simons and Bradshaw (2016).[56]

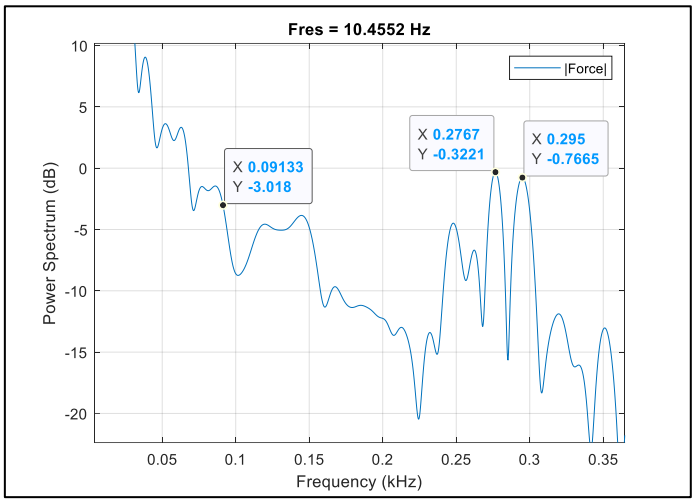

Figure 21: Scaled-up power spectrum of Force M.

Acceleration Filter Design

However, it would not be effective to apply this same filter over the acceleration data. Since the sampling rate of the accelerometer was originally 148.1 Hz, the original minimum frequency for a non-aliasing signal would have been 74.05 Hz:

$$f_{NQ} = \frac{f_s}{2} = \frac{148.1\ Hz}{2} = 74.05\ Hz$$

Although 74.05 Hz could be taken as a much better indicator for an appropriate pole location, even this may not be suitable, for the bandwidth of the device was 50 ± 5 Hz.[57] On closer inspection of the acceleration power spectrum, it is observed that all frequencies above 52 Hz attenuate to P ≪ -19.25 dB; with the final primary frequency occurring at approximately 44 Hz (Figure 22). In light of this, the acceleration cut-off frequency was selected at 50 Hz, acknowledging that a gradual roll-off will allow the frequencies on the upper limit of the device bandwidth to still be effectual within the analysis.

[56] Chapter 2.1.5, *Qualifying Articles*.
[57] Chapter 7.1.1, *Background*.

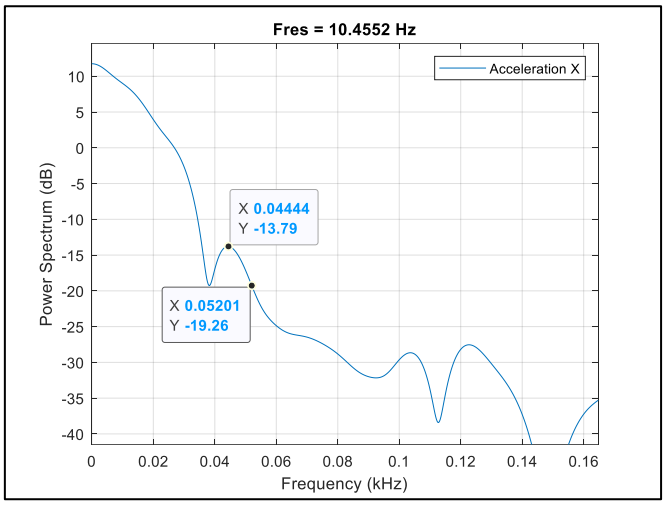

Figure 22: Scaled-up power spectrum of Acceleration X.

Filter Application

Filters were designed with poles at the selected locations. So as not to modulate frequencies below the cut-off (apart from minor attenuation), a Butterworth filter was selected as opposed to a Chebyshev or elliptical design; and it chosen over a Bessel filter for its sharper roll-off. A 4th order filter was chosen; though, similar orders may have also been suitable. The filtered spectra are shown in Figure 23. As seen, the undesired frequencies have been significantly attenuated.

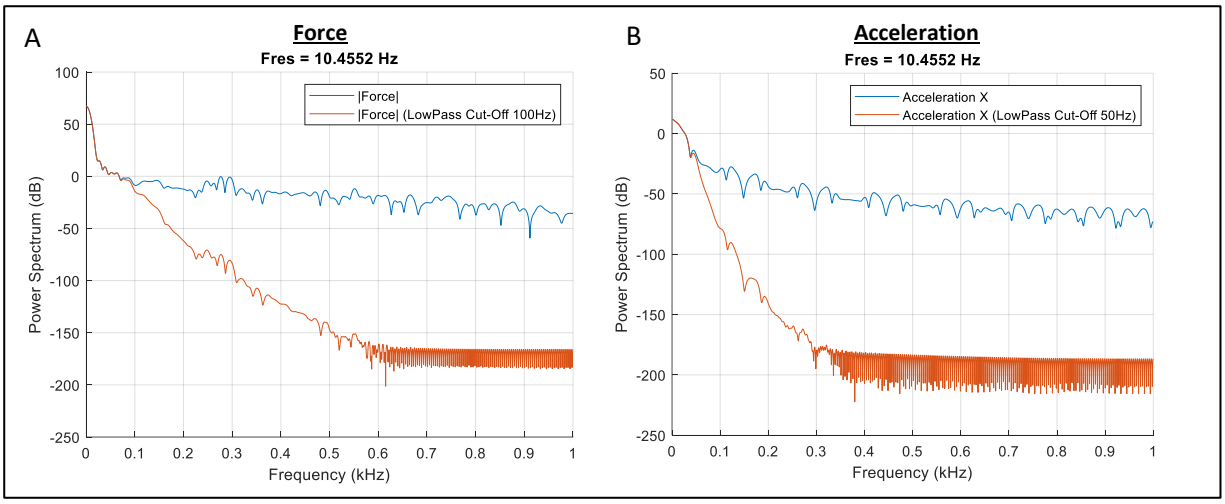

Figure 23: Power spectra pre- and post-filtering of (A) resultant force and (B) axial acceleration.

The result of this application is shown in Figure 24, where each signal has been appropriately smoothed, without having lost its main signal characteristics. The *absolute* peak reduction of each

curve here was -0.09% for force[58] and $+0.21\%$ for acceleration.[59] The assumption was made that the noise present within the resultant force and axial acceleration signals were consistent in each axis of both variables, and as such these filters were applied over the entire dataset: a 100 Hz filter was applied to each force axis, and a 50 Hz filter was applied to each acceleration axis.[60]

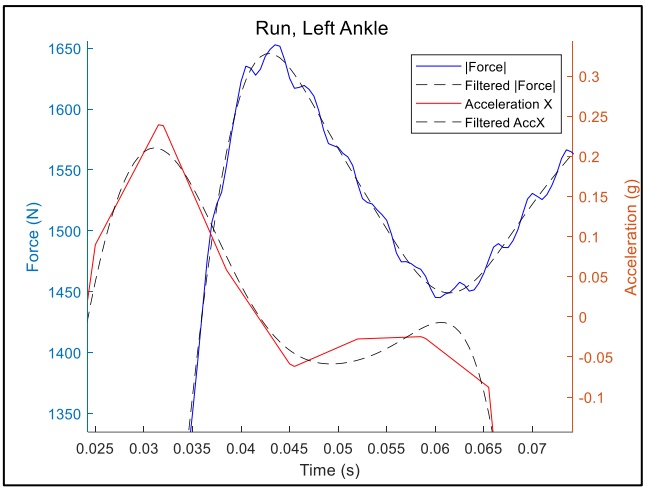

Figure 24: Force and acceleration before and after filtering (scaled).

7.2.2. Variable Isolation

The events that were selected for identification are shown in Figure 25. These events were selected for analysis primarily based on the findings of the literature; and the analysis was further extended to consider the peak events in the data of all three acceleration axes. In addition to these events, the integrals of the resultant and vertical force and acceleration waveforms were also calculated. These are shown in Figure 26.

[58] $\text{Peak }|\text{Force}|\text{ Reduction} = \frac{1769.4N - 1770.9N}{1770.9N} \times 100 = -0.09\%$ (i.e. before filtering $= 1770.9N$; after filtering $= 1769.4N$).

[59] $\text{Peak }|\text{Acc X}|\text{ Reduction} = \frac{6.9711g - 6.9567g}{6.9567g} \times 100 = +0.21\%$ (i.e. before filtering $= -6.9567g$; after filtering $= -6.9711g$).

[60] It is not expected that the difference in peak magnitude here will be equivalent between every trial, nor at every point within the signal. However, it is assumed that this calculation is an acceptable and indicative error for the variables which will be investigated, and as such that these filters may be appropriated to the entire dataset.

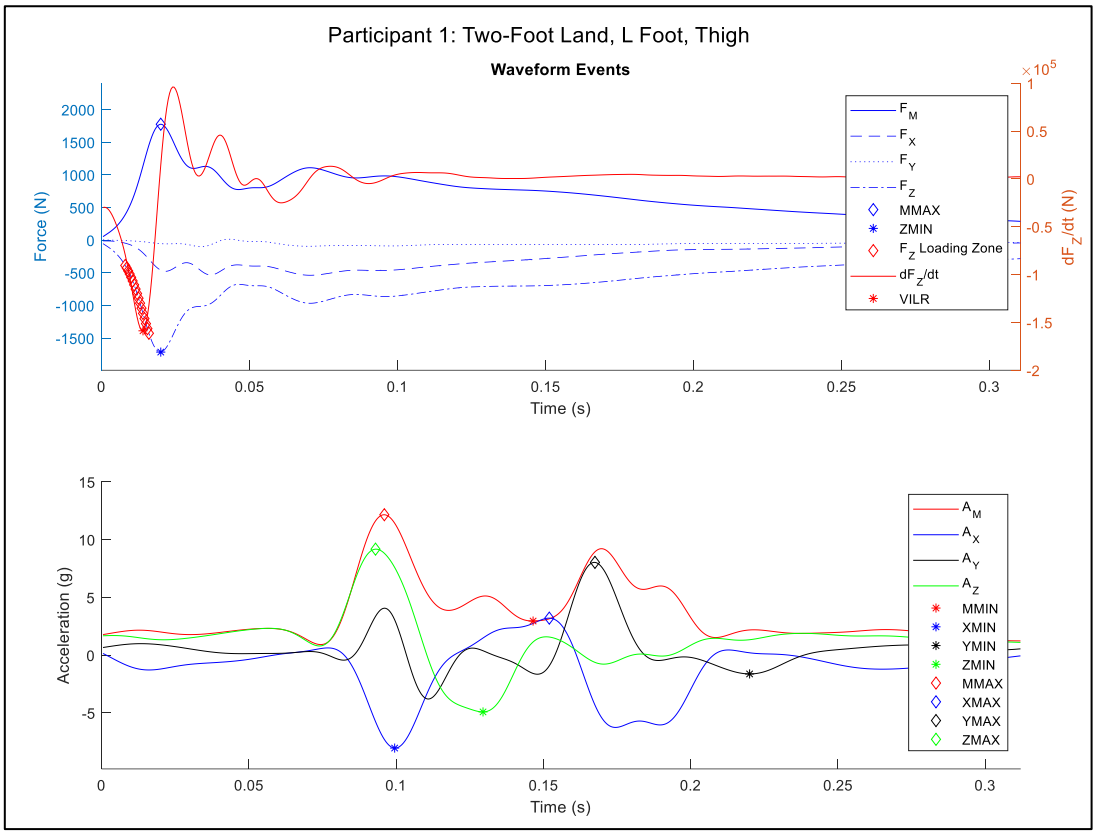

Figure 25: The force and acceleration events identified for analysis.

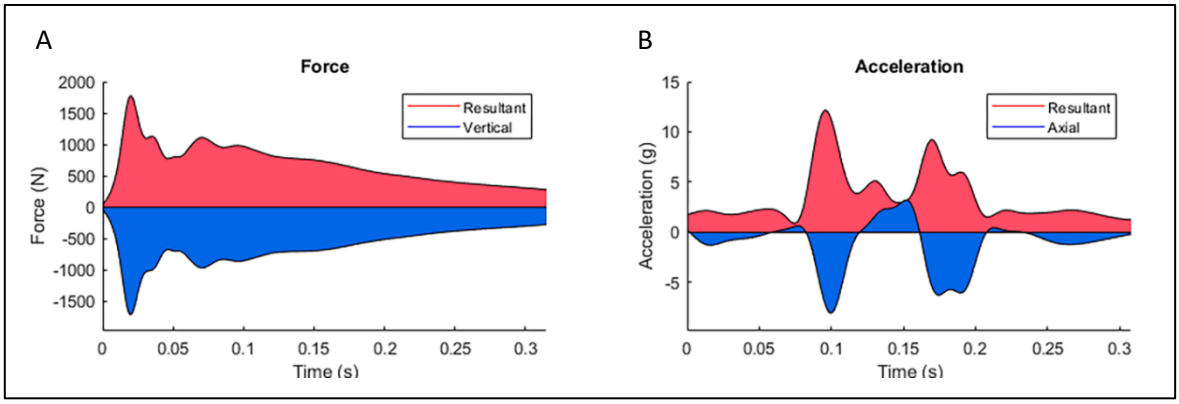

Figure 26: The integrals (the area under the curves) of resultant and vertical (A) force and (B) acceleration.

The force and acceleration variables identified in these figures are further defined in Table 14 and Table 15.

Table 14: Force variables and events considered in this investigation.

Force Variables and Events	
Variable/Event	**Explanation**
$\boldsymbol{F_M}$	Resultant Force - i.e. Magnitude - $F_M = \sqrt{F_X^2 + F_Y^2 + F_Z^2}$
$\boldsymbol{F_X, F_Y, F_Z}$	Uniaxial force plate data - F_Z is equivalent to vertical ground reaction force (vGRF)
MMAX	Peak Resultant Force
ZMIN	Peak Vertical Force - Since F_Z is directed towards the ground, this is always negative
$\boldsymbol{F_Z}$ **Loading Zone**	Vertical Force Loading Zone - The zone between 20-80% of the first F_Z local maximum - Specified as above 100 N to account for initial non-event oscillation.
$\boldsymbol{dF_Z/dt}$	Vertical Force Loading Rate - Derivative of F_Z
VALR	Vertical Average Loading Rate - The *average* slope of the F_Z Loading Zone.
VILR	Vertical Instantaneous Loading Rate - The *peak* slope of the F_Z Loading Zone.
MINTEG, ZINTEG	The integrals of the resultant and vertical waveforms.

Table 15: Acceleration variables and events considered in this investigation.

Acceleration Variables and Events	
Variable/Event	**Explanation**
$\boldsymbol{A_M}$	Resultant Acceleration - i.e. Magnitude - $A_M = \sqrt{A_X^2 + A_Y^2 + A_Z^2}$
$\boldsymbol{A_X, A_Y, A_Z}$	Uniaxial acceleration data - A_X is equivalent to axial acceleration
MMAX	Peak Resultant Acceleration - The global maximum of A_M
XMIN	Peak Axial Acceleration - The global minimum of A_X - Since the first peak is at heel-strike, A_X is directed towards the ground and this is always negative
YMAX, ZMAX	Global maximum A_Y, A_Z
XMAX	The *maximum* value within the 100 ms after XMIN.
MMIN, YMIN, ZMIN	The *minimum* value within the 100 ms after MMAX, YMAX, ZMAX.
MINTEG, XINTEG	The integrals of the resultant and vertical waveforms.
MHEIGHT, XHEIGHT YHEIGHT, ZHEIGHT	*Not shown in figure.* The peak-to-peak height of the maximum and minimum waveform events. - $H_M = abs(\mathrm{MMAX} - \mathrm{MMIN})$ etc.

7.3. Phase 1: Linear Modelling

An event-to-event investigation was performed with the aim of identifying whether accurate linear relationships can be defined between acceleration and force events, and whether these relationships are transferable between participants. The predictive power of linear models is considered, and a baseline for the comparison of future non-linear models is established.

7.3.1. Event-to-Event Correlations

Event Outputs

All identified force and acceleration events for each participant at each position, and for the entire cohort at each position, were linearly correlated in *MATLAB R2020a*. The correlations were colour graded according to the scale shown in Figure 27, with red indicating a *trivial* correlation and green indicating an *almost perfect* correlation.

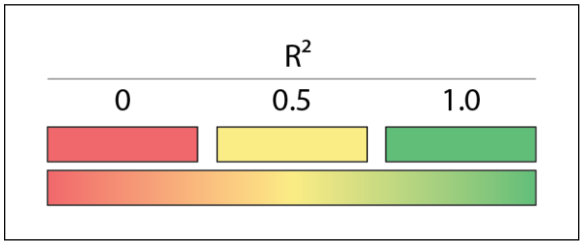

Figure 27: Colour grading of correlations.

The shank events from all trials completed by Participant 2 are shown in Table 16, where the cells that contained *trivial* or *low* correlations ($R^2 < 0.3$) have been cleared.[61] Every correlation for this participant, and for every other participant, at every location, is given in Appendix A, completely summarising the results of the event-to-event based correlation investigation.

Table 16: Event-to-Event correlations for Participant 2 at the shank, $R^2 > 0.3$.

Force	Acceleration													
P2Shank	MHEIGHT	MINTEG	MMAX	MMIN	XHEIGHT	XINTEG	XMAX	XMIN	YHEIGHT	YMAX	YMIN	ZHEIGHT	ZMAX	ZMIN
MINTEG		0.9060				0.9351								
MMAX	0.3794		0.3906		0.3957		0.3455	0.3252						0.3339
VALR	0.6079	0.3324	0.5813		0.3758		0.3646					0.6185	0.5460	0.4508
VILR	0.6258	0.3877	0.5423		0.4023		0.3645	0.3084				0.5158	0.4820	0.3367
ZINTEG		0.9029				0.9345								
ZMIN	0.3569		0.3623		0.3840		0.3332	0.3193						0.3115

On initial inspection, it may be concluded that except for the integrals, there are no waveform events that produce *very large* or *almost perfect* correlations. The highest correlations produced

[61] The printing of Table 17 for initial consideration was chosen in this way: the primary interest of this thesis is the shank, so the shank was selected; and a random number between 1 and 4 was generated in MATLAB using $\mathrm{randi}(4)$; Participant 2 was selected. This table is used as a starting point for the discussion and display of relative results.

are *large* and were obtained from the correlations of peak resultant and Z-Axis acceleration (MMAX, MHEIGHT, ZMAX, ZHEIGHT) with vertical average and instantaneous load rate (VILR and VALR). Participant 2 produced *no* correlations that were higher than moderate between peak force and peak acceleration, along any axis; and especially in the Y-axis, for which there were no correlations above $R^2 = 0.3$. If this table were taken as globally conclusive, the conclusion could be made that peak events do *not* correlate well. But these results are not consistent between participants. Whereas Participant 2 had a shank correlation between vertical instantaneous loading rate (VILR) and resultant maximum-minimum peak height (MHEIGHT) of $R^2 = 0.63$, Participant 1 had $R^2 = 0.44$ and Participant 4 had $R^2 = 0.09$. Perhaps this implies that Participant 2 was an outlier; but perhaps not. The overall participant event variance, and similarities, would seem to indicate that these results are not due to Participant 2 being an outlier. For example, whereas Participant 2 produced a *moderate* shank correlation of $R^2 = 0.39$ between resultant acceleration (MMAX) and resultant force (MMAX), Participant 4 had $R^2 = 0.65$ and Participants 1 and 3 both had $R^2 < 0.18$ (Figure 28). In this event, Participant 2 was closer to the mean than the boundary.

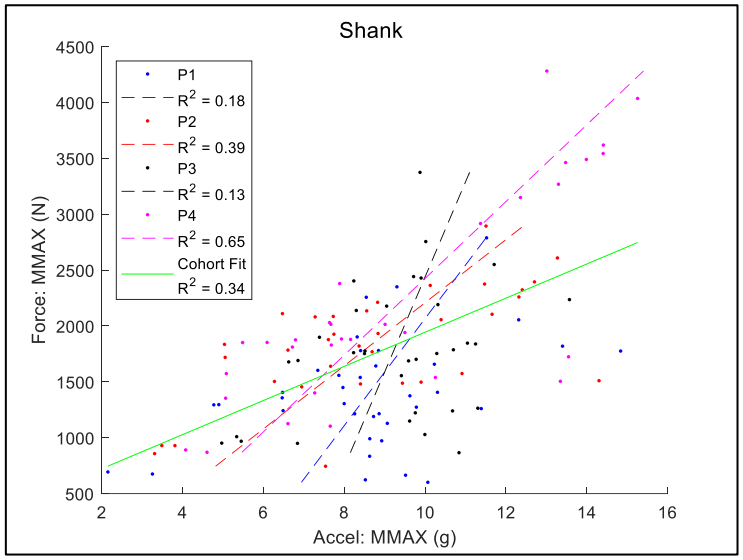

Figure 28: Correlations between resultant force and resultant acceleration at the shank.

Although weak, relationships do seem present between the waveform events. At the thigh, the resultant force and resultant acceleration (MMAX-MMAX) correlations (Figure 29) were $R^2 = 0.40$, 0.25, 0.64, and 0.74 for Participants 1-4 respectively. Yet, despite the correlation of Participant 3 being *large*, and of Participant 4 being *very large*, when the cohort data were combined, the correlation was only $R^2 = 0.43$, indicating an overall *moderate* relationship. However, the subject-specific effects of mass are yet to be considered; and will be, after the higher integral correlations are considered.

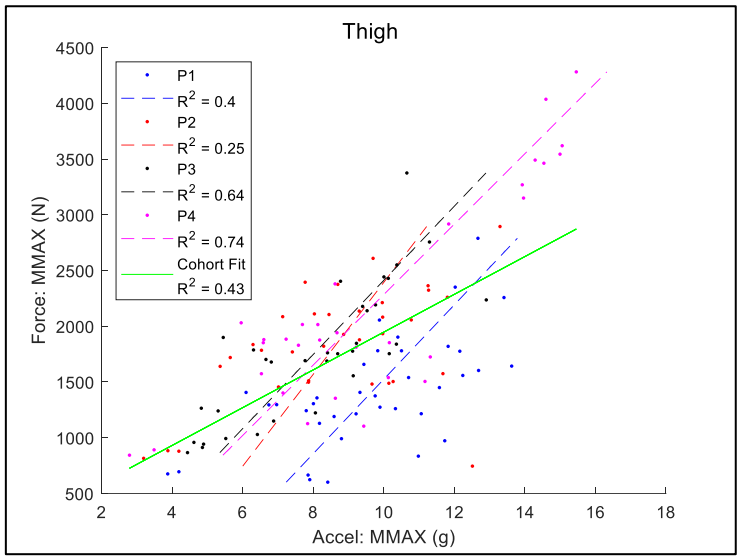

Figure 29: Correlations between resultant force and resultant acceleration at the thigh.

The previous results have shown substantial variability between the event correlation results for individual participants. In fact, there were only four events that produced at least moderate correlations ($R^2 > 0.3$) for all four participants. These *somewhat* higher correlations occurred at the *shank only* and were between peak resultant and vertical force (MMAX, ZMIN) and peak axial acceleration (XMAX, XHEIGHT). This may seem to indicate that the shank is the best location for predicting peak force from acceleration. However, even these correlations had much variability: for each of these four correlations, the minimums were between $R^2 = 0.33$ to 0.35 and the maximums between $R^2 = 0.72$ to 0.79. In other words, *no* events had a correlation of $R^2 > 0.36$ for every participant.

If these events were the only available data from which to predict impact dose, then these results would suggest that they are inadequate for long term, inter-participant reliability. To be valid for extended use, these predicted impact levels would need to be at a much high accuracy and in the order of at least 80%.[62] This would necessitate the obtaining of at least *very large* correlations in every person.

Integration

As briefly mentioned above, the correlation between force and acceleration waveform integration was *almost perfect* for Participant 2 at the shank. The correlation of the axial acceleration (XINTEG) and vertical force (ZINTEG) integral was $R^2 = 0.93$, which is *almost perfect*, as illustrated in Figure

[62] Chapter 4.1.4, *Result Validation*.

30. This high correlation was consistent with the correlations from Participant 1 ($R^2 = 0.90$) and Participant 4 ($R^2 = 0.95$) which were also *almost perfect*, but far greater than Participant 1 ($R^2 = 0.50$) which was only *moderate*.

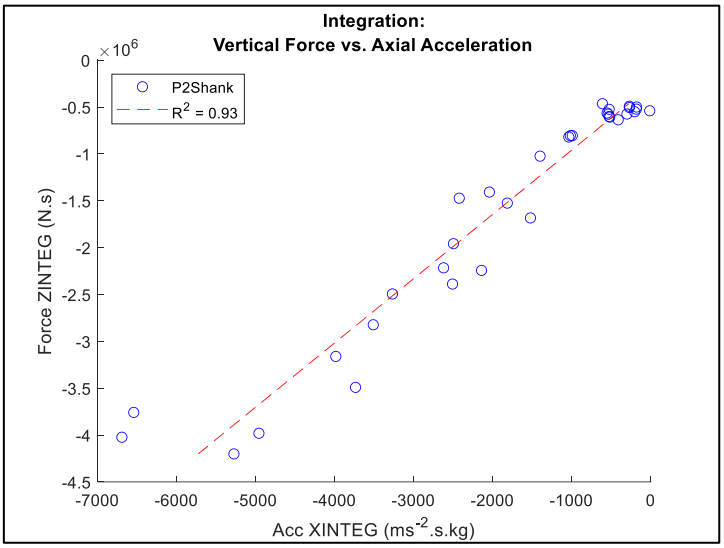

Figure 30: Integration of the vertical force and axial acceleration waveforms.

In fact, every integration correlation across participants and locations was *at least moderate*, with most correlations *very large* to *almost perfect*, as shown in Table 17. And on further consideration, it is seen that the *moderate* correlation of Participant 1 was in fact a clear outlier.

Table 17: Correlations between the integration of force and acceleration.

	Integration: Force-Acceleration					
	Thigh		Shank		Ankle	
R^2	Vertical-Axial*	Resultant-Resultant**	Vertical-Axial	Resultant-Resultant	Vertical-Axial	Resultant-Resultant
P1	0.88	0.84	0.50	0.86	0.76	0.88
P2	0.92	0.91	0.93	0.91	0.97	0.94
P3	0.93	0.83	0.90	0.91	0.98	0.98
P4	0.92	0.79	0.95	0.92	0.91	0.90
Mean	0.91	0.85	0.82	0.90	0.91	0.92
Cohort	0.78	0.83	0.89	0.90	0.95	0.93

**Vertical Force* (ZINTEG) - *Axial Acceleration* (XINTEG)
***Force Magnitude* (MINTEG) - *Acceleration Magnitude* (MINTEG)

Concluding on the participant *means* in Table 17, the optimal location for predicting the force integral is the ankle, which produces a mean resultant and axial correlation almost equivalent to, or greater than, the thigh and the shank ($p < 0.05$).[63] Considering the *entire* cohort, the ankle is also more effective than the thigh and shank ($p < 0.03$).

[63] *Almost equivalent* was defined as a difference of not more than $R^2 = 0.01$.

However, when comparing the vertical-axial participant correlations at the thigh ($R^2 = 0.88$ to 0.93) with the same *cohort* correlation ($R^2 = 0.78$), it is peculiar that the cohort regression value was so low. To understand this, the effects of participant mass must be understood.

Further two-tailed paired-sample t-Tests were performed for calculating the statistical difference between the original cohort and mass-scaled correlation differences.[64] It was hypothesised for each test that the means of the samples were the same (i.e. $H_0 = 0$). The results show that scaling by mass increases the cohort regression at every location for each *integration* correlation between force (ZINTEG, MINTEG) and acceleration (XINTEG, MINTEG):

- The difference was statistically significant ($p = 0.0027$, $MD_{R_2} = 0.02$), so it was statistically likely that mass had increased the regression coefficient.[65]
- The smallest increase was between *resultant* force and acceleration, where mass increased the regression coefficient from $R^2 = 0.90$ to 0.90 (the increase was $R^2 = 0.0031$).

The effect of mass-scaling in the cohort regression is also shown above in the extension of Table 17 below, where the inclusion of mass increases every cohort correlation; and is further illustrated in Figure 31.

Table 18: Extension of Table 17, showing the cohort mass-induced correlation differences.

	Thigh		Shank		Ankle	
R^2	Vertical-Axial	Resultant-Resultant	Vertical-Axial	Resultant-Resultant	Vertical-Axial	Resultant-Resultant
Cohort	0.78	0.83	0.89	0.90	0.95	0.93
Cohort: mass-scaled	0.83	0.85	0.90	0.90	0.96	0.95

[64] All tests were calculated using the *Microsoft Excel t-Test: Paired Two Sample for Means* (*two-tailed).*
[65] Average unscaled: $\mu_{R^2} = 0.88$; average mean-scaled: $\mu_{R^2 mass} = 0.90$; mean difference $MD_{R^2} = 0.02$.

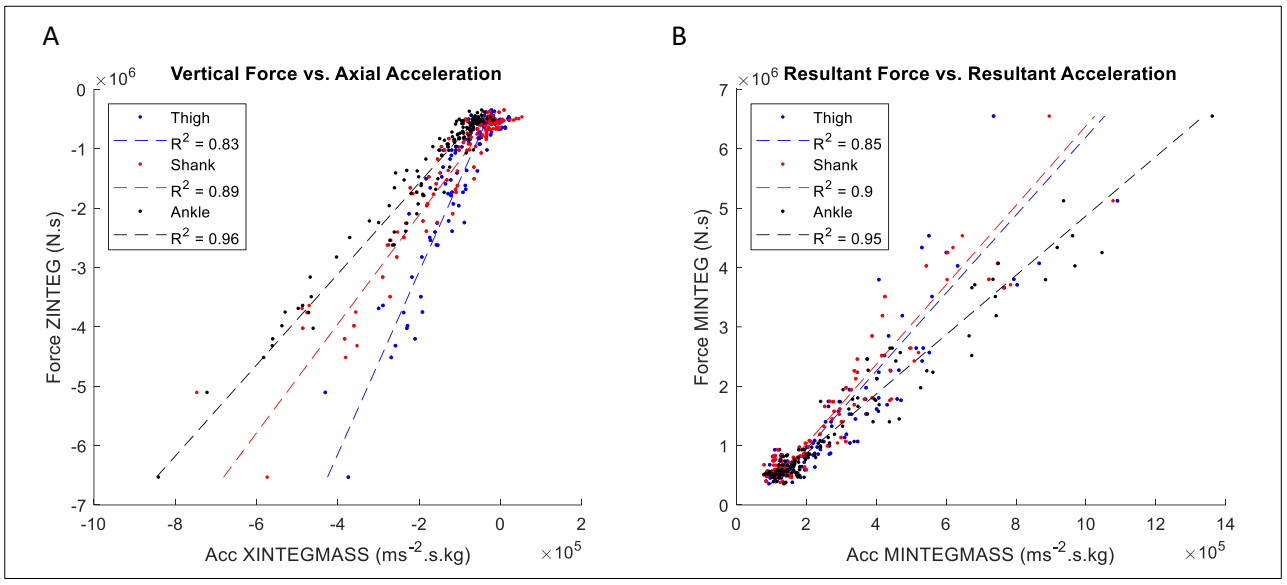

Figure 31: Mass-scaled integral correlations.
(A) Vertical force (ZINTEG) and axial acceleration (XINTEGMASS).
(B) Resultant force (MINTEG) and resultant acceleration (MINTEGMASS).

The prediction model for the integral of vertical force (ZINTEG) from mass-scaled axial acceleration (XINTEGMASS) at the ankle can then be given as:

$$F_{\text{ZINTEG}} = 5367.3 + 0.13039 \times A_{\text{XINTEGMASS}}$$

This model returns a correlation accuracy of $R^2 = 0.96$ and a root mean squared error of $RMSE = 3.01 \times 10^4\ N.s$. Equivalently, this model can furthermore be expressed in terms of vertical impulse:

$$\overrightarrow{I_V} = 5367.3 + 0.13039 \times \int \overrightarrow{A_X}\, dt \times mass$$

Cohort Mass-Scaled Event Correlations

In light of the favourable effect of mass-scaling that has been observed, event correlations were also revisited with the inclusion of mass-scaling. Following an analysis of the cohort regression results in Appendix A, the following event-to-event *cohort-combined* conclusions were made:

- Scaling by mass increased the cohort regression at every location between both peak resultant and vertical force (MMAX, ZMIN) and every peak acceleration (MMAX, XMAX, YMAX, ZMAX) ($p < 0.0001$).[66]
    - Initial range: $0.10 < R^2 < 0.54$

[66] Average unscaled: $\mu = 0.32$; average mean-scaled: $\mu_{mass} = 0.39$; mean difference $MD_{R^2} = 0.07$.

- Mass-scaled range: $0.15 < R^2 < 0.59$

- Scaling by mass increased the cohort regression at every location between both vertical loading rates (VALR, VILR) and every peak acceleration (MMAX, XMAX, YMAX, ZMAX) ($p = 0.0105$).[67]
  - Initial range: $0.05 < R^2 < 0.35$
  - Mass-scaled range: $0.07 < R^2 < 0.35$

The increase in correlations of peak resultant force (MMAX) and peak resultant acceleration (MMAX) after scaling by mass (MMAXMASS) are shown in Figure 32, where it is observed that the cohort correlations were highest at the thigh; then the shank; then the ankle.

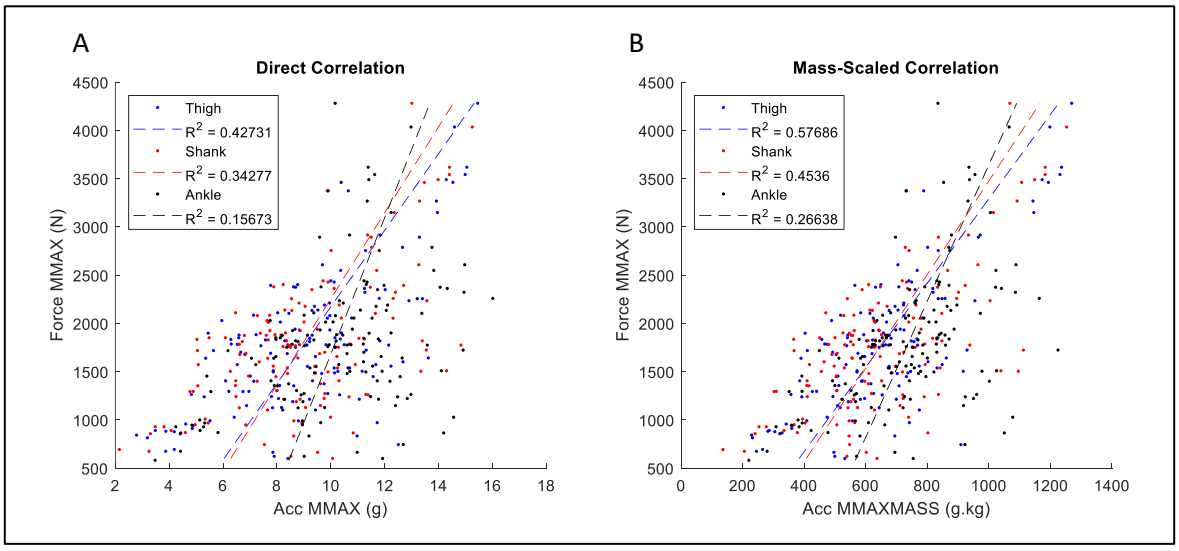

Figure 32: Correlation differences after scaling by mass for resultant force (MMAX) and resultant acceleration (MMAX). (A) Direct correlations. (B) Mass-scaled correlations.

As shown above, the highest cohort correlation obtained at the thigh, which was between peak resultant force (MMAX) and mass-scaled peak resultant acceleration (MMAXMASS), was $R^2 = 0.5769$. Interestingly, between *vertical* force (ZMIN) and the same mass-scaled peak resultant acceleration (MMAXMASS), the correlation was $R^2 = 0.5694$, which is only a difference of -1.3%.[68] The same resultant-resultant correlations from the shank and ankle were $R^2 = 0.45$ and 0.27 respectively.

The highest correlation obtained at the ankle, which was between peak resultant force (MMAX) and mass-scaled peak *Y-axis* acceleration (YMAXMASS), was $R^2 = 0.5364$. Between *vertical* force (ZMIN) and the same mass-scaled peak *Y-axis* acceleration (YMAXMASS), it was $R^2 = 0.5318$

[67] Average unscaled: $\mu = 0.19$; average mean-scaled: $\mu_{mass} = 0.20$; mean difference $MD_{R^2} = 0.01$.
[68] Percent Decrease $= \frac{0.5694 - 0.5769}{0.5769} \times 100 = -1.300\%$.

(-0.86%).[69] The same resultant-*Y-axis* correlations from the thigh and shank were $R^2 = 0.52$ and 0.38 respectively.

The highest correlation obtained at the shank, which was between peak resultant force (MMAX) and mass-scaled peak axial acceleration (XMAXMASS), was $R^2 = 0.5927$. Between *vertical* force (ZMIN) and the same mass-scaled peak axial acceleration (XMAXMASS) correlation of $R^2 = 0.5924$ (-0.05%).[70] The same resultant-axial correlations as obtained at the thigh and ankle were $R^2 = 0.29$ and 0.25 respectively.

In each case, the vertical correlation was within 2% of the resultant correlation:

$$0.98 \times R_{F_M}^2 < R_{F_V}^2 < 1.02 \times R_{F_M}^2$$

Although these results were all only *large* $(0.5 < R^2 < 0.7)$, the proximity of these resultant and vertical force correlations do indicate that the resultant magnitude of each waveform for both acceleration and force in the recorded activities is primarily dependent on the magnitude of the vertical force axis. In light of the previous investigation, where direct linear correlations have been considered for individuals and for the entire cohort, the investigation will now turn to consider whether these correlations can be improved with the application of a 20 Hz lowpass filter.

7.3.2. Filter-Induced Differences

Overview

This investigation must determine whether filtering the data using a lower cut-off frequency prepares the acceleration data for predictive analysis more effectively than the previous 50 Hz filter. Following the recommendations given by Simons and Bradshaw (2016), a 20 Hz filter will be applied to the acceleration data, and if there are major differences between the results, may inform this investigation of the location of the primary frequencies which contribute to the efficacy of a predictive model.

To best understand the effect of a different filter, the entire correlation set will be compared. However, it would be quite arduous to repeat the previous investigation and comment on the change of every possible variable for both filters and with different models; for even at this stage,

[69] $\text{Percent Decrease} = \frac{0.5318-0.5364}{0.5364} \times 100 = -0.8576\%$.
[70] $\text{Percent Decrease} = \frac{0.5924-0.5927}{0.5927} \times 100 = -0.0506\%$.

many correlations have not been considered.[71] The decision was therefore made to perform a cell-to-cell t-test for each correlation in the tables of Appendix A, with the aim of determining whether the 20 Hz filtered correlation results were statistically different to the 50 Hz filter. If the 20 Hz filter were found to produce statistically different results, the 20 Hz filtered data would be retained in the following investigation; if the results were *not* statistically different, only the 50 Hz filtered data would be retained.

Applying the 20 Hz Filter

Identical in all other regards to the previous filter of 50 Hz, a new 4th order Butterworth lowpass filter with its poles at 20 Hz was designed and applied to the acceleration data. The effect that this has to the waveform is shown in Figure 33, where the normal, 50 Hz filtered, and 20 Hz filtered waveforms are compared for a trial of Participant 1. The change in the *absolute* maximum of this waveform (i.e. the negative peak) due to the 50 Hz filter was +0.07%, and for the 20 Hz filter was -18.3%.

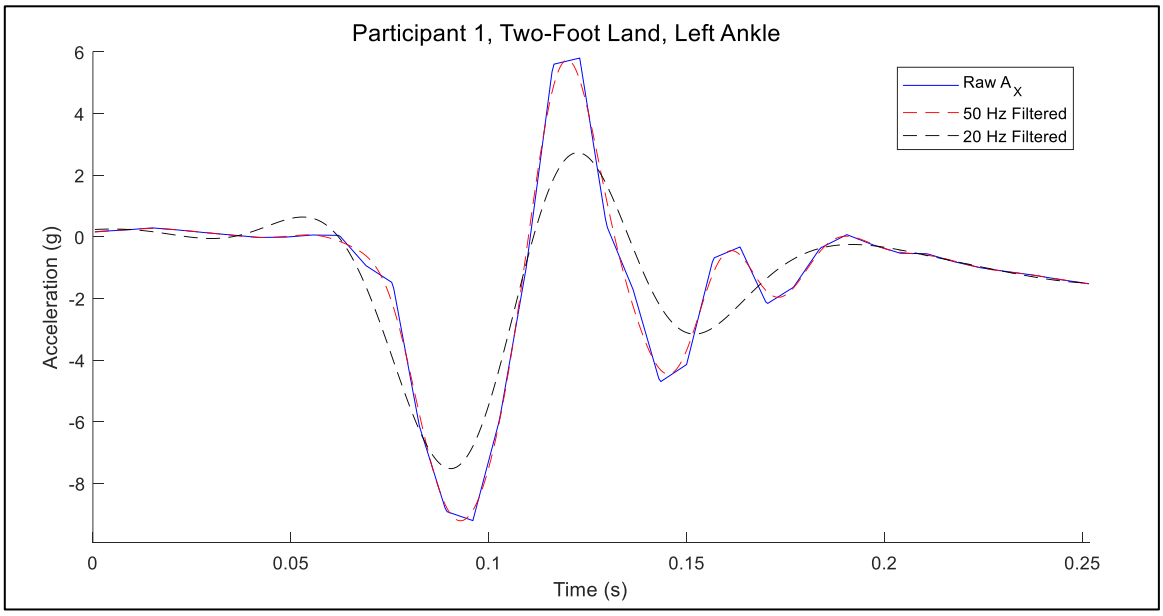

Figure 33: Comparison of raw, 50 Hz filtered, and 20 Hz filtered acceleration data.

[71] It would be quite impractical to comment on every correlation present in the tables of Appendix 2. So far, the investigation has attempted to summarise and explain the most informative and insightful correlations for the purpose of this investigation, but the summary which has been provided is by no means exhaustive of the potential meaning which could be wrought through a more extensive consideration of the entire correlation set. For what is possible, these considerations will be explained in more detail in the later discussion (Chapter 7.5), but this will be predominantly based on the information which has been explicitly mentioned in this investigation.

The same tables as in Appendix A were generated for the 20 Hz filtered data. A two-tailed paired t-test was performed for each set within the generated correlations: the 50 Hz filtered correlations from Participant 1 at the thigh were compared the 20 Hz filtered correlations from Participant 1 at the thigh; etc. for each participant, location and cohort correlation. It was hypothesised for each test that the mean difference was equal (i.e. $H_0 = 0$). The results are shown below in Table 19.

Table 19: Comparison of correlation coefficients between 20 and 50 Hz filtered data. Green indicates a stronger correlation.

Persons				
	P1Thigh	**P2Thigh**	**P3Thigh**	**P4Thigh**
50 Hz Mean (R^2)	0.2095	0.2191	0.2665	0.3497
20 Hz Mean (R^2)	0.1542	0.1825	0.1881	0.2352
p-value	0.0002	0.0035	< 0.0001	< 0.0001
	P1Shank	**P2Shank**	**P3Shank**	**P4Shank**
50 Hz Mean (R^2)	0.2001	0.2640	0.2104	0.3435
20 Hz Mean (R^2)	0.1591	0.2082	0.1768	0.2454
p-value	0.0040	< 0.0001	**0.0528**	< 0.0001
	P1Ankle	**P2Ankle**	**P3Ankle**	**P4Ankle**
50 Hz Mean (R^2)	0.1941	0.2191	0.1965	0.2266
20 Hz Mean (R^2)	0.1390	0.1699	0.1648	0.1903
p-value	0.0001	0.0001	0.0362	0.0252
Cohort				
	Thigh	**Shank**	**Ankle**	
50 Hz Mean (R^2)	0.1985	0.2270	0.1768	
20 Hz Mean (R^2)	0.1463	0.1774	0.1506	
p-value	< 0.0001	< 0.0001	0.0113	

The null hypothesis was rejected in almost every test: the difference between the means of the 50 Hz- and 20 Hz filtered data *is statistically significant*. The one exception to this was for Participant 3 at the shank, where $p > 0.05$ and the null hypothesis was not rejected. However, this seemed to be an anomaly: aside from this one situation, the mean of the 50 Hz filtered data was *greater* than the 20 Hz filtered data *on every occasion.* The statistical significance was in favour of the 50 Hz filtered data, for on average, the 20 Hz filter actually *reduced* the correlations.

In the previous section, a consideration was made as to what correlations produced *at least* moderate locations for all four participants. It was found that apart from the integral correlations, this only occurred for the shank correlations between peak resultant and vertical force (MMAX,

ZMIN) and peak axial acceleration (XMAX, XHEIGHT). The same consideration was made to understand the reduced 20 Hz filtered data correlations, and it was found that *none* of these events achieved correlations of greater than $R^2 = 0.3$ for all four participants.

However, there was *one* event correlation that produced at least *moderate* correlations for all four participants in the 20 Hz filtered data. This was between peak resultant force (MMAX) and peak resultant acceleration (MMAX) at the *thigh*, where the correlations were $R^2 = 0.42, 0.31, 0.47,$ and 0.75 for each participant, respectively. These same resultant-resultant correlations in the 50 Hz filtered data were: $R^2 = 0.40, 0.25, 0.64,$ and 0.74 respectively. Several observations may be made on this:

- Although the 20 Hz filter reduced most correlations, it did increase others, such that the 20 Hz filtered thigh data correlated higher for this event than the 50 Hz filtered data.
- The 20 Hz filter increased the location correlation consistency of single events at the thigh, since values which were not consistently predictable at the shank between participants were more consistently predictable at the thigh.
- Although the 20 Hz filter increased this correlation in comparison with the 50 Hz data and shank correlations, the increase was not uniform across the correlations. The 20 Hz filtered data for this event at this location was only higher for Participants 1, 2, and 4; for Participant 3, the 50 Hz filtered data was still higher.

Similar to the 50 Hz filter, the 20 Hz filter obtained *moderate* to *almost perfect* integral correlations of $R^2 = 0.47$ to 0.98 (the 50 Hz filter had obtained $R^2 = 0.50$ to 0.98). There were no other events for which the 20 Hz filtered data obtained *at least moderate* correlations for more than three participants. In light of all of these results, it was concluded that the 20 Hz filter does *not* produce stronger correlations than the 50 Hz filter, and that the 50 Hz filter was overall more effective.

Having determined that applying a 20 Hz filter does not, on average, increase the mean of the event correlations, it was decided that all future analysis would continue using the 50 Hz filtered dataset. The final validation method for determining the predictive power of these linear models would be to determine the inter-participant predictive accuracy of the linear models with a leave-one-out cross-validation study. However, since the previous results have shown that in general, the events of this dataset do not have greater than large correlations, it was determined that a cross-validation study would not add value to this investigation; for worse correlations would not

be practically useful, and higher correlations would be due to chance. Therefore, it was decided that the only waveform characteristics that would be considered in the cross-validation study were the 50 Hz filtered data integral correlations.

7.3.3. Leave-One-Out Cross-Validation for Linear Integration

Overview

The leave-out-out cross-validation will entail the development of a model based on the 50 Hz filtered data of *three* participants, and then validating the model against the *fourth* participant. This will provide an understanding into generalisable physiological waveform events, where if a model were consistently accurate for a general population, the models can be assumed as physiologically representative of a general population.[72] Indeed, if there are not characteristic relationships that are true for every participant, then it is expected that a cross-validation model would enable the identification of this.

Method

This process will be completed four times per model, with a different participant left out each time. This was chosen because if the conclusions of a single model were generalised over the entire population, then they may misrepresent the actual resolving power of the model, since the results generated may have only worked for that combination of training data. This would also provide an understanding of how training sets can influence the results. This method necessarily involves each model being trained *without* the data of the person on whom the model will be validated, increasing the validity of the trained model. If the validation person's data was included in the training model, as it effectively was in the previous *cohort correlations*, then it is expected that these results of an applied model would be high, since the model would have originally been trained with the data of the validation participant, nullifying its predictive argument.

The method that will be used to perform this cross validation is illustrated in Figure 34. The predicted values obtained from the model will be compared with the actual measured values.

[72] Assuming that the four participants represent the general population.

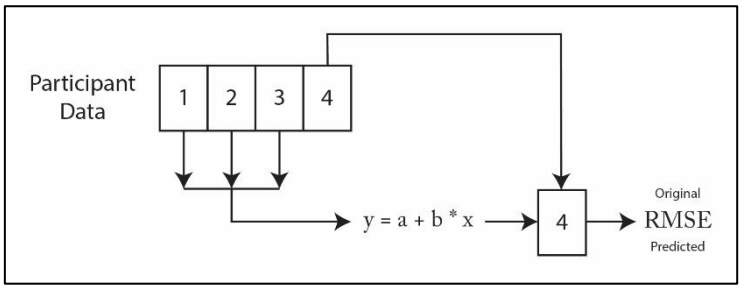

Figure 34: Flow-structure for the cross-validation protocol.

This method will be used to determine the ability of the model to predict the activity force integral, or *impulse.* Specifically, the variables that will be modelled and predicted are:

- Integration of resultant force with mass-scaled resultant acceleration (MINTEG-MINTEGMASS).
- Integration of vertical force with mass-scaled axial acceleration (ZINTEG-XINTEGMASS).

Because the correlations between uniaxial and resultant events are so similar,[73] it is assumed that these correlations will be similar again to the resultant-axial and vertical-resultant correlations; and as such these will not also be tested.

Results

The data of Participants 1 to 3 were taken, from which a generalised linear model was developed. The correlations are shown in Figure 35.

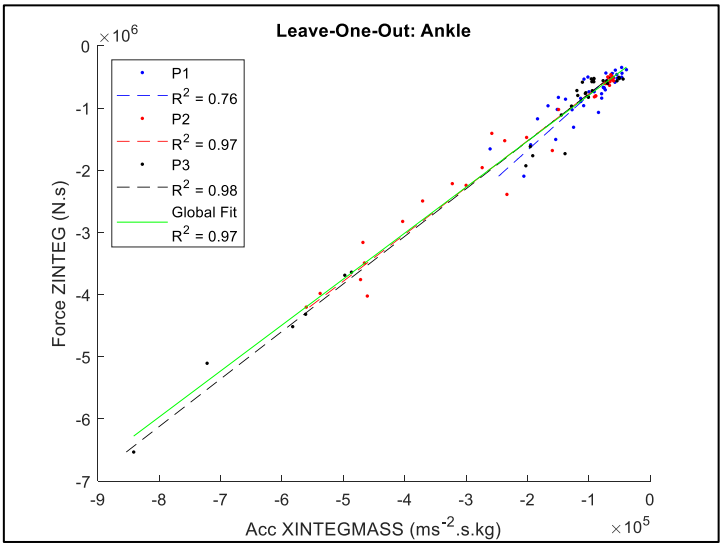

Figure 35: Developing a global model for the integration of force (impulse) from the data of Participants 1 to 3.

[73] Chapter 7.3.1, *Event-to-Event Correlations.*

The global model that was developed from this regression is given directly and in terms of vertical impulse:

$$F_{\text{ZINTEG}} = -54790.5388 + 7.3916 \times A_{\text{XINTEGMASS}}$$

$$\overrightarrow{I_V} = -54790.5388 + 7.3916 \times \int \overrightarrow{A_X}\, dt \times mass$$

This model was applied to the data of Participant 4, where Figure 36 shows the actual and predicted values for the integration of vertical force, and the correlation accuracy of the actual and predicted force.

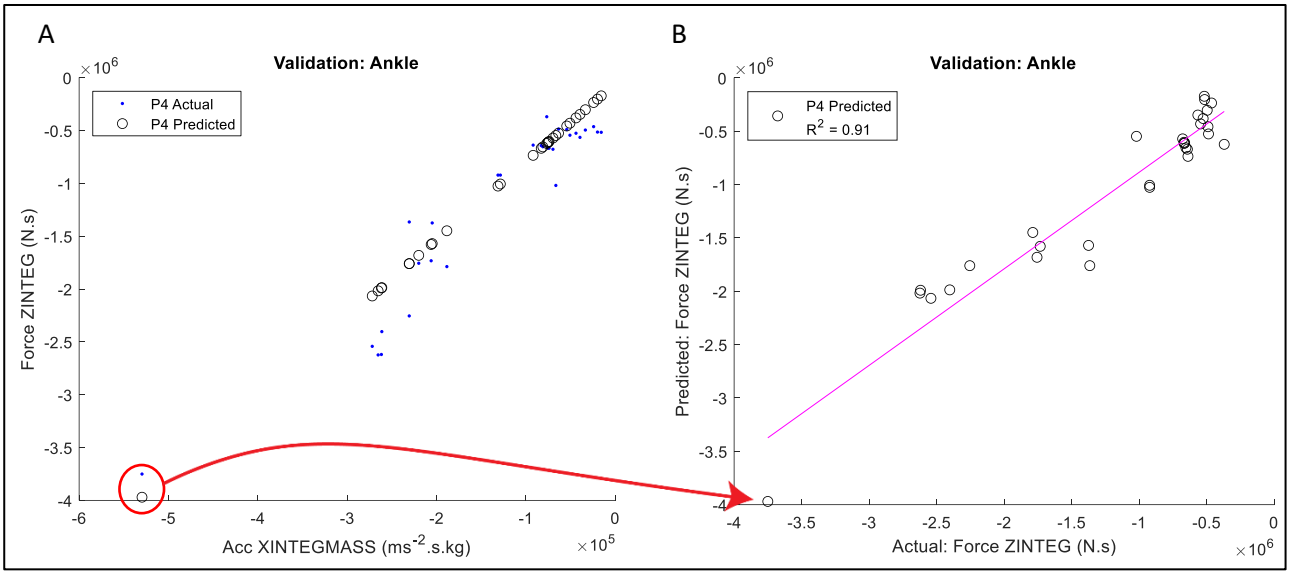

Figure 36: Predicting the vertical force integral.

(A) Predicting the force integration of Participant 4 from the developed model.

(B) The correlation between predicted vs. actual force integration values for Participant 4.

As seen, the predicted model produced a correlation coefficient of $R^2 = 0.9147$. When the acceleration integral was originally correlated with the force integral at the ankle of Participant 4, the correlation was also $R^2 = 0.9147$. However, this should not be surprising, since all that has occurred within this cross-validation is a shifting and scaling of the original acceleration values. As such, a much better indicator of the effectiveness of this cross-validation method is to consider the root mean squared error of the predicted data. These results for all participants and locations are given in Table 20, with the cell that corresponds to the preceding analysis highlighted in blue in the lower right corner.

To clarify, the errors given below are not direct equivalent comparisons because:

- the *original* RMSE pertains to the correlation between the original FZINTEG and AXINTEGMASS, whose magnitudes were in the order of 10^6 and 10^5, and therefore had an RMSE in the order of 10^5.
- the *predicted* RMSE pertains to the correlation between the original FZINTEG and the predicted FZINTEG, whose magnitudes were both in the order of 10^6, and therefore had an RMSE in the order of 10^6.

As such, it is expected that the RMSE for the predicted force will be an order higher than the RMSE of the original prediction; and as such, these results should be taken as relative indicators of accuracy. Considering the results below, it can be seen that for every situation, the predicted RMSE is between 4.4 to 13.6 times the size of the original error, as expected. It is therefore reasonable to conclude that the cross-validation models have predicted force from acceleration to a similar degree of accuracy as the original cohort correlations.

Table 20: Results of the linear Leave-One-Out investigation.

Comparison of Original vs. Predicted Force Integration					
Left-Out Participant	**Location**	$\boldsymbol{RMSE\ (N.s \times 10^3)}$ **3.s.f.**			
		Resultant-Resultant		**Vertical-Axial**	
		Original	**Predicted**	**Original**	**Predicted**
Participant 1	*Thigh*	17.5	235	37.6	211
	Shank	36.3	292	26.5	156
	Ankle	25.9	191	29.8	141
Participant 2	*Thigh*	21.2	250	64.2	356
	Shank	35.3	273	57.5	325
	Ankle	31.3	233	70.8	356
Participant 3	*Thigh*	30.6	373	102	540
	Shank	60.3	490	77.6	461
	Ankle	26.8	194	47.1	209
Participant 4	*Thigh*	20.8	283	75.2	430
	Shank	27.3	226	47.7	289
	Ankle	33.4	247	56.5	267

Having considered the resolving power of linear models to relate the waveform characteristics of acceleration and force, the investigation will now turn to consider non-linear prediction models: namely, logarithmic and machine learning. This second phase will closely follow the methods as presented in the present phase.

7.4. Phase 2: Non-Linear Modelling

The aim of Phase 2 is to determine whether the mass-scaled, 50 Hz filtered data is better approximated by the previous linear, or by a logarithmic, correlation. The literature-identified

strategies for relating acceleration to force are logarithmic event-based modelling and machine learning waveform modelling. These algorithms have been suggested for comparison according to the literature models that produced three of the highest qualifications.[74] Since there were no linear event-to-event correlations in Phase 1 that for all participants produced correlations of $R^2 > 0.6$, Phase 2 will specifically target those events that produced moderate to large correlations in Phase 1, to see if these correlations can be improved by non-linear models.

7.4.1. Logarithmic Event Modelling

Overview

This section on logarithmic models will follow the method presented in a previous study by Charry *et al.* (2013), who used the axial acceleration (XMIN, XMAX, XHEIGHT) of the shank to logarithmically approximate peak vertical force (ZMIN).[75] The initial model used by Charry *et al.* (2013) was:[76]

$$F_V = \log_2(A_X + 1)$$

However, they had then linearly generalised the formula according to participant mass:

$$F_V(m, A_X) = a(m) + b(m) \times log_2(A_X + 1)$$

In this formula, since $\log(A_X)$ cannot be resolved with a real answer for $A_X \leq 0$, Charry *et al.* (2013) included the shifting constant $c = 1$ to account for any negative acceleration values. However, although this was sufficient to correct *their* data, this did not account for any *future* generalisation of this formula. Indeed, in the participant data of the present investigation, there *were* values less than -1, which would have failed the model. To rectify this in the present investigation, the entire dataset was linearly shifted according to the magnitude of the minimum value in the dataset, normalising the trials such that the minimum value of each dataset was 1:

$$F_V(m, A_X) = a(m) + b(m) \times log_2\big(A_X + abs\big(min(A_X)\big) + 1\big)$$

Results

Ordinarily, as was shown for the waveforms in the previous section, the direction of the vertical force vectors is negative. However, it seemed more intuitive to present the logarithmic results in terms of positive numbers, and as such, for this section on logarithms, the negative values for

[74] See Chapter 4.2.3, *Table 11.*
[75] Chapter 3.2.2, *Non-Linear Models*.
[76] The notation used by Charry *et al.* (2013) has been changed here to reflect the common notation within this thesis.

vertical force (FZMIN) and axial acceleration (AXMIN) will be given as rectified displays. As this is only a linear scaling of the output, there is no change in correlation. As a reference example, the linear fit between vertical force (FZMIN) (which has been rectified) and axial acceleration (AXMAX) (which did not need rectification) for Participant 1 is illustrated Figure 37.

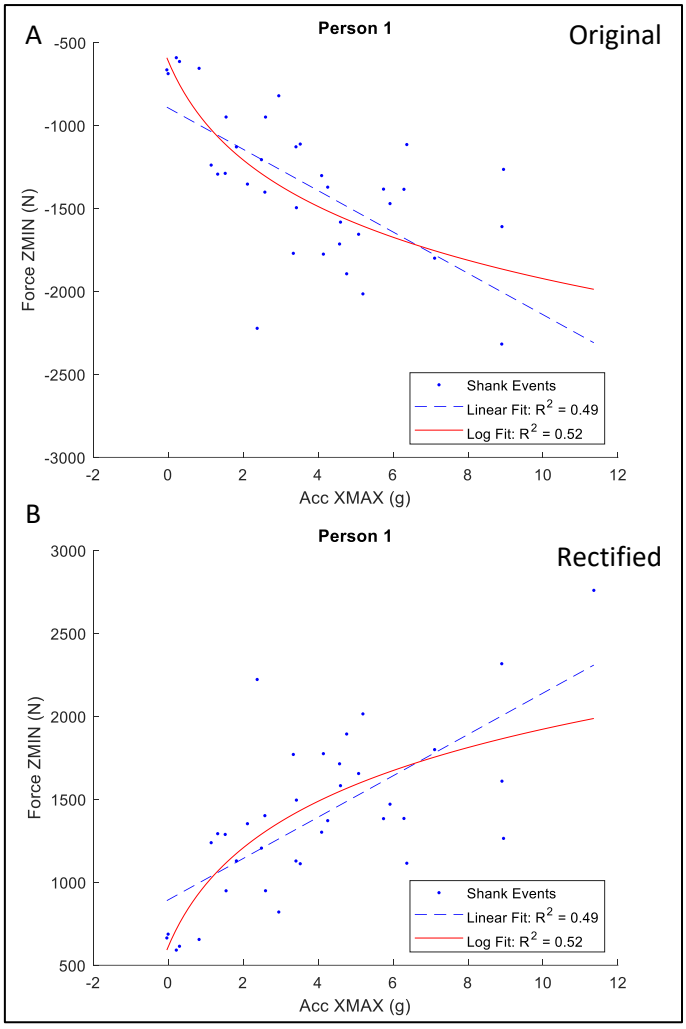

Figure 37: Rectifying negative vertical force (ZMIN). (B) Original fit. (A) Rectified fit.

The effective equation that describes the rectified logarithmic fit in Figure 37 is:

$$F_V = 591.8 + 384.3 \times \log_2(A_X + abs(\min(A_X)) + 1)$$

This logarithmic fit of peak vertical force (ZMIN) can be also compared linearly with the actual peak vertical force (ZMIN), as illustrated in Figure 38.

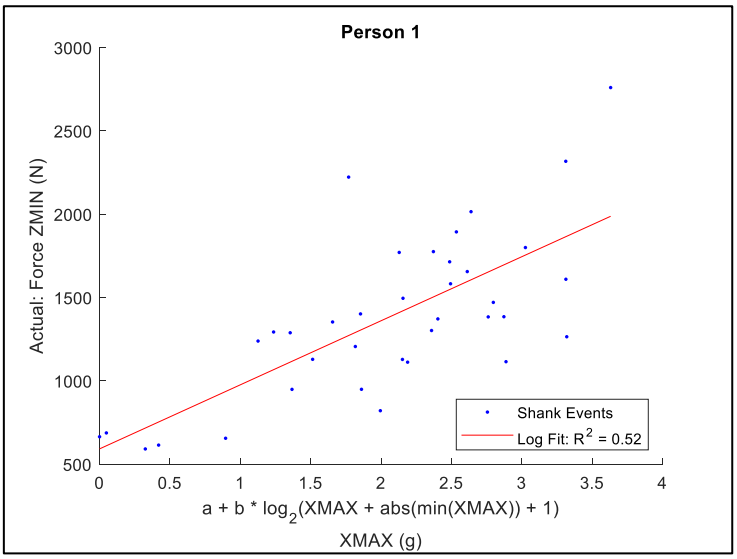

Figure 38: Logarithmic prediction of force (ZMIN) from acceleration (XMAX) against the actual value.

Comparing this relationship for each of the four participants, the logarithmic fit is found to have an inconsistent effect, producing higher correlations for Participants 1 and 3; but lower for 2 and 4. This data is summarised in Table 21.

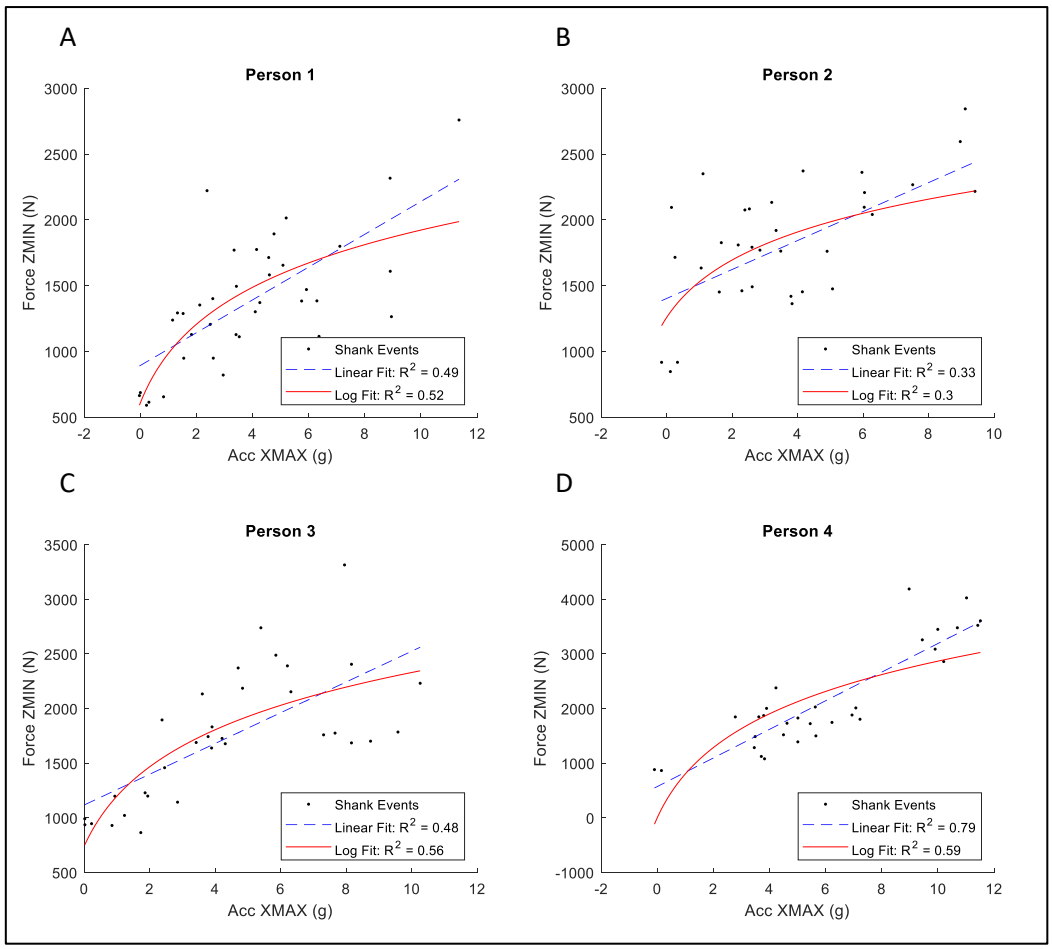

Figure 39: Comparison of linear and logarithmic correlations between vertical force (ZMIN) *and axial acceleration* (XMAX).
(A) Participant 1. (B) Participant 2. (C) Participant 3. (D) Participant 4.

Table 21: Logarithmic models and respective correlations.

Individual Logarithmic Approximation Coefficients				
	a	b	R^2 (Linear Fit)	R^2 (Logarithmic Fit)
Participant 1	591.8	384.3	0.4956	0.4615
Participant 2	1196	301.0	0.3332	0.2972
Participant 3	733.1	461.4	0.4838	0.5624
Participant 4	-115.7	859.3	0.7865	0.5876

To demonstrate the application of this data to a general relationship, following the method of Charry *et al.* (2013), let the coefficients a and b be assumed as linearly dependent on the mass of each participant. Then, they can be plotted, and a linear relationship derived between them. Applying the *leave-one-out* method, this has been calculated and illustrated for Participants 1, 2, and 3 in Figure 40, in preparation for validating the model on Participant 4.[77]

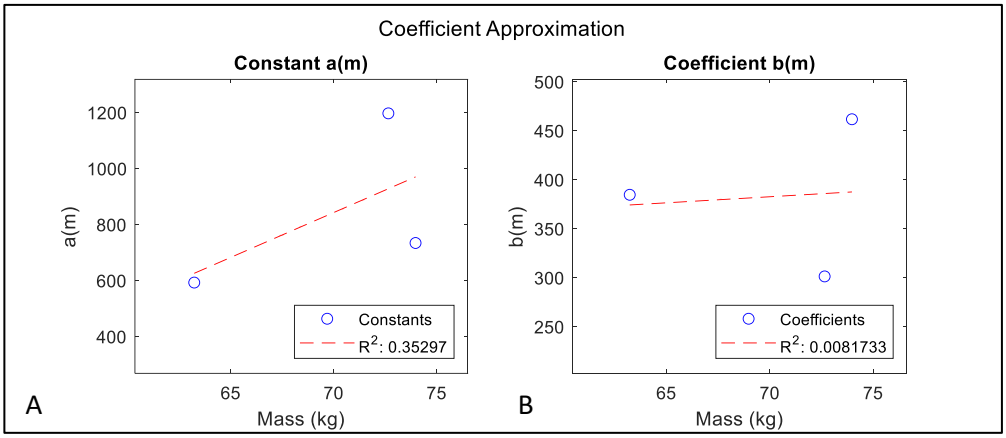

Figure 40: Using linear approximations to obtain coefficients for the global logarithmic model. (A) a(m). (B) b(m).

These mass-derived coefficients may then be used to complete the logarithmic model:

$$F_V(m, A_X) = a(m) + b(m) \times log_2\big(A_X + abs\big(min(A_X)\big) + 1\big)$$

$$a(m) = -1401.7495 + 32.0516 \times mass$$

$$b(m) = 295.6782 + 1.2375 \times mass$$

[77] This method has clearly not obtained an accurate linear relationship between mass and the relative coefficients, but it will be used to remain consistent with the method presented by Charry et al. (2013). In light of these results, it is probably a reasonable assumption to say that these correlation coefficients are not linearly related by mass. As it is, Charry et al. (2013) did not provide a correlation coefficient for this part of their study, so the results of the coefficient linear fit cannot be directly compared.

This model was applied to Participant 4 and the results are shown in Figure 39. Naturally, the new logarithmic model will have the same correlation coefficient (R^2) and $RMSE$ as the original log model, since they are only a scaling and shifting of the original data values:

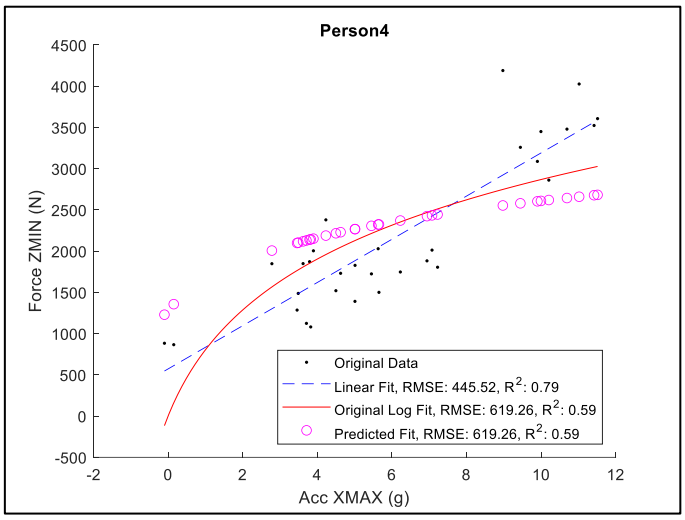

Figure 41: Comparison of the linear and logarithmic models for vertical-axial shank prediction.

Modelling for All Participants and Locations

The analysis was extended to the thigh and ankle, where in each case, one participant was left out of development and used to test the model. The results of this extension are shown below in Table 22. $RMSE$ cells are shaded green if they were lower (better) and red if higher (worse), where a lower $RMSE$ corresponds to a higher R^2 value. The corresponding results of Participants 1-3 have been included in Appendix B.

Table 22: Logarithmically modelling the vertical force and axial acceleration of Participant 4 at each location.

Results of Logarithmic Modelling							
Participant	**Location**	**Correlation**		**R^2**		**$RMSE$ (N)**	
		Force	**Acceleration**	**Linear**	**Log**	**Linear**	**Log**
4	**Thigh**	ZMIN	XMAX	0.17	0.12	879.9	903.7
		ZMIN	XMIN	0.52	0.43	672.5	726.6
		ZMIN	XHEIGHT	0.36	0.31	774.7	804.9
	Shank	ZMIN	XMAX	0.79	0.59	445.5	619.3
		ZMIN	XMIN	0.47	0.44	699.0	722.8
		ZMIN	XHEIGHT	0.73	0.62	504.6	593.9
	Ankle	ZMIN	XMAX	0.17	0.22	884.6	857.2
		ZMIN	XMIN	0.02	0.04	957.2	947.4
		ZMIN	XHEIGHT	0.12	0.16	908.5	889.7

Although the correlation was higher in each ankle correlation, this was not indicative of the entire dataset (c.f. Appendix B). To confirm this, a two-tailed paired t-test was performed on the

correlation coefficients of the linear set and the logarithmic set.[78] It was found that the logarithmic model correlation coefficients were overall *not* statistically different to the linear results ($p = 0.39$).

Cohort Prediction

However, where this has the greatest effect difference is when considering the combined cohort correlation. In this case, although each participant will have been scaled and shifted linearly (and so the intra-participant RMSE will not have changed), precisely *because* each data set has been scaled differently, the *cohort* will have an overall different correlation.

In addition to performing this scaling of the function, the input to the function was changed from being only peak axial acceleration (MMAX) to being mass-scaled peak axial acceleration (MMAXMASS). To illustrate this, consider that if the above method is repeated for the *entire cohort*; and Participants 1-3 are used to train the model; and where the data of every participant has been individually scaled by their respective mass, then the model coefficients describing the relationship between peak vertical force (ZMIN) and peak axial acceleration (XMAX), according to $F_V(m, A_X)$, are below. The graph generated by this is shown in Figure 42.

$$a(m) = 4677.9 - 76.7872 \times m$$

$$b(m) = -1513.0 + 31.0445 \times m$$

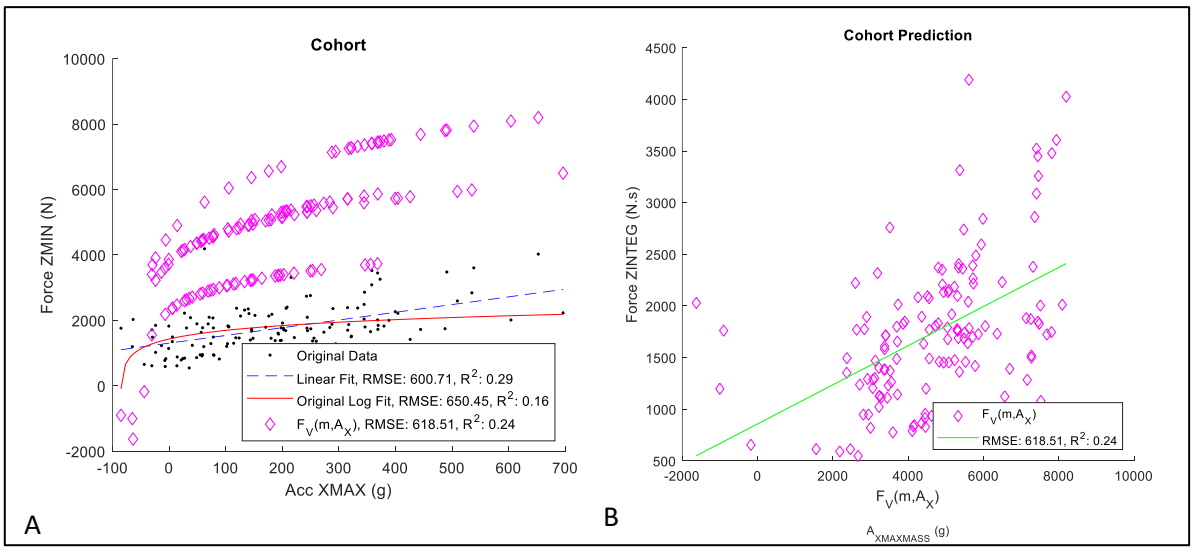

Figure 42: Cohort correlation of peak vertical force (MMAX) with peak axial acceleration (XMAX). (A) Comparison of correlations. (B) Cohort $F_V(m, A_X)$ predicted fit against the actual force.

[78] The level of significance was set at $p = 0.05$. Results: $\mu_{Linear} = 0.32$, $\mu_{Log} = 0.32$, $p = 0.3943$. The null hypothesis was not rejected: the correlations between the linear and logarithmic models were not statistically different.

Although this model for these events produced a correlation of $R^2 = 0.24$ and an $RMSE = 619$, and although there seems to be quite a large overestimation, what can be observed is that this fit is actually *closer* to the linear fit than the original logarithmic fit was. The regression equation that produced this correlation, shown in Figure 42 (B) was:

$$y = 858.43 + 0.18932 \times F_V(m, A_X)$$

This relationship may be visualised more clearly if the above prediction is scaled according to this linear fit; the result of this is shown in Figure 43.

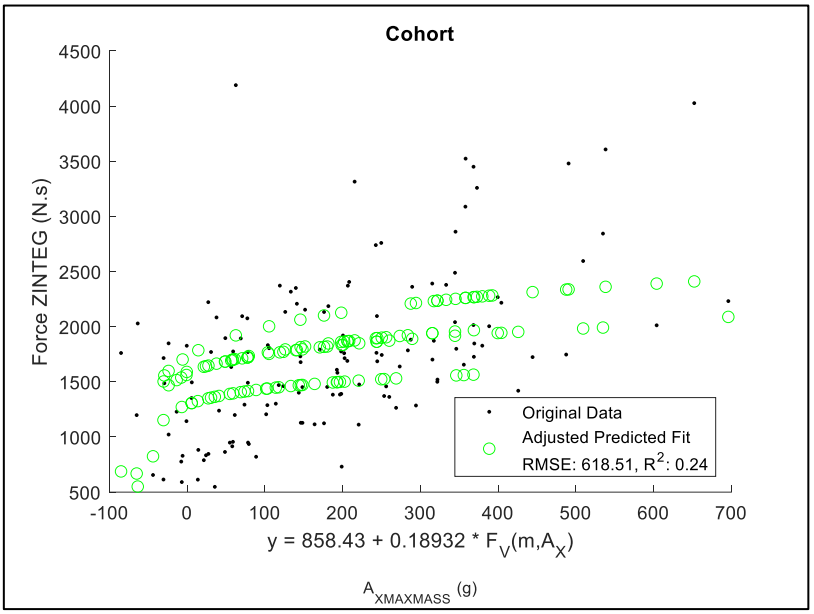

Figure 43: Adjusted predicted cohort fit.

Accounting for both y and $F_V(m, A_X)$, the final equation form is written as:

$$y = a + b \times \Big(\underbrace{(c + d \times m)}_{a(m)} + \underbrace{(e + f \times m)}_{b(m)} \times \log_2(A_X + abs(\min A_X) + 1)\Big)$$

$$F_V(m, A_X)$$

The results of the remaining locations and events for Participant 4 are shown in Table 23. The results of the model that was generated in Figure 42 and Figure 43 may be read in the top line of this table. Because it was found in Phase 1 that mass increased linear model accuracy, only the mass-scaled events were correlated here; except for the peak height (XHEIGHT), as this was not

considered with respect to mass in the analysis.[79] The cohort results of all four participants have been included in Appendix B.

Table 23: Logarithmically modelling the vertical force and axial acceleration of the entire cohort at each location.

Results of Logarithmic Modelling									
Participant	Location	Correlation		R^2			$RMSE\ (N)$		
		Force	Acceleration	Linear	Log	Adjusted Log	Linear	Log	Adjusted Log
4	Thigh	ZMIN	XMAXMASS	0.29	0.16	0.24	601	650	619
		ZMIN	XMINMASS	0.42	0.36	0.23	541	567	623
		ZMIN	XHEIGHT	0.32	0.29	0.41	584	600	546
	Shank	ZMIN	XMAXMASS	0.59	0.39	0.44	449	552	528
		ZMIN	XMINMASS	0.30	0.27	0.21	589	602	627
		ZMIN	XHEIGHT	0.50	0.41	0.52	498	539	489
	Ankle	ZMIN	XMAXMASS	0.26	0.16	0.26	611	647	611
		ZMIN	XMINMASS	0.16	0.17	0.19	651	646	636
		ZMIN	XHEIGHT	0.19	0.20	0.31	637	635	589

The results lean in favour of the linear models: the linear model correlation coefficients were statistically different to the original logarithmic results ($p < 0.0001$) and the adjusted logarithmic results ($p = 0.035$), with the linear models higher in both cases ($MD_{R^2} = 0.07$ and 0.05).[80] The adjusted logarithmic model was not statistically different to the original logarithmic model ($p = 0.27$), but it was on average higher ($MD_{R^2} = 0.02$). Based on these results, there is not sufficient evidence to affirm that the vertical force waveform is better approximated logarithmically than linearly, and as such, the results of Charry *et al.* (2013) were not reproduced. The final part of Phase 2 will now consider a machine learning model to see if this can possibly lift these lower correlations.

7.4.2. Machine Learning Waveform Modelling

Overview

The purpose of using machine learning within this investigation was to consider the effectiveness of an advanced non-linear timeseries algorithm to predict an output force from an input acceleration series. These predictions were made in MATLAB, using the Deep Learning Toolbox. This toolbox was chosen rather than manual design because the aim of this investigation was to evaluate machine learning as a whole; not to determine whether a *new* kind of machine learning

[79] But for the record, the mean of the mass-scaled logarithmic models ($\mu = 0.27$) was also higher than the un-scaled event data ($\mu = 0.25$).

[80] Two-tailed paired t-test; level of significance: $p = 0.05$. Results: $\mu_{Linear} = 0.34$, $\mu_{Log} = 0.27$, $MD = 0.07$, $p = 0.016$. Null hypothesis rejected: statistically different, linear models higher.

algorithm could be manually developed. Within this section, triaxial acceleration data will be used to predict both vertical force (F_Z) and resultant force (F_M).

Model Types

Since the peak events in the force and acceleration waveform do not occur simultaneously,[81] then if there is a relationship between them, it is probably time-dependent, based on the kinematics preceding the peak. The Deep Learning Toolbox contains three types of predictive functions for neural network *timeseries* modelling (MathWorks, 2020):

1) Non-linear auto-regressive with external exogenous input:
    - Both the input x and the output y are fed as inputs into the transfer function.

$$\mathrm{y(t)} = \mathrm{f(y(t-1),\ldots,\ y(t-d),\ x(t-1),\ldots,(t-d))}$$

2) Non-linear autoregressive:
    - Only the output y is fed as an input into the transfer function.

$$y(t) = f(y(t-1),\ldots,\ y(t-d))$$

3) Non-linear input-output:
    - Only the input x is fed as an input into the transfer function.

$$y(t) = f(x(t-1),\ldots,x(t-d))$$

Model 1 would be useful for predicting the future values of stock or financial systems, and Model 2 for the control of various mechanical systems. However, since in a practical application of a wearable device the actual force values will not be known and cannot be verified (without an accompanying device), neither Models 1 nor 2 can be used for this investigation. Model 3, which considers only the previous values of the input, is appropriate for the prediction of unknown force values.

As previously, this model will be trained on three participants, and then tested against the fourth participant. Note that whereas the previous sections had considered event-to-event correlations, and as such only a single event per movement and waveform was considered, this section is considering the *entire* waveform, and so will also display these similarities in terms of the full

[81] See Chapter 3.2.4, *Algorithm Variables*.

waveform, rather than only in terms of point-to-point correlations. Prediction models for both vertical and resultant force will be generated.

Data Preparation

All trial data at the shank was concatenated in the following way.

Let the concatenated axial acceleration data of Participant 1, for all trials, be written as:

$$A_{X_{P1}} = \begin{bmatrix} A_{X_{Trial\ 1}} \\ \vdots \\ A_{X_{Trial\ n}} \end{bmatrix}$$

Then for the triaxial data of each training participant, the model input can be written as:

$$\text{Shank Input} = \left[\begin{bmatrix} A_{X_{P1}} \\ A_{X_{P2}} \\ A_{X_{P3}} \end{bmatrix} \begin{bmatrix} A_{Y_{P1}} \\ A_{Y_{P2}} \\ A_{Y_{P3}} \end{bmatrix} \begin{bmatrix} A_{Z_{P1}} \\ A_{Z_{P2}} \\ A_{Z_{P3}} \end{bmatrix} \right]$$

The vertical force data of the test participant was similarly concatenated into an output array:

$$\text{Shank Output} = \begin{bmatrix} F_{Z_{P1}} \\ F_{Z_{P2}} \\ F_{Z_{P3}} \end{bmatrix}$$

Data was divided randomly into a 70% training set (205,056 timesteps), a 15% validation set (43,941 timesteps), and a 15% testing set (43,941 timesteps). The *Levenberg-Marquardt* training algorithm was chosen over a *Bayesian Regularisation* or a *Scaled Conjugate Gradient* because it typically requires less time than the others, though it uses more memory (MathWorks, 2020).

Non-Linear Input-Output Waveform Modelling

A non-linear input-output model was trained on the shank data. The network in Figure 44 was designed for this purpose. Consistent with the default given within the toolbox, it was designed with 10 hidden neurons and 2 delays.

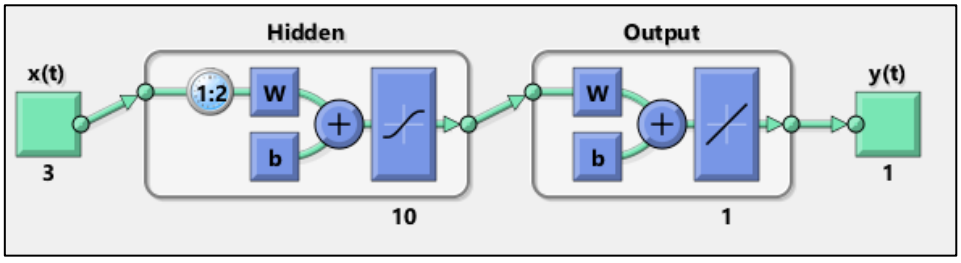

Figure 44: Non-linear input-output network design.

The response of the network is shown in Figure 45, where it is seen that a substantial amount of error was observed.

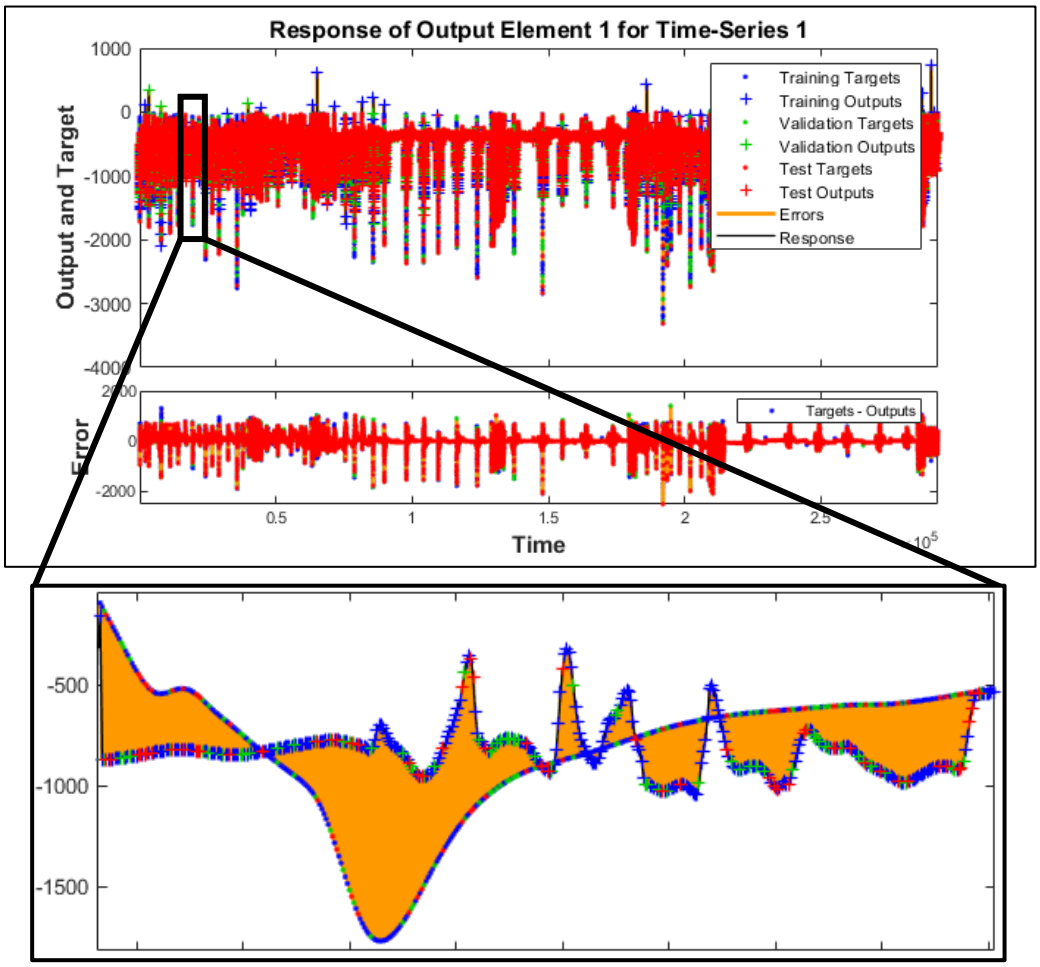

Figure 45: Non-linear network training. Vertical axes: force (N). Horizontal axes: time in samples, where 1 sample equals 0.5ms.

Considering this waveform prediction sample-by-sample, the equivalent correlations for the training, validation and testing datasets are shown in Figure 46.

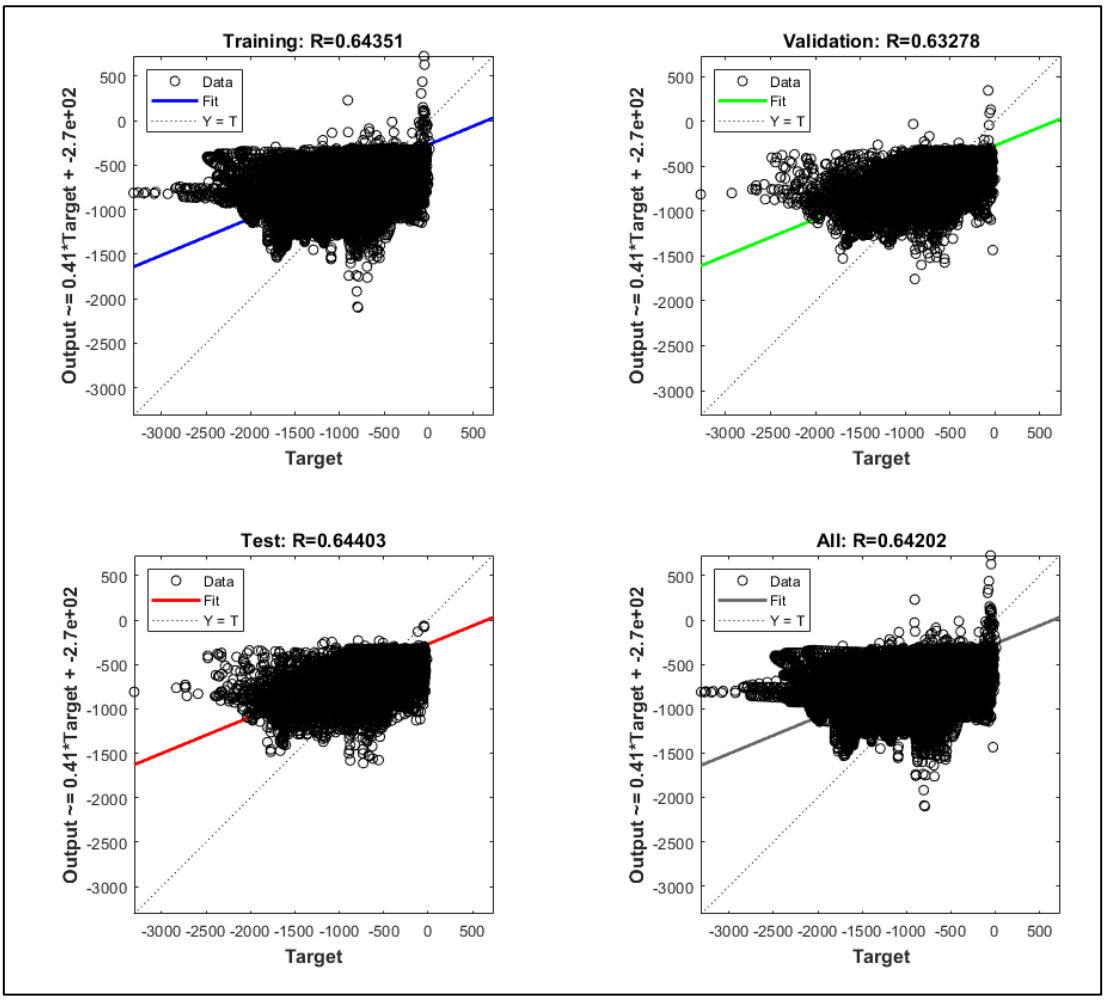

Figure 46: Correlation of input and output samples following the waveform prediction.

The model produced a validation dataset $RMSE = 217.6\ N$, $R^2 = 0.41$. When applied to Participant 4, the model produced a validation dataset $RMSE = 324.3\ N$, $R^2 = 0.36$. In each case, the correlation and the RMSE of the *test* participant performed slightly poorer than the *training* results: $MD_{R^2} = -0.08$, $MD_{RMSE} = +28\ N$. The method was applied also to the other participant combinations, and the results are shown in Table 24.

Table 24: Correlation and RMSE results of non-linear input-output waveform modelling.

Non-Linear Input-Output Waveform Modelling						
Training Participants	**Timesteps**	R^2	$RMSE\ (N)$	**Test Participant**	R^2	$RMSE\ (N)$
1,2,3	292,938	0.41	218	4	0.36	324
1,2,4	253,409	0.45	237	3	0.38	228
1,3,4	242,983	0.41	247	2	0.37	222
2,3,4	291,471	0.48	230	1	0.31	270
Average	-	0.44	233	-	0.36	261

Furthermore, it may be noticed that the model that was tested on Participant 4 produced an RMSE of 324 N. The original linear model for Participant 4 (non-prediction; direct correlation) for vertical peak force (MMAX) and axial peak acceleration (XMAX) had an RMSE of 446 N. The machine learning

prediction model for the entire waveform has produced a correlation with less error than the initial Participant 4 linear correlation of the single event.

Including Mass

Following this, the same investigation was performed where mass was included as an input into the model, where *mass* is an array of the same size as each acceleration input, with every value in the array equivalent to the particular participant mass:

$$m_{P1} = \begin{bmatrix} m \\ \vdots \\ m \end{bmatrix}$$

$$\text{Input} = \begin{bmatrix} \begin{bmatrix} A_{X_{P1}} \\ A_{X_{P2}} \\ A_{X_{P3}} \end{bmatrix} \begin{bmatrix} A_{Y_{P1}} \\ A_{Y_{P2}} \\ A_{Y_{P3}} \end{bmatrix} \begin{bmatrix} A_{Z_{P1}} \\ A_{Z_{P2}} \\ A_{Z_{P3}} \end{bmatrix} \begin{bmatrix} m_{P1} \\ m_{P2} \\ m_{P3} \end{bmatrix} \end{bmatrix}$$

The results of including as an input in the model is shown below in Table 25.

Table 25: Correlation and RMSE results of non-linear input-output waveform modelling, where mass has been included as an input.

Non-Linear Input-Output Waveform Modelling						
Training Participants	**Timesteps**	R^2	$RMSE\ (N)$	**Test Participant**	R^2	$RMSE\ (N)$
1,2,3	292,938	0.46	230	4	0.21	588
1,2,4	253,409	0.46	230	3	0.36	241
1,3,4	242,983	0.46	238	2	0.37	221
2,3,4	291,471	0.48	226	1	0.27	508
Average	-	0.47	231	-	0.30	390

The inclusion of mass has not made a substantial difference to the accuracy of the model. The average correlation coefficient of the training data has slightly increased ($MD_{R^2} = +0.03$), but the average test data correlation coefficient reduced ($MD_{R^2} = -0.06$). In contrast to the clear increase that mass produced in the linear models, this is surprising. However, since mass was constant for each third of the training data, it likely did not provide value to the timeseries model, for the model would have expected a series of fluctuating, interdependent points; not a static value.

Resultant Force

The same method as above was repeated for determining resultant force, rather than for vertical force. The results are shown in Table 26 and Table 27. The differences between the results of the

resultant force and vertical force data were not significant ($p_{R^2} = 0.40$, $p_{RMSE} = 0.60$). Based on these results, it can be concluded that the non-linear input-output model has used triaxial acceleration data and predicted resultant force *at least as well as* it predicted vertical force, but there was not a significant difference in the predictive power of the model between these variables.

Table 26: Correlation and RMSE results of non-linear input-output waveform modelling.

Non-Linear Input-Output Waveform Modelling						
Training Participants	**Timesteps**	$\boldsymbol{R^2}$	$\boldsymbol{RMSE\ (N)}$	**Test Participant**	$\boldsymbol{R^2}$	$\boldsymbol{RMSE\ (N)}$
1,2,3	292,938	0.45	218	4	0.35	333
1,2,4	253,409	0.42	248	3	0.41	230
1,3,4	242,983	0.42	247	2	0.40	222
2,3,4	291,471	0.49	232	1	0.34	272
Average	-	0.45	236	-	0.38	264

Table 27: Correlation and RMSE results of non-linear input-output waveform modelling, where mass has been included as an input.

Non-Linear Input-Output Waveform Modelling						
Training Participants	**Timesteps**	$\boldsymbol{R^2}$	$\boldsymbol{RMSE\ (N)}$	**Test Participant**	$\boldsymbol{R^2}$	$\boldsymbol{RMSE\ (N)}$
1,2,3	292,938	0.48	208	4	0.31	420
1,2,4	253,409	0.45	244	3	0.29	314
1,3,4	242,983	0.49	237	2	0.38	227
2,3,4	291,471	0.49	233	1	0.21	470
Average	-	0.48	231	-	0.30	358

Although the correlations of these machine learning models were nearly always only *moderate*, they were still higher, on average, than the event-to-event correlation results of Phase 1: for whereas only four correlations in Phase 1 had consistently measured above $R^2 = 0.3$ in every person, the machine learning algorithms have here predicted *the entire waveform* at an accuracy above this.[82]

Having considered the resolving power of linear, logarithmic, and non-linear timeseries machine learning models, a more comprehensive discussion will now ensue, to tie together both the literature and the results of this investigation.

[82] The correlations in Phase 1 that consistently produced $R^2 > 0.3$ were for the shank between peak resultant and vertical force (MMAX, ZMIN), and peak axial acceleration (XMAX, XHEIGHT).

Chapter 8. Discussion

8.1. Investigation Discussion

The preceding investigation was undertaken to assess and validate the performance of several acceleration-force models as presented within the literature. This section will summarise the results of this investigation and use them to conclude on the investigation hypotheses. It will provide a discussion on the challenges and limitations that were present in the investigation. Finally, it will offer a selection of recommendations for future research in these areas and suggest a strategy for this to proceed.

8.1.2. Synopsis

Having extracted 14 events from each acceleration waveform, and six events from each force waveform, the acceleration and force data from 111 activities of four participants were linearly correlated.

Phase 1

The only variables that had *very large* to *almost perfect* correlations for all participants and locations were the integral correlations between resultant and vertical force (MINTEG, ZINTEG), and resultant and axial acceleration (MINTEG, XINTEG). The exception to this was the result of Participant 1 at the shank, who obtained $R^2 = 0.50$ between vertical force and axial acceleration; but this was a clear outlier, with all other participant and location correlations above $R^2 = 0.76$. These integral correlations were the strongest at the ankle ($p < 0.05$), but in general were *at least very large* at all locations. When each integral and waveform event was scaled according to participant mass, the entire cohort correlations always increased ($p = 0.0027$). The highest mass-scaled cohort integration correlation was between vertical force (ZINTEG) from mass-scaled axial acceleration (XINTEGMASS) at the ankle. In terms of vertical impulse ($I_V = F_{\text{ZINTEG}}$), this model was expressed as:

$$\overrightarrow{I_V} = 5367.3 + 0.13039 \times \int \overrightarrow{A_X}\, dt \times mass$$

Although individual participants would at times show other strong event correlations, they were generally not consistent between participants, with the strongest correlations of one participant often being substantially higher than the others. The only four events that were *at least moderate* ($R^2 > 0.3$) for all four participants occurred at the *shank only* and were between peak resultant

and vertical force (MMAX, ZMIN) and peak axial acceleration (XMAX, XHEIGHT). However, the variability even between these was still significant ($R^2 = 0.33$ to 0.79), and there were *no* events that had a correlation of $R^2 > 0.36$ for every participant. These inter-participant differences often reduced the entire cohort correlations, making them a better indicator of the weak strength of the generalised physiological relationship. Scaling the cohort-combined events by mass increased the cohort correlation at every location, between both peak resultant and vertical force (MMAX, ZMIN) and every peak acceleration (MMAX, XMAX, YMAX, ZMAX) ($p < 0.0001$).

- The highest cohort event correlation coefficient of the investigation was obtained at the shank, between peak resultant force (MMAX) and mass-scaled peak axial acceleration (XMAXMASS) ($R^2 = 0.59$).
- The highest cohort event correlation at the thigh was between peak resultant force (MMAX) and mass-scaled peak resultant acceleration (MMAXMASS) ($R^2 = 0.58$).
- The highest cohort event correlation at the ankle was between peak resultant force (MMAX) and mass-scaled peak Y-Axis acceleration (YMAXMASS) ($R^2 = 0.54$).

The respective acceleration components were different between locations, which may indicate that device location changes the variable that must necessarily be used as the primary indicator in the model. If so, then these reflect the research of Takeda *et al.* (2009), who observed that different locations contain different waveform components; and these components may be more or less helpful depending on the location that they are observed. That these maximum events were all quite similar may indicate that resultant force can similarly be predicted from any of these three locations on the leg, but that the shank is slightly favourable for the prediction of these events.

In each of the three maximum correlations, the relevant force event was the triaxial *resultant* force. This may indicate that resultant force should be the target variable in future studies for the correlation of acceleration with force. However, in each case, the *vertical* correlations between the same variables were within 2% of the *resultant* correlations. This indicated that the resultant magnitude of each waveform for both acceleration and force in the recorded activities was primarily dependent on the magnitude of the vertical force axis.

The primary frequencies for force were under 100 Hz, and the primary frequencies for acceleration were under 50 Hz; and these were the filters that had been initially designed for each dataset, and for which the above results were obtained. Following the application of a *20 Hz* filter

to the acceleration data, the event correlations did not on average increase; but rather *decreased* the correlations ($p > 0.05$). However, there was *one* event that improved when compared to the 50 Hz filter: this was between peak resultant force (MMAX) and peak resultant acceleration (MMAX) at the *thigh* ($0.31 < R^2 < 0.75$); the same correlations in the 50 Hz data at the shank and ankle had at least one participant with a correlation coefficient of $R^2 < 0.3$. Similar to the aforementioned integral correlation results, the 20 Hz filter also obtained *moderate* to *almost perfect* integral correlations of $R^2 = 0.47$ to 0.98. It was concluded in light of these that the 20 Hz filter *does not* produce stronger correlations than the 50 Hz filter, and that the 50 Hz filter was overall more effective.

To validate the high integral correlations of the 50 Hz experiment, a leave-one-out cross-validation study was performed, wherein the data of three participants was used to develop a model that was tested on the fourth participant. As the properties of the regression coefficient meant that the applied linear models would not change the correlation of the acceleration values after applying the new linear model, only the RMSE of the predicted force values was considered. Although the results of the RMSE were one order of magnitude out, this was considered to *not* be inaccurate since the comparison was considering actual force (10^6) against predicted force (10^6) rather than actual force (10^6) against mass-scaled acceleration (10^5). As such, the linear integral force-acceleration models were not considered to be substantially different when predicted by a generalised model.

Phase 2

Logarithmic models were applied to the same 50 Hz filtered shank data of peak vertical force (ZMIN) with axial acceleration (XMIN, XMAX, XHEIGHT) data to validate the study results of Charry *et al.* (2013). The generated models were dependent on participant mass and were of the form:

$$F_V(m, A_X) = a(m) + b(m) \times log_2\big(A_X + abs\big(min(A_X)\big) + 1\big)$$

The formulas of the coefficients $a(m)$ and $b(m)$ were generated by the results of three participants, and the overall model was tested on the fourth. Overall, the logarithmic model correlation coefficients were *not* statistically different to the linear results ($p = 0.39$). The method was extended to the cohort correlations, where the same process was repeated, and in addition to this, a second logarithmic equation was defined:

$$y = a + b \times \big((c + d \times m) + (e + f \times m) \times \log_2(A_X + abs(\min A_X) + 1)\big)$$

Neither of these cohort-applied logarithmic models increased the event correlations; however, the mean of the adjusted logarithmic equation did produce slightly higher correlations than the original logarithmic equation. The previous *linear* model correlation coefficients were statistically different to both the original logarithmic results ($p < 0.0001$) and the adjusted logarithmic results ($p = 0.035$), with the linear models higher in both cases ($MD_{R^2} = 0.07$ and 0.05). As such, the results of Charry *et al.* (2013) were not reproduced, and it was concluded that vertical force is *not* better approximated logarithmically than linearly.

Following the logarithmic investigation, a non-linear input-output timeseries machine learning model was designed and applied to the data. Using triaxial acceleration as the input variable (x) and vertical force as the desired output (y), the model designed was of the form:

$$y(t) = f(x(t-1), \ldots, x(t-d))$$

Three participants were used to train each model, with the fourth used to test it. The average training correlation coefficient was $R^2 = 0.44$, and the average test coefficient was $R^2 = 0.36$. Considering that these results were predicting the *entire* waveform, rather than only events, this was considered to be a better result than the linear approximations, which had produced only four events that between participants had $R^2 > 0.3$.

This process was then repeated using mass as a fourth input alongside the triaxial acceleration data. Although the average training correlation coefficient slightly increased ($MD_{R^2} = +0.03$), the average test data correlation coefficient reduced ($MD_{R^2} = -0.06$). It was concluded that including participant mass did not substantially improve the model accuracy, but that since mass is not technically a *timeseries* input, the limited change in accuracy was not unusual.

This machine learning process was finally repeated with resultant force as the desired output rather than vertical force. The resultant and vertical force prediction correlations were not statistically different ($p_{R^2} = 0.40$, $p_{RMSE} = 0.60$).

8.1.2. Conclusions

Linear Modelling

Regarding waveform *events*, the correlation variance does not provide confidence for the future use of these variables. Despite there being more *moderate* to *very large* correlations at the shank, the correlations of FMMAX and FZMIN with AXHEIGHT and AXMAX were not consistently high, and as such should not be used as accurate estimations. However, since there were more consistent

event correlations on the shank that correlated *at least moderately*, and since the ankle was found to overall produce the best *integral* correlations, there seems to be evidence supporting the notion that the lower limb *is* optimal for predicting force from acceleration.

Although the vertical and resultant *force* correlations were often almost equal, the *acceleration* variables that produced these similar correlations were *not similar* between locations. Rather, different acceleration axes were found to be more or less correlated. The literature had recommended that triaxial accelerometers be used (Elvin et al., 2007), and the evidence seems to suggest that triaxial devices are indeed necessary to determine strong correlations. However, Elvin *et al.* (2007) was the only study that actually used uniaxial accelerometers, so in light of these results their recommendation towards triaxial devices is justified.

That the vertical average and instantaneous loading rates did not correlate well was surprising in light of the large correlations produced by Davis *et al.* (2018). However, they had used a sample size of $n = 169$, where each participant ran for eight steps (in total, 1,325 events); whereas the present investigation had only a sample size of $n = 4$ with a combined 135 events from different activities. In light of this, there was highly likely not substantial evidence to reject the conclusions of Davis *et al.* (2018) based on the results of the present investigation.

Despite the waveform events generally not correlating consistently, the acceleration integral did consistently and strongly correlate with the force integral. The prediction of integrals may therefore bode well for the future of impact dose prediction; and especially when linearly scaled according to participant mass. That this was high also seems to align with the literature, for as Hunter *et al.* (2005) explains, *"when horizontal, braking, propulsive, and vertical impulses* [i.e. force integration] *are expressed relative to body mass, they reflect the change in velocity* [i.e. acceleration] *of the center of mass… during the respective periods and in the respective directions."*

In this case, the ankle is the optimum position to place this to detect the highest acceleration forces, since this is going to be the closest to the foot accelerations which were highest as measured within this study. These positive results at the ankle are promising in the case of an eventual device implementation, especially considering the preference of athletes to use this lower location.[83] However, expanded research will be required to determine the repeatability of these results with a larger sample size. These differences between location hold further relevance in understanding future implementation, especially regarding the position on each segment. When

[83] Chapter 1.1.2, *Considering a Device*.

the device was placed on the ankle (near the distal tibia), versus on the shank (the medial tibia), the results were different, and when applied in real life, the location will most certainly vary in these small ways between participants.

When compared to the results that were originally obtained by Corbo (2018), it is found that the results are substantially and surprisingly different. The highest correlation obtained by Corbo (2018) was $\mathrm{R}^2 = 0.64$, which was also between the integration of vertical force and axial acceleration at the ankle. With the correlations of the present investigation being approximately $R^2 = 0.3$ higher for this same variable, it is likely that the analysis method used between the original evaluation and the present re-evaluation was different. In the study by Corbo (2018), force threshold, noise filtering and an activity start time had not been included; and in the present investigation, the events selected for analysis had been re-evaluated for validity, with several events used in the previous analysis discarded, and some retained that may not have been used previously; so there were several differences in analysis that may have contributed to this. As the exact method of analysis that was used by Corbo (2018) was not known, understanding the cause of the correlation differences may not be possible.

Filtering

In the present investigation, although the thigh generally did not produce stronger correlations than the shank or ankle, this is not to say that the thigh is sub-optimal in all circumstances. After the 20 Hz filter had been applied, there was one particular thigh event correlation that increased for every participant beyond what the 50 Hz filtered shank and ankle correlation for that event had produced. There may therefore be particular waveform characteristics of the thigh that are better for predicting different events, especially if the particular frequencies of that event are isolated; and vice versa for the shank and ankle. This may confirm the notion that a single location is not necessarily the best for predicting every feature, but that different locations are more helpful for predicting different waveform features. This would be consistent with the earlier discussion which showed that different waveform features are present at different locations (Takeda *et al.*, 2009). Generally speaking, across all locations, the events that included frequencies between 0 to 50 Hz predicted force more accurately than when only the 0 to 20 Hz waveform content had been considered.

In the literature, it had been recommended that lowpass filters with poles between 20 to 50 Hz be further considered when predicting force from acceleration (Simons and Bradshaw, 2016). In the

present investigation, both of these filters were used: 50 Hz was experimentally chosen, and 20 Hz was chosen following this recommendation from Simons and Bradshaw (2016). However, no significant positive difference in the analysis was found, meaning that either the results of Simons and Bradshaw (2016) were not generalisable to the kind of investigation that was here performed; of that its application in the present investigation was errant because of systematic problems in the dataset.

In light of these results, the conclusion from Simons and Bradshaw (2016) that resultant acceleration filtering is more important that peak force-acceleration agreements does not seem to hold true, for it was found that the filter did *not* make a significant differences, which was more in line with the results of Rantalainen *et al.* (2018), who had also found no major differences. From the present investigation, it would sooner be concluded that identifying force-acceleration agreement is more important than understanding which filter to use. However, it is expected that these two procedures are not mutually exclusive of each other: understanding the frequency components of the acceleration data may be totally necessary for determine *which* events are the events that cause an agreement; and therefore, although the application of these filters is important, they may be secondary to understanding *which* events are the desired events for correlation. These results also seem to justify the recommendation by the literature that higher frequencies be further considered in future studies (Lafortune *et al.*, 1995, Wundersitz *et al.*, 2013).

To be sure, filters must be chosen carefully, based on the targeted frequency content of each activity and the elimination of noise. The optimal filter will inform not only which physiological events correlate the strongest, but also of the frequency content of those events. However, this all assumes that impact dose is optimally predicted by event-to-event correlations, and as such is not necessarily exhaustive of the use or validity of the noise-eliminated raw data for the purpose of predicting impact dose.

Logarithmic Modelling

The logarithmic modelling in the present investigation was based closely upon the work of Charry *et al.* (2013), but did not replicate their results for the conditions that were specified. Whereas Charry *et al.* (2013) had produced *very large* to *almost perfect* correlations, this investigation at most only produced *large* correlations; and this was fairly uncommon. Charry *et al.* (2013) had three participants, so the differences were not likely due to sample size. It is expected that the

differences primarily arose due to the activity variations that were involved in the present investigation, for Charry *et al.* (2013) only had their participants *run*.

Charry *et al.* (2013) had only recorded their acceleration data at 100 Hz, but without their data, it is not possible to determine whether this caused significant differences in the recording ability of their device when compared to the 148.1 Hz of the present investigation. These relatively lower sampling rates may have missed the sharper accelerations during breaking or pushing off in the change of direction tasks. Without a second reference point for validating the acceleration in addition to the accelerometers, it is not possible to determine this. Although it is not expected that the recorded acceleration in the present investigation peaked during these sharp activities, the higher dynamic range of ± 24 g that Charry *et al.* (2013) used may have provided an advantage.

Regarding the actual logarithmic model, the present investigation linearly shifted the acceleration data according to the magnitude of the minimum axial acceleration data of each event set; whereas Charry *et al.* (2013) had simply shifted their dataset by +1. This will have slightly changed the correlation coefficient due to the properties of logarithmically scaling, but it is not expected that this was the primary cause of why the correlation difference between studies was in excess of $R^2 = 0.3$.[84] Rather, it is expected that the primary cause of the reduced correlations was due to the activity type and the shape of the model. Between linear and logarithmic modelling, for a sample set characterised by that within this investigation, linear modelling is superior.

Machine Learning Modelling

The non-linear input-output timeseries neural network did not approximate force higher than moderately, and as such cannot be concluded as a reliable method for predicting force from acceleration. However, the fact that it produced an overall correlation coefficient of $R^2 > 0.3$, indicates that on average it has performed more favourably than the linear correlations, since the linear models only had several *events* that correlated above this for every participant. However, the events that did correlate linearly, for the entire cohort, correlated more strongly than the machine learning model.

The results of the machine learning algorithms in this section cannot be directly compared with the machine learning studies in the literature review because the neural network training models were different between these. This indicates the different predictive abilities of different models

[84] Maximum logarithmic correlations: Charry *et al.* (2013): $R^2 = 0.95$; this investigation: $R^2 = 0.59$.

for different purposes, as was explained in the investigation. However, it might actually be possible that the method used by Guo *et al.* (2017) would not be applicable for a wearable device, because it seems that their training algorithm incorporated known force values, using a model similar to what was proposed as for a stock market. The results of an individual in any commercialised device would never be confirmed though an accurate validation of true force. It is uncertain whether the method used by Guo *et al.* (2017) is implementable for this kind of approximation. However, in the long term, a model which, based on the known force values of a large training set during manufacturing may become generalisable to an unknown future user, if subject specific characteristic can be understood and implemented within this algorithm such that it in effect becomes an input-output, rather than a model relying on known force data.

The weak resolving power of the neural network may further indicate that the acceleration data lacked key information that contributes to the prediction of force. Perhaps this could be resolved in a future machine learning model by including information from a gyroscope or magnetometer. Any future model will also need to consider that whilst a real-time output is ideal, a complicated machine learning algorithm may be limited in its application due to its power requirements and the time that may be necessary to evaluate the model. As Pieper *et al.* (2020) has said, "*the tuning required from such methodology introduces distinct challenges which may limit the ease of translation."*[85]

Mass

In every model, except the machine learning timeseries model, the inclusion of mass increased the cohort and predictive model correlations, demonstrating the importance of the subject-specific relationship. If these relationships and methods are to be generalised, it may be helpful to establish the kind of participants for whom they may apply. It could be proposed that the results of Participant 3 may provide insight into the relevance of these results to the general netball population, for this participant was female and was closest to the mean weight of netballers; and Participant 3 was representative of the mean mass of the trial participants:

i. The mean mass of elite female netballers has been reported as 73.42 ± 6.95 kg (Simpson *et al.*, 2019). The mass of Participant 3 was 73.97 kg (+0.75% elite mean mass).

[85] This was stated in conclusion to their study on random forest networks.

ii. The mean mass of all four participants was 72.99 kg. Participant 3 was +1.35% of this mean participant mass. Participant 2 (male, 72.65 kg) was also closer to mean participant mass (-0.46% mean).

However, it must be considered that the training set was *not* entirely representative of elite netballers, since it included two non-elite males. As such, although Participant 3 may be the closest in mass, since the model was not developed from a representative population, these results may not be generalisable. But then again, because the results *did* include non-representative participants, they may actually inform a *more* generalised model, since there is no certainty as to the end user; only generalised estimates can be used for this. Alas, these conclusions are still limited, for the sample size and inclusion is not likely sufficient to describe the general population of elite netballers.

Challenges in Analysis

There were many system variables that could not be isolated or controlled within the investigation, and the influence of which therefore could not be knowingly accounted for. For example, it is expected that a major contributor to the inter-participant correlation differences were different landing techniques. If a generalisable model for all subjects was to be developed, it would need to incorporate the differences that are present in groups, including for amateur athletes with inconsistent techniques and for those with physical limitations due to impairment. Perhaps there is a generalised population dataset on which a model could be trained, such that these predictive algorithms are more representative of a future user. As mentioned, the variety of movements that were recorded in this investigation made it difficult to directly answer or validate the movements of each other study. But this is not to say that a variety of movements cannot produce strong correlations, because Meyer *et al.* (2015) had obtained *very large* correlations using a similar variety of movements with 13 participants with devices placed on the hip. Due to the number of different variables present between each study and movement, it is difficult to isolate the precise cause of these differences.

Although the variance between activities may have been a contributing factor to the wide range of correlations, understanding that the *similarities* between different movements in the future may make multi-activity studies easier to compare and apply to other sports. Callaghan *et al.* (2018) had recommended that an understanding of segment kinematics be provided regarding pace bowling performance. Although pace bowling performance was clearly not considered in the

present investigation, the *two-foot land* and the *cut* may have been similar in that both movements involve a sharp movement deceleration (the landing of both feet and the change of direction) which are similar to the sharp planting of the single foot during a delivery. So, although bowling was not specifically considered, such movements may contribute understanding to similar activities and therefore be generalisable between different sports.

A summary of factors that have been raised within this report, by which the relationship is affected, and between which a relationship may be modelled, are shown in Figure 47. These factors are not necessarily mutually exclusive of one another, and it is likely that there are more factors that were not considered in this investigation that have not been included in this summary.

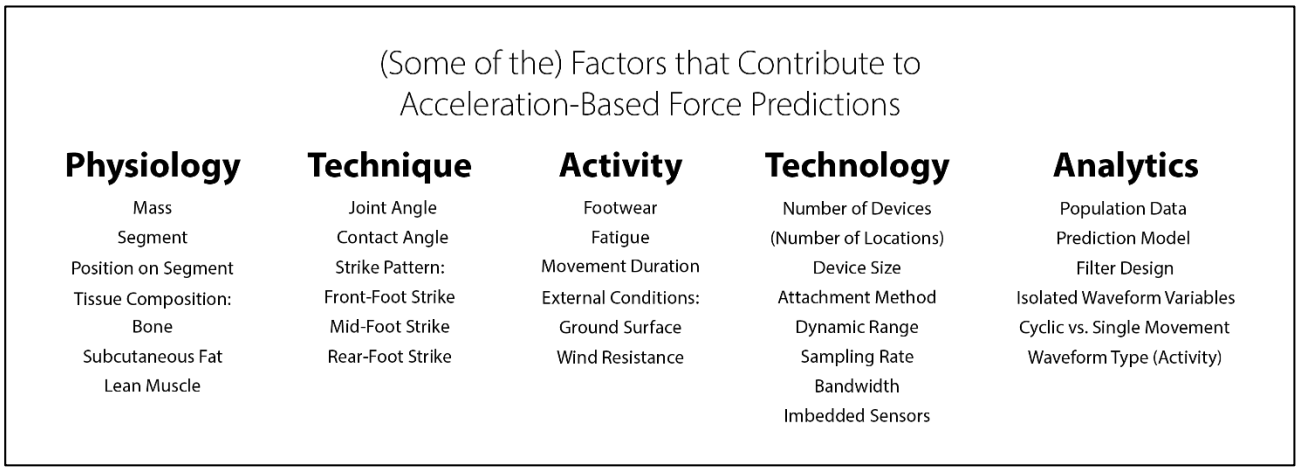

Figure 47: Factors that contribute to model predictions, ascertained from the literature.

8.1.3. Limitations

The limitations of the investigation will now be considered. These have been outlined in five main areas: study design, physiology, hardware, analysis, and research.

Study Design

The investigation had a limited sample size of $n = 4$, wherein the participants had masses of between 63.2 to 82.0 kg (range: 18.9 kg, +29.8%). It is expected that a more normalised distribution of sample points provided by a larger cohort size would have provided more insight into the physiological accuracy of the presented models. Although the inclusion of mass was found to positively increase the cohort correlations, precisely *how, why,* and in *what capacity* this occurs was not studied, for the investigation primarily focused on the efficacy of different predictive models. However, this may be simply due to the kinematics of movement being consistent with Newton's Second Law of Motion, $F = m \times a$.

As the available patient data did not include information on their physical health before or after the trial, the consideration of kinematics in relation to injuries could not be determined. As such, these results cannot be generalised to a population with physiological impairments. Although noise-attenuating filters were applied to the acceleration data, the study was not able to determine and account for the effects of soft tissue attenuation between participants and locations that may have been present within the selected frequency range.

The study was confined to a laboratory environment, and so cannot be generalised to external environments or for environments with wind resistance or uneven terrain. The physical characteristics of the footwear of each participant was not available, so differences between participants due to this were considered as unknown systematic errors and were not accounted for.

Physiology

The participants were not elite athletes and did not necessarily have the same level of fitness, and as such the results cannot be generalised directly to elite athletes. Furthermore, since the study did not consider how leg dominance affects technique, but only generalised these results by position, and the results may have been skewed due to the inclusion of unequal leg support during landing. The two contralateral devices therefore provided insight into combined, *position-based* predictions, but not into the kinematics of a *single* location. This decision had been originally made to increase the sample size by pooling the event data from both legs, but rather than increasing the distribution due to the greater amount of data, this may have actually limited the results by masking any potential side-specific correlations. If leg dominance had further been incorporated into this, and if the dominant leg was the leg that carried the most impact during these movements (as it may have done during the change-of-direction movements), then the leg-specific dominant-side data may have produced more consistent and comparable relationships.

In addition to not considering *single* placements, the investigation also did not consider multiple *locations.* As only the ankle, shank, and thigh were individually investigated, the literature-based results pertaining to the other locations could not be validated, and as such although the lower leg was here identified as optimal, this is not globally conclusive regarding all potential locations. This is particularly so for the logarithmic and machine learning estimations, which were only calculated on the shank.

Within the qualified articles, several had recorded cyclic activities; but the present investigation only considered single movements. Therefore, these cyclic-movement studies cannot be validated according to the generated results. However, these studies lack the generalisability to a wide range of movements, and their results must be applied accordingly. Although the movements that were compared included a range of speed variations and models, the exact contribution of the different events remains unknown. Although the waveforms of each event were visually sighted during the analysis, the shape of each waveform was not formally analysed, so the exact means behind the conjecture that different events have largely contributed to the variance in results is yet to be proven for this dataset. It had been suggested in the literature that the average of several events from multiple strides be used to predict calculations, rather than only correlating the events of individual strides (Raper et al., 2018). As this was not considered in the study, the benefits of using this method could not be evaluated; and considering the variability of the data, this method may have been quite helpful. Alas, only a selection of variables and analysis methods could be chosen for consideration.

Hardware

There were also several technological limitations present. As the study did not have access to gyroscopic output, joint and contact angles could not be considered; meaning that angular acceleration could not be considered. Global vertical acceleration was not correlated with vertical force, which may have produced different correlations according to the linear $F = m \times a$ model. Although it did not seem that acceleration had peaked, since the literature said that accelerations can be up to 12 g, the 9 g accelerometers used may not have correctly captured the kinematics of every activity.

However, if the high magnitude accelerations were also generated at high frequencies, then the devices may have missed them anyway, because the sampling rate of the accelerometer was quite low (148.1 Hz). The available data was therefore jagged, and the analysis had to be completed based on the approximated waveform via a filter. It is impossible to know whether the events that were analysed were true representations of the physiological magnitudes. To get a more accurate representation and prediction, a higher sampling rate may be necessary.

This study did not consider the presence of internal device bias. This was predominantly due to only having access to the trial data, rather than being able to test the measurement ability of the devices and calibrate them prior to the data analysis. Several of the original devices that were

used by Corbo (2018) had been replaced due to failure, and for the ones that remained, the bias present would not have been accurate to the state of the device during the original recording. It had to be assumed that the device specifications given in the original device documentation and in the previous study were indeed representative of the true original device performance.

Analysis

The analysis was limited in that it did not assess every potential acceleration or force event and did not exhaust the list of potential models by which these events may be related. Fourier and event-based machine learning were two models that were presented in the literate but were not validated. The conclusion must not be made that waveforms *do not correlate,* but only that the strategies that were used here to model these events were not effective for producing strong correlations.

It was assumed that the filters that were applied were acceptable for both datasets, with the original filters being applied only to remove non-physiological noise. However, the design of the filter was based on the results of a single trial and may not have been indicative of the primary frequencies of every waveform. Although 50 Hz had been recommended in the literature as a filter to consider, there may have been high power frequencies that were filtered out, significantly and unfavourably reducing the respective waveforms; but confirming this would require further investigation.

After the 20 Hz filter was later applied on the data, and poor results obtained, 20 Hz filtered data was put aside, assumed to not produce stronger correlations than the 50 Hz filtered dataset. Since the effectiveness of this filter for non-linear modelling was not validated, the conclusion that the 20 Hz filter resulted in weaker correlations than the 50 Hz filter is limited to prediction via the linear models demonstrated.

Several conclusions were made based on the statistical significance generated by t-tests. Although these do not seem inappropriate considering the context, it is acknowledged that other kinds of statistical analysis could have been used to demonstrate the strength of correlations in additional ways. It is also assumed that even though several of the t-tests used in this investigation did not have more than eight samples per group, their conclusions need not be rejected simply because they are small (Bland and Altman, 2009).

Research

A significant assumption was made in the literature review regarding the comparison of correlation coefficients. As not every study reported the method by which they produced their correlations, and not every correlation presented their results in terms of the same correlation coefficient, there was no way to directly compare each result with certainty of correlation equivalence. As such, it was assumed that the available correlations could be taken as *indications* of the results of each study, and the correlation coefficients of the studies were therefore compared indiscriminately of their correlation terms. Although this was avoided where at all possible, this may have meant that several of the correlations that were compared in the literature review were not equivalent. If there were any occasions that this was the case, it is acknowledged that the conclusions drawn may be invalid. Therefore, unless explicitly clear, the presented results must be held with this caveat.

Finally, the limited number of articles that were retrieved from within this search (16), as compared to the total number of articles reviewed (99), may indicate that the original search term presented was inadequate to retrieve relevant articles comprehensively. As such, additional qualifiable articles likely exist, but were not included within this study. For example, it was later identified that the study written by Davis *et al.* (2018) was more comprehensively reported in Tenforde *et al.* (2020), but this was only identified towards the end of this investigation and so was not included.

In the search exclusion criteria, articles were only included if they had explicitly targeted ground reaction force, because it had been assumed that peak force was the most appropriate factor to model. As such, studies that had considered power and impulse had been excluded. In light of the results of the investigation, which found that impulse was actually the highest correlating variable, there were very likely studies that were excluded which may have held more relevance than was first thought. It is acknowledged that existing articles that were not included in this study may include information that supersedes the results and conclusions presented within this thesis and maintained that the conclusions drawn here were made in response to investigation and the articles that were originally identified.

8.1.4. Hypothesis Conclusion

In the *Investigation Outline (Chapter 7.1)*, six hypotheses were made regarding the development of an acceleration-force relationship. Based on the results of the investigation, each of these will now be concisely concluded on as either *supported* or *rejected*, followed by a brief explanation.

1. **There is a very large relationship ($\mathbf{R^2 = 0.7}$ to $\mathbf{0.9}$) between force and acceleration at the lower limb, with the shank being optimal for developing this model.**

Supported

With the exception of a single outlier ($R^2 = 0.5$), the participant correlations between the integrals of force (resultant and vertical) and acceleration (resultant and axial) at every location were *very large* to *almost perfect* ($R^2 = 0.76$ to 0.98). However, there were no waveform events that correlated consistently above $R^2 = 0.36$ for all participants, and in this regard the hypothesis is rejected.

2. **The shank is the most effective position for modelling this relationship.**

Rejected

The strongest correlations were measured between the integrals of force and acceleration at the ankle ($p < 0.05$). However, participant and cohort correlation were also at least *very large* between the integral of resultant force and acceleration at the shank ($R^2 = 0.86$), so although the shank was not the *most* effective, it was yet highly effective.

3. **Generalised models are the most effective when they incorporate subject-specific characteristics.**

Supported

On average, the inclusion of mass increased the cohort regression value between the integral of force and acceleration by $R^2 = 0.02$ ($p = 0.0027$). Scaling by mass also increased the cohort regression values of every peak force and acceleration event ($p = 0.0001$).

4. **The correlations after filtering the data with a 20 Hz filter will be higher than when the data is only filtered for noise.**

Rejected

For every participant and cohort correlation set, except for Participant 3 at the shank, the correlations between the 50 Hz and the 20 Hz filtered data models were statistically significant ($p < 0.05$), and in every instance the mean correlation of the 50 Hz models was greater.

5. **Logarithmic modelling predicts force more accurately than linear modelling.**

Rejected

The linear model correlation coefficients were statistically different to all logarithmic models results ($p < 0.05$), with the linear models higher in both cases ($MD_{R^2} > 0.05$).

6. **Machine learning modelling predicts force more accurately than logarithmic and linear modelling.**

Supported

Although the correlations of the machine learning models were nearly always only *moderate*, with an entire waveform predictive ability of up to $R^2 = 0.41$, they were on average higher than the linear and logarithmic event-to-event correlation results.

8.2. Future Research

Finally, having considered the conclusions of the investigation, this section outlines areas of research that are yet to be explored. It is followed by a very brief recommendation for the continuance of this project.

8.2.1. Future Research Areas

The following list of research areas have been collated to summarise the areas that have been put forward in this thesis as necessary objectives towards further research in this field. These recommendations include research that may inform the prediction of impact risk from impulse, and also regard how waveform event correlations may be further considered and improved upon.

Injuries

- Determine whether the established relationship between the force and acceleration waveform integrals can be used as an indicator for impact dose and used to quantify injury risk.
- Determine whether other waveform event correlations can be improved for this end and determine what locations are optimal for recording these values.

- Determine precisely *how* this information relates to injuries and identify an objective count of impact dose.
- Determine how fatigue affects technique and prediction model accuracy.
- Determine how post-injury recovery will affect the performance of a prediction model, and in what capacity a predictive model may be used to assess and aid rehabilitation programs such as following ACL reconstruction.
- In Figure 48, an *arbitrary* risk measurement assessment has been generated to demonstrate the application of this future research. In this, the peak forces from each activity of each individual have been given. This arbitrary indication has been designed with the assumption that level of risk may depend on the ability of a person to adapt their technique to deal with landing force, and therefore that the risk level at the same forces may differ between people.

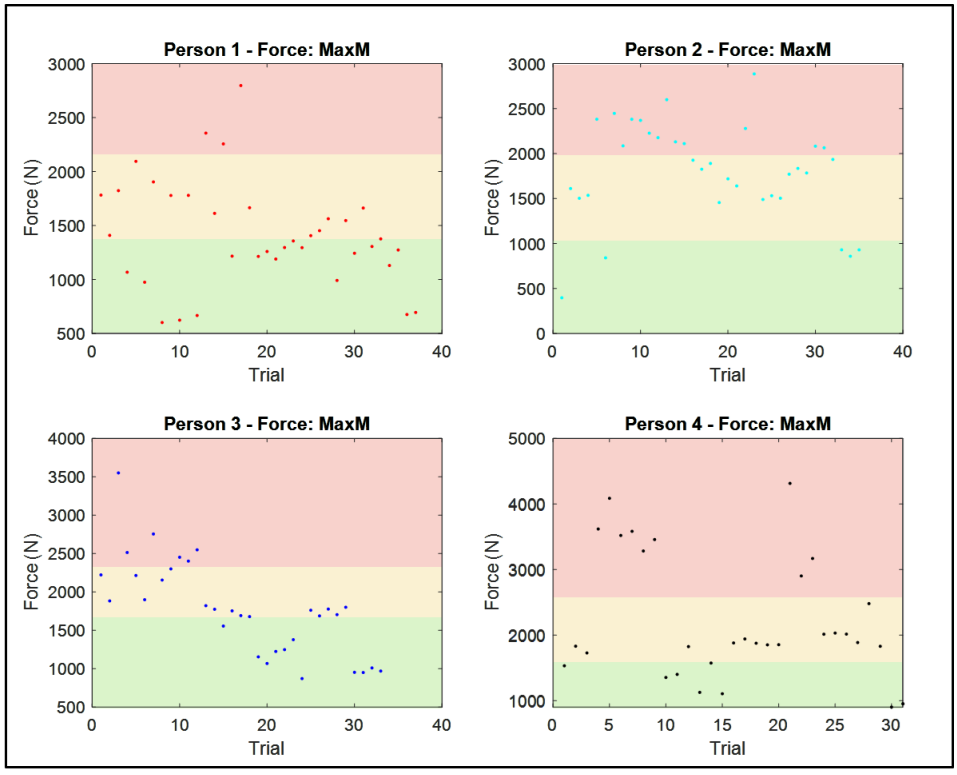

Figure 48: Conceptualising the long-term goal of this research - a risk scale generated for resultant peak force.

Activities and Technique

- Determine how specific activity types contribute towards model kinetics.
- Consider whether a model that *identifies movement* and uses an algorithm to predict the force based on the identified movement can make an effective prediction model design.

- Determine how differences in landing technique change prediction accuracy and how the models should adapt to a change in technique over time.
- Determine the primary factors that contribute to inter-participant correlation variability.
- Determine how participant athletic ability affects model accuracy across age, gender, skill, and impairment.
- Determine whether leg dominance is an indicator of model performance; and whether the kinematics of one leg can predict the kinematics of the other leg; and whether leg-specific performance is important for model accuracy.
- Determine whether the effects of footwear and terrain (e.g. timber vs. concrete) must be factored into the model, or whether the effects of these are negligent.
- Determine whether the kind of knee and ankle stabilisation braces as frequently worn by netball players[86] diminishes propulsive power and will inhibit the accuracy of a predicted model.

Data Analysis

- Determine activity frequency components such that an appropriate sampling frequency can be selected.
- Determine exactly what portion of the frequency spectrum pertain to the events that correlate and design filters accordingly.
- Determine whether acceleration in the global vertical axis or in the transverse plane (as relative to the axial axis) are beneficial for load prediction.
- Determine whether different and applicable machine learning models are more effective at modelling force with acceleration than the non-linear input-output timeseries neural network that was used in this investigation.
    - Consider single event prediction rather waveform prediction.
    - Perhaps consider sinusoidal or polynomial approximation models.
- Consider revisiting linear and logarithmic correlations following a *large, uniform, single-activity cohort study.*

[86] Chapter 1.1.2, *Considering a Device*.

Study Design

- Determine whether it is necessary to first validate a prediction model for a single kind of movement, rather than a range of different movements. This may eliminate the variability of results as obtained in the preceding investigation.
    - Perhaps consider undertaking a cyclic activity study.
- Eventually, design a study that collects data from a comprehensive list of activities, such that the force prediction of *any* activity that may be monitored with the device can be validated.
- Determine inter-session location repeatability and effect (i.e. whether minimal placement changes dramatically negatively affect model prediction accuracy).
- Determined how the presence of movement artefact and soft tissue attenuation can be detected, perhaps through a calibration routine with a motion capture system. Use this information to determine an optimal method for securing the device to remove such noise.
- Determine an effective method of device attachment such that movement artefact is minimised.
    - Perhaps undertake a study in which several people are given different kinds of devices, collecting information on overall device preference, comfortability, and intrusive features.

8.2.1. Recommended Priority

In light of all that has been considered, the following steps are a recommended as a way forward:

1. Determine whether and in what way impulse can be used as a measure of impact dose, and how this can contribute to injury prevention and a measure of participant risk.
2. Identify or design a wearable accelerometer that has minimum movement artefact when attached.
3. Conduct a trial with a large sample size in an attempt to reproduce the high integration correlation results and prove the relevance of the prediction for overuse injury risk.

Chapter 9. Thesis Conclusion

9.1. Conclusion

Having reviewed the literature and undertaken an investigation into the characteristics of the force-acceleration relationship, the preceding research will now be concluded on.

9.1.1. Conclusion

The aim of this investigation was to determine whether there is a relationship between force and acceleration at the lower limb that can be accurately modelled using data from wearable accelerometers; and whether this relationship can be generalised across subjects, movements, and external conditions such that it is useful for injury management and prevention.

This research has demonstrated that there is a relationship between ground reaction force and acceleration at the lower limb. But, as seen in both the literature and in the investigation, this relationship is highly dependent on activity, technique, model, and data preparation, and it may be observed to produce inconsistent results. The results of the validation investigation were not consistent with the literature-based correlations, but this was likely due to variance in study design, cohort size, and activities undertaken in the trial.

The strongest relationship identified was between the integration of force, which is impulse, and acceleration. This was consistently *very large* to *almost perfect* across participants, and the highest linear correlation was obtained at the ankle. Although the shank and thigh also produced, on average, at least *very large* impulse correlations, the ankle lateral malleolus was generally higher and was deemed optimal. The strongest correlation at the ankle was between vertical force and axial acceleration. The variability of results may indicate that although a relationship is present, it may not be immediately generalisable between subjects, movements, and external conditions.

The small cohort used in the present investigation did not produce consistently high event-based correlations. Although the linear and logarithmic models were at times able to predict accurately between events, the results between participants were not consistent. The best indicator of event-based relationships was the global cohort averages. These indicated that the force magnitude increases with acceleration magnitude, but that there are many challenges that must be yet overcome before the accuracy of these inter-person results will be consistent. As the machine learning model that was applied did not predict the force waveform above a *moderate* accuracy, it was deemed more accurate than the linear and logarithmic event modelling. With the qualification that there were no correlations that consistently measured above moderate in all

models (except for integration at the ankle), the medial shank was determined to be the most accurate location from which to predict force waveform events.

The study has demonstrated both from the literature and from the investigation that an accurate relationship between force and acceleration can be modelled using wearable accelerometers. However, the accuracy variance between literature studies and this investigation demonstrated that there are factors deeper than surface acceleration that contribute to an accurate model of force. The generalised relationships produced a similar degree of accuracy as the subject-specific models, but the variability between studies indicates that further research is necessary to confirm the global validity of these models.

The investigation was unable to contribute to an understanding of injury prediction and objective impact dose, but based on the literature, there does seem to be clinical relevance for the prediction of force from acceleration. Future research must now consider precisely how these objective kinematic quantities can be used to define an objective and accurate assessment of risk level between individuals. Future studies should consider larger cohorts and determine whether the results of this investigation can be reproduced. If an objective measure of injury risk can be established, and be objectively quantified in terms of these results, then the strong relationships that have been observed may become a broadly used level of preventative and rehabilitative study.

The sooner that these safe dosage levels can be quantified, the sooner that this technology can be applied in aiding chronic pain and reducing the risk of overuse injury for elite and non-elite athletes, and in both rehabilitation and physiological monitoring.

References

ABDELHADY, M., VAN DEN BOGERT, A. J. & SIMON, D. 2019. A High-Fidelity Wearable System for Measuring Lower-Limb Kinetics and Kinematics. *IEEE Sensors Journal,* 19**,** 12482-12493.

ALAQTASH, M., YU, H., BROWER, R., ABDELGAWAD, A. & SARKODIE-GYAN, T. 2011. Application of wearable sensors for human gait analysis using fuzzy computational algorithm. *Engineering Applications of Artificial Intelligence,* 24**,** 1018-1025.

ALAQTASH, M., YU, H., BROWER, R., ABDELGAWAD, A., SPIER, E. & SARKODIE-GYAN, T. 2010. *Application of Wearable Miniature Non-invasive Sensory System in Human Locomotion Using Soft Computing Algorithm,* Berlin, Heidelberg, Berlin, Heidelberg: Springer Berlin Heidelberg.

ANTONSSON, E. K. & MANN, R. W. 1985. The frequency content of gait. *Journal of biomechanics,* 18**,** 39-47.

ARAMI, A., AMINIAN, K., FORCHELET, D. & RENAUD, P. 2014. Implantable and wearable measurement system for smart knee prosthesis.

AUSTRALIAN FOOTBALL LEAGUE 2019. *Laws of Australian Football,* Melbourne, Victoria.

BAILEY, A. M., MCMURRY, T. L., SALZAR, R. S. & CRANDALL, J. R. 2018. An Injury Risk Function for the Leg, Foot, and Ankle Exposed to Axial Impact Loading Using Force and Impulse. *Journal of Biomechanical Engineering,* 141.

BAILEY, J. A., GASTIN, P. B., MACKEY, L. & DWYER, D. B. 2017. The Player Load Associated With Typical Activities in Elite Netball. *Int J Sports Physiol Perform,* 12**,** 1218-1223.

BERNARDS, J. R., SATO, K., HAFF, G. G. & BAZYLER, C. D. 2017. Current Research and Statistical Practices in Sport Science and a Need for Change. *Sports (Basel),* 5**,** 87.

BEST, G. 2017. EPIDEMIOLOGY AND INCIDENCE OF INJURY IN ELITE NETBALL PLAYERS - AN INJURY AUDIT OF THE 2016 NETBALL SUPERLEAGUE SEASON. *British Journal of Sports Medicine,* 51**,** 297.

BISSELL, L. & LORENTZOS, P. 2018. The prevalence of overuse injuries in Australian non-elite netballers. *Open Access Journal of Sports Medicine,* 9**,** 233+.

BLAND, J. M. & ALTMAN, D. G. 2009. Analysis of continuous data from small samples. *BMJ,* 338**,** a3166.

BOBBERT, M. F., YEADON, M. R. & NIGG, B. M. 1992. Mechanical analysis of the landing phase in heel-toe running. *Journal of Biomechanics,* 25**,** 223-234.

BROWNE, M. G. & FRANZ, J. R. 2019. Ankle power biofeedback attenuates the distal-to-proximal redistribution in older adults. *Gait & Posture,* 71**,** 44-49.

BRUCE, O. L., FIRMINGER, C. R., WANNOP, J. W., STEFANYSHYN, D. J. & EDWARDS, W. B. 2019. Effects of basketball court construction and shoe stiffness on countermovement jump landings. *Footwear Science,* 11**,** 171-179.

BRUKNER, P. D. & BENNELL, K. L. 2020. *Chapter 3 - Stress Fractures: Their Causes and Principles of Treatment*.

CALLAGHAN, S. J., LOCKIE, R. G., ANDREWS, W. A., CHIPCHASE, R. F. & NIMPHIUS, S. 2018. The relationship between inertial measurement unit-derived 'force signatures' and ground reaction forces during cricket pace bowling. *Sports Biomechanics***,** 1-15.

CHARRY, E., WENZHENG, H., UMER, M., RONCHI, A. & TAYLOR, S. 2013. Study on estimation of peak Ground Reaction Forces using tibial accelerations in running. IEEE Eighth International Conference on Intelligent Sensors, Sensor Networks and Information Processing.

CLARK, K. P., RYAN, L. J. & WEYAND, P. G. 2014. Foot speed, foot-strike and footwear: linking gait mechanics and running ground reaction forces.(Report). *Journal of Experimental Biology,* 217**,** 2037.

CLARK, K. P., RYAN, L. J. & WEYAND, P. G. 2017. A general relationship links gait mechanics and running ground reaction forces. *The Journal of experimental biology,* 220**,** 247-258.

COLBY, J. M., DAWSON, J. B., HEASMAN, J. J., ROGALSKI, J. B. & GABBETT, J. T. 2014. Accelerometer and GPS-Derived Running Loads and Injury Risk in Elite Australian Footballers. *Journal of Strength and Conditioning Research,* 28**,** 2244-2252.

CORBO, E. 2018. The Design and Development of a Wearable Device to Assess Lower-Limb Impact Dose during Competitive Netball Play. *Flinders University*.

COVENTRY, E., O'CONNOR, K. M., HART, B. A., EARL, J. E. & EBERSOLE, K. T. 2006. The effect of lower extremity fatigue on shock attenuation during single-leg landing. *Clinical Biomechanics,* 21**,** 1090-1097.

CROWELL, H. P. & DAVIS, I. S. 2011. Gait retraining to reduce lower extremity loading in runners. *Clinical Biomechanics,* 26**,** 78-83.

DAN, M. J., LUN, K. K., DAN, L., EFIRD, J., PELLETIER, M., BROE, D. & WALSH, W. R. 2019. Wearable inertial sensors and pressure MAT detect risk factors associated with ACL graft failure that are not possible with traditional return to sport assessments. *BMJ Open Sport & Exercise Medicine,* 5.

DAVIS, I., HAYANO, T. & TENFORDE, A. 2018. The Relationship Between Vertical Loadrates and Tibial Acceleration Across Footstrike Patterns. *Foot & Ankle Orthopaedics,* 3.

DEVITA, A. P. & SKELLY, A. W. 1992. Effect of landing stiffness on joint kinetics and energetics in the lower extremity. *Medicine & Science in Sports & Exercise,* 24**,** 108-115.

EHRMANN, E. F., DUNCAN, S. C., SINDHUSAKE, N. D., FRANZSEN, A. W. & GREENE, A. D. 2016. GPS and Injury Prevention in Professional Soccer. *Journal of Strength and Conditioning Research,* 30**,** 360-367.

ELVIN, N., ELVIN, A. & ARNOCZKY, S. 2007. Correlation between Ground Reaction Force and Tibial Acceleration in Vertical Jumping. *Journal of applied biomechanics,* 23**,** 180-9.

FÉDÉRATION INTERNATIONALE DE VOLLEYBALL 2016. *Official Volleyball Rules 2017-2020*.

FUTRELL, E. E., GROSS, K. D., REISMAN, D., MULLINEAUX, D. R. & DAVIS, I. S. 2020. Transition to forefoot strike reduces load rates more effectively than altered cadence. *Journal of Sport and Health Science,* 9**,** 248-257.

GABBETT, J. T. & ULLAH, J. S. 2012. Relationship Between Running Loads and Soft-Tissue Injury in Elite Team Sport Athletes. *Journal of Strength and Conditioning Research,* 26**,** 953-960.

GOKELER, A., WELLING, W., ZAFFAGNINI, S., SEIL, R. & PADUA, D. 2017. Development of a test battery to enhance safe return to sports after anterior cruciate ligament reconstruction. *Knee Surgery, Sports Traumatology, Arthroscopy,* 25**,** 192-199.

GUO, Y., STORM, F., ZHAO, Y., BILLINGS, S. A., PAVIC, A., MAZZÀ, C. & GUO, L.-Z. 2017. A New Proxy Measurement Algorithm with Application to the Estimation of Vertical Ground Reaction Forces Using Wearable Sensors. *Sensors (Basel, Switzerland),* 17.

HAVENS, K. L., COHEN, S. C., PRATT, K. A. & SIGWARD, S. M. 2018. Accelerations from wearable accelerometers reflect knee loading during running after anterior cruciate ligament reconstruction. *Clinical Biomechanics,* 58**,** 57-61.

HENNIG, E. & LAFORTUNE, M. Tibial bone and skin accelerations during running. Cotton CE, Lamontagne M, Robertson DGE, Stothart JPProceedings of the Fifth Biennial Conference of the Canadian Society for Biomechanics. Ottawa: Spodym Publishers, 1988. 74-5.

HENNIG, E. & LAFORTUNE, M. A. 1991. RELATIONSHIPS BETWEEN GROUND REACTION FORCE AND TIBIAL BONE ACCELERATION PARAMETERS. *International Journal Of Sport Biomechanics,* 7**,** 303-309.

HOPKINS, W. 2006. *A New View of Statistics: A Scale of Magnitudes for Effect Statistics* [Online]. Available: http://www.sportsci.org/resource/stats/index.html [Accessed 29 August 2020].

HOPKINS, W. G., MARSHALL, S. W., BATTERHAM, A. M. & HANIN, J. 2009. Progressive Statistics for Studies in Sports Medicine and Exercise Science. *Medicine & Science in Sports & Exercise,* 41.

HOPPER, D. & ELLIOTT, B. 1993. Lower limb and back injury patterns of elite netball players. *Sports Med,* 16**,** 148-62.

HOPPER, D., ELLIOTT, B. & LALOR, J. 1995. A descriptive epidemiology of netball injuries during competition: a five year study. *British Journal of Sports Medicine,* 29**,** 223.

HUME, P. A. & STEELE, J. R. 2000. A preliminary investigation of injury prevention strategies in netball: Are players heeding the advice? *Journal of Science and Medicine in Sport,* 3**,** 406-413.

HUNTER, J. P., MARSHALL, R. N. & MCNAIR, P. J. 2005. Relationships between ground reaction force impulse and kinematics of sprint-running acceleration. *Journal of applied biomechanics,* 21**,** 31-43.

INTERNATIONAL BASKETBALL FEDERATION 2020. *2020 Official Basketball Rules: Basketball Rules & Basketball Equipment,* Mies, Switzerland.

INTERNATIONAL NETBALL FEDERATION 2020. Rules of Netball, 21-23.

JACOBS, D. A. & FERRIS, D. P. 2015. Estimation of ground reaction forces and ankle moment with multiple, low-cost sensors. *Journal of NeuroEngineering and Rehabilitation,* 12.

JIANG, X., GHOLAMI, M., KHOSHNAM, M., ENG, J. J. & MENON, C. 2019. Estimation of Ankle Joint Power during Walking Using Two Inertial Sensors. *Sensors (Basel, Switzerland),* 19.

KIERNAN, D., HAWKINS, D. A., MANOUKIAN, M. A. C., MCKALLIP, M., OELSNER, L., CASKEY, C. F. & COOLBAUGH, C. L. 2018. Accelerometer-based prediction of running injury in National Collegiate Athletic Association track athletes. *Journal of Biomechanics,* 73**,** 201-209.

LAFORTUNE, M. A. 1991. Three-dimensional acceleration of the tibia during walking and running. *Journal of Biomechanics,* 24**,** 877,881-879,886.

LAFORTUNE, M. A., LAKE, M. J. & HENNIG, E. 1995. Transfer function between tibial acceleration and ground reaction force. *Journal of Biomechanics,* 28**,** 113-117.

LAFORTUNE, M. A., LAKE, M. J. & HENNIG, E. M. 1996. Differential shock transmission response of the human body to impact severity and lower limb posture. *Journal of biomechanics,* 29**,** 1531-1537.

LEE, Y.-S., HO, C.-S., SHIH, Y., CHANG, S.-Y., RÓBERT, F. J. & SHIANG, T.-Y. 2015. Assessment of walking, running, and jumping movement features by using the inertial measurement unit. *Gait & Posture,* 41**,** 877-881.

LEWIS, L. M., NAUNHEIM, R., STANDEVEN, J., LAURYSSEN, C., RICHTER, C. & JEFFORDS, B. 2001. Do Football Helmets Reduce Acceleration of Impact in Blunt Head Injuries? *Academic Emergency Medicine,* 8**,** 604-609.

LIIKAVAINIO, T., BRAGGE, T., HAKKARAINEN, M., JURVELIN, J. S., KARJALAINEN, P. A. & AROKOSKI, J. P. 2007. Reproducibility of Loading Measurements With Skin-Mounted Accelerometers During Walking. *Archives of Physical Medicine and Rehabilitation,* 88**,** 907-915.

MACADAM, D. P., SIMPERINGHAM, B. K. & CRONIN, B. J. 2017. Acute Kinematic and Kinetic Adaptations to Wearable Resistance During Sprint Acceleration. *Journal of Strength and Conditioning Research,* 31**,** 1297-1304.

MACWILLIAMS, B. A., COWLEY, M. & NICHOLSON, D. E. 2003. Foot kinematics and kinetics during adolescent gait. *Gait & Posture,* 17**,** 214-224.

MAHDAVIAN, M., ARZANPOUR, S. & PARK, E. J. Motion Generation of a Wearable Hip Exoskeleton Robot Using Machine Learning-Based Estimation of Ground Reaction Forces and Moments. 2019 IEEE/ASME International Conference on Advanced Intelligent Mechatronics (AIM), 8-12 July 2019 2019. 796-801.

MARIN, F., LEPETIT, K., FRADET, L., HANSEN, C. & BEN MANSOUR, K. 2020. Using accelerations of single inertial measurement units to determine the intensity level of light-moderate-vigorous physical activities: Technical and mathematical considerations. *J Biomech,* 107**,** 109834.

MATHWORKS. 2020. *Shallow Neural Network Time-Series Prediction and Modeling* [Online]. Available: https://www.mathworks.com/help/deeplearning/gs/neural-network-time-series-prediction-and-modeling.html [Accessed 9 October 2020].

MCMANUS, A., STEVENSON, M. R. & FINCH, C. F. 2006. Incidence and risk factors for injury in non-elite netball. *Journal of Science and Medicine in Sport,* 9**,** 119-124.

MERO, A. 1988. Force-Time Characteristics and Running Velocity of Male Sprinters during the Acceleration Phase of Sprinting. *Research Quarterly for Exercise and Sport,* 59**,** 94-98.

MEYER, U., ERNST, D., SCHOTT, S., RIERA, C., HATTENDORF, J., ROMKES, J., GRANACHER, U., GÖPFERT, B. & KRIEMLER, S. 2015. Validation of two accelerometers to determine mechanical loading of physical activities in children. *Journal of Sports Sciences,* 33**,** 1702-1709.

MUNDT, M., KOEPPE, A., DAVID, S., WITTER, T., BAMER, F., POTTHAST, W. & MARKERT, B. 2020. Estimation of Gait Mechanics Based on Simulated and Measured IMU Data Using an Artificial Neural Network. *Frontiers in bioengineering and biotechnology,* 8**,** 41-41.

NETBALL AUSTRALIA. 2016. *Footwork and Movement skills* [Online]. Available: https://www.youtube.com/watch?v=rtnDm52t_eM [Accessed 13 October 2020].

NETBALL AUSTRALIA. 2019. *Netball continues to lead for women and girls* [Online]. Available: https://netball.com.au/news/netball-continues-lead-women-and-girls [Accessed 8 October 2020].

NOSHADI, H., DABIRI, F., AHMADIAN, S., AMINI, N. & SARRAFZADEH, M. 2013. HERMES: Mobile system for instability analysis and balance assessment. *ACM Transactions on Embedded Computing Systems (TECS),* 12**,** 1-24.

PENGHAI, W., HAIYANG, Q. & LIDONG, L. 2014. A Wireless Wearable Human Jump Analysis System. *International journal on smart sensing and intelligent systems,* 7.

PIEPER, N. L., LEWEK, M. D. & FRANZ, J. R. 2020. Can shank acceleration provide a clinically feasible surrogate for individual limb propulsion during walking? *Journal of Biomechanics,* 98.

PRADKO, F., LEE, R. A. AND GREENE, J. D., BYARS, E. F., CONTINI, R. & ROBERTS, V. L. 1967. *Human vibration-response theory, in: Biomechanics monograph*, American Society of Mechanical Engineers.

PUYAU, M. R., ADOLPH, A. L., VOHRA, F. A. & BUTTE, N. F. 2002. Validation and calibration of physical activity monitors in children. *Obes Res,* 10**,** 150-7.

RANTALAINEN, T., GASTIN, P. B., SPANGLER, R. & WUNDERSITZ, D. 2018. Concurrent validity and reliability of torso-worn inertial measurement unit for jump power and height estimation. *Journal of Sports Sciences,* 36**,** 1937-1942.

RAPER, D. P., WITCHALLS, J., PHILIPS, E. J., KNIGHT, E., DREW, M. K. & WADDINGTON, G. 2018. Use of a tibial accelerometer to measure ground reaction force in running: A reliability and validity comparison with force plates. *Journal of Science and Medicine in Sport,* 21**,** 84-88.

REENALDA, J., MAARTENS, E., HOMAN, L. & BUURKE, J. H. 2016. Continuous three dimensional analysis of running mechanics during a marathon by means of inertial magnetic measurement units to objectify changes in running mechanics. *Journal of Biomechanics,* 49**,** 3362-3367.

ROUHANI, H., FAVRE, J., CREVOISIER, X. & AMINIAN, K. 2014. A wearable system for multi-segment foot kinetics measurement. *Journal of Biomechanics,* 47**,** 1704-1711.

SAZONOV, E. S., FULK, G., HILL, J., SCHUTZ, Y. & BROWNING, R. 2011. Monitoring of Posture Allocations and Activities by a Shoe-Based Wearable Sensor. *IEEE Transactions on Biomedical Engineering,* 58**,** 983-990.

SCHNEUER, F., BELL, J., ADAMS, S., BROWN, J., FINCH, C. & NASSAR, N. 2018. The burden of hospitalized sports-related injuries in children: an Australian population-based study, 2005–2013. *Injury Epidemiology,* 5**,** 1-10.

SCOTT, S. H. & WINTER, D. A. 1993. Biomechanical model of the human foot: Kinematics and kinetics during the stance phase of walking. *Journal of Biomechanics,* 26**,** 1091-1104.

SHAHABPOOR, E. & PAVIC, A. 2017. Measurement of Walking Ground Reactions in Real-Life Environments: A Systematic Review of Techniques and Technologies. *Sensors (Basel, Switzerland),* 17.

SIMONS, C. & BRADSHAW, E. J. 2016. Do accelerometers mounted on the back provide a good estimate of impact loads in jumping and landing tasks? *Sports Biomechanics,* 15**,** 76-88.

SIMPSON, M. J., JENKINS, D. G., LEVERITT, M. D. & KELLY, V. G. 2019. Physical profiles of elite, sub-elite, regional and age-group netballers. *Journal of Sports Sciences,* 37**,** 1212-1219.

STEVENSON, M. R., HAMER, P., FINCH, C. F., ELLIOT, B. & KRESNOW, M. 2000. Sport, age, and sex specific incidence of sports injuries in Western Australia. *British journal of sports medicine,* 34**,** 188-194.

TAKEDA, R., TADANO, S., TODOH, M., MORIKAWA, M., NAKAYASU, M. & YOSHINARI, S. 2009. Gait analysis using gravitational acceleration measured by wearable sensors. *Journal of Biomechanics,* 42**,** 223-233.

TALUKDER, A. 2020. *The design and development of a wearable device to assess lower-limb impact dose during competitive netball play.* Masters by Coursework, Thesis (Masters).

TAN, T., STROUT, Z. A. & SHULL, P. B. 2020. Accurate impact loading rate estimation during running via a subject-independent convolutional neural network model and optimal IMU placement. *IEEE Journal of Biomedical and Health Informatics***,** 1-1.

TAO, L., INOUE, Y., SHIBATA, K. & RENCHENG, Z. 2007. Measurement of human lower limb orientations and ground reaction forces using wearable sensor systems.

TENFORDE, A. S., HAYANO, T., JAMISON, S. T., OUTERLEYS, J. & DAVIS, I. S. 2020. Tibial Acceleration Measured from Wearable Sensors Is Associated with Loading Rates in Injured Runners. *PM&R,* 12**,** 679-684.

TONG, K. & GRANAT, M. H. 1999. A practical gait analysis system using gyroscopes. *Medical Engineering and Physics,* 21**,** 87-94.

TRAN, J., NETTO, K., AISBETT, B. & GASTIN, P. 2012. *Validation of accelerometer data for measuring impacts during jumping and landing tasks*.

UDOFA, A. B., RYAN, L. J. & WEYAND, P. G. 2016. Impact forces during running: Loaded questions, sensible outcomes.

WILLY, R., BUCHENIC, L., ROGACKI, K., ACKERMAN, J., SCHMIDT, A. & WILLSON, J. 2016. In-field gait retraining and mobile monitoring to address running biomechanics associated with tibial stress fracture. *Scandinavian journal of medicine & science in sports,* 26**,** 197-205.

WINTER, M. E. 2005. JUMPING: POWER OR IMPULSE? *Medicine & Science in Sports & Exercise,* 37**,** 523-523.

WORLD RUGBY. 2019. *World Rugby Handbook: Regulation 12. PROVISIONS RELATING TO PLAYERS' DRESS* [Online]. Available: https://www.world.rugby/handbook/regulations/reg-12 [Accessed 4 September 2020].

WOUDA, F. J., GIUBERTI, M., BELLUSCI, G., MAARTENS, E., REENALDA, J., VAN BEIJNUM, B. F. & VELTINK, P. H. 2018. Estimation of Vertical Ground Reaction Forces and Sagittal Knee Kinematics During Running Using Three Inertial Sensors. *Front Physiol,* 9**,** 218.

WUNDERSITZ, D. W., GASTIN, P. B., RICHTER, C., ROBERTSON, S. J. & NETTO, K. J. 2015. Validity of a trunk-mounted accelerometer to assess peak accelerations during walking, jogging and running. *European journal of sport science,* 15**,** 382-390.

WUNDERSITZ, D. W. T., NETTO, K. J., AISBETT, B. & GASTIN, P. B. 2013. Validity of an upper-body-mounted accelerometer to measure peak vertical and resultant force during running and change-of-direction tasks. *Sports Biomechanics,* 12**,** 403-412.

ZATSIORSKY, V. M. & ZACIORSKIJ, V. M. 2002. *Kinetics of human motion*, Human Kinetics.

ZECA, I., GUO, Y., STORM, F., MAZZA, C. & GUO, L. 2018. Estimation of Centre of Pressure from Wearable Intertial Sensors. *UKACC 12th International Conference on Control***,** 450-455.

ZHANG, S., DERRICK, T. R., EVANS, W. & YU, Y.-J. 2008. Shock and impact reduction in moderate and strenuous landing activities. *Sports Biomechanics,* 7**,** 296-309.

Appendices

Appendix A. Linear Correlations

The following tables provide the results of the event-to-event linear correlation experiment using the 50 Hz filtered data.

Table 28: Individual participant thigh correlations.

Force	Acceleration													
P1Thigh	MHEIGHT	MINTEG	MMAX	MMIN	XHEIGHT	XINTEG	XMAX	XMIN	YHEIGHT	YMAX	YMIN	ZHEIGHT	ZMAX	ZMIN
MINTEG	0.2366	0.8429	0.1684	0.0255	0.0011	0.8747	0.0491	0.0431	0.0624	0.0312	0.0690	0.0218	0.1210	0.0159
MMAX	0.3782	0.0342	0.3984	0.0300	0.3309	0.0213	0.2219	0.2198	0.3545	0.3195	0.2138	0.6012	0.3993	0.4806
VALR	0.0746	0.0054	0.1201	0.0885	0.3685	0.0392	0.4168	0.0991	0.1443	0.2103	0.0338	0.2694	0.1434	0.2647
VILR	0.0836	0.0040	0.1334	0.0962	0.3657	0.0378	0.3922	0.1116	0.1486	0.2176	0.0344	0.2882	0.1667	0.2634
ZINTEG	0.2297	0.8388	0.1621	0.0266	0.0025	0.8781	0.0560	0.0385	0.0531	0.0242	0.0628	0.0186	0.1191	0.0205
ZMIN	0.3691	0.0297	0.3952	0.0352	0.3312	0.0178	0.2156	0.2279	0.3288	0.2915	0.2028	0.5827	0.3915	0.4603
P2Thigh	MHEIGHT	MINTEG	MMAX	MMIN	XHEIGHT	XINTEG	XMAX	XMIN	YHEIGHT	YMAX	YMIN	ZHEIGHT	ZMAX	ZMIN
MINTEG	0.1505	0.9146	0.2034	0.1018	0.1961	0.9215	0.1646	0.1672	0.0948	0.0112	0.1490	0.0888	0.1716	0.0105
MMAX	0.2241	0.1305	0.2520	0.0547	0.2817	0.0869	0.2381	0.2382	0.1204	0.1184	0.0520	0.1816	0.0592	0.2911
VALR	0.2078	0.3251	0.2882	0.1577	0.4446	0.2321	0.4463	0.3067	0.2477	0.1761	0.1561	0.2775	0.2016	0.2503
VILR	0.2232	0.3813	0.2909	0.1273	0.4305	0.3429	0.4052	0.3218	0.1924	0.1030	0.1546	0.2488	0.1994	0.2022
ZINTEG	0.1466	0.9126	0.1992	0.1016	0.1914	0.9196	0.1608	0.1629	0.0928	0.0109	0.1459	0.0846	0.1659	0.0094
ZMIN	0.2035	0.1282	0.2290	0.0499	0.2498	0.0871	0.2082	0.2145	0.1103	0.1158	0.0433	0.1486	0.0416	0.2562
P3Thigh	MHEIGHT	MINTEG	MMAX	MMIN	XHEIGHT	XINTEG	XMAX	XMIN	YHEIGHT	YMAX	YMIN	ZHEIGHT	ZMAX	ZMIN
MINTEG	0.0655	0.8347	0.1318	0.1553	0.3202	0.9319	0.3781	0.1646	0.0669	0.1005	0.0119	0.1107	0.0880	0.1024
MMAX	0.5220	0.1359	0.6396	0.1108	0.5290	0.1861	0.3335	0.5820	0.3702	0.3573	0.2097	0.4565	0.3192	0.4718
VALR	0.3425	0.0082	0.3609	0.0115	0.3032	0.0142	0.1984	0.3229	0.2723	0.1994	0.2326	0.2232	0.1113	0.2927
VILR	0.2799	0.0031	0.2861	0.0047	0.2092	0.0007	0.1242	0.2419	0.2207	0.1466	0.2117	0.1704	0.0758	0.2387
ZINTEG	0.0669	0.8340	0.1340	0.1563	0.3228	0.9319	0.3798	0.1669	0.0688	0.1027	0.0127	0.1119	0.0890	0.1036
ZMIN	0.5161	0.1351	0.6283	0.1038	0.5221	0.1835	0.3281	0.5759	0.3498	0.3392	0.1965	0.4526	0.3131	0.4717
P4Thigh	MHEIGHT	MINTEG	MMAX	MMIN	XHEIGHT	XINTEG	XMAX	XMIN	YHEIGHT	YMAX	YMIN	ZHEIGHT	ZMAX	ZMIN
MINTEG	0.4178	0.7939	0.4483	0.0001	0.2459	0.9152	0.1662	0.2671	0.4882	0.4630	0.3520	0.3985	0.4122	0.2584
MMAX	0.6787	0.6321	0.7420	0.0002	0.3451	0.3337	0.1595	0.5096	0.6609	0.6740	0.4127	0.7801	0.7491	0.5738
VALR	0.1041	0.0320	0.1970	0.1304	0.0354	0.0000	0.0042	0.0935	0.1172	0.1128	0.0821	0.2593	0.1790	0.2952
VILR	0.1400	0.0477	0.2371	0.1062	0.0419	0.0015	0.0045	0.1129	0.1495	0.1561	0.0887	0.2956	0.2142	0.3187
ZINTEG	0.4176	0.7954	0.4474	0.0001	0.2471	0.9166	0.1677	0.2673	0.4880	0.4616	0.3534	0.3959	0.4095	0.2568
ZMIN	0.6800	0.6434	0.7444	0.0002	0.3568	0.3450	0.1703	0.5153	0.6675	0.6717	0.4285	0.7754	0.7418	0.5737

Table 29: Individual participant shank correlations.

Force	Acceleration													
P1Shank	MHEIGHT	MINTEG	MMAX	MMIN	XHEIGHT	XINTEG	XMAX	XMIN	YHEIGHT	YMAX	YMIN	ZHEIGHT	ZMAX	ZMIN
MINTEG	0.0049	0.8579	0.0033	0.0046	0.0069	0.4961	0.0035	0.0061	0.0711	0.0066	0.1705	0.0476	0.0106	0.1374
MMAX	0.1738	0.0459	0.1753	0.0126	0.3549	0.0836	0.4957	0.0067	0.3257	0.4546	0.0487	0.3123	0.2821	0.2706
VALR	0.4260	0.0016	0.4909	0.2256	0.3040	0.0869	0.2451	0.1171	0.2061	0.4191	0.0008	0.4031	0.3748	0.3330
VILR	0.4367	0.0011	0.4971	0.2040	0.3009	0.0783	0.2366	0.1231	0.2171	0.4208	0.0025	0.4081	0.3859	0.3273
ZINTEG	0.0028	0.8541	0.0015	0.0060	0.0060	0.5028	0.0033	0.0047	0.0660	0.0043	0.1720	0.0399	0.0076	0.1228
ZMIN	0.1611	0.0375	0.1614	0.0097	0.3492	0.0862	0.4903	0.0061	0.3033	0.4303	0.0424	0.2887	0.2645	0.2444
P2Shank	MHEIGHT	MINTEG	MMAX	MMIN	XHEIGHT	XINTEG	XMAX	XMIN	YHEIGHT	YMAX	YMIN	ZHEIGHT	ZMAX	ZMIN
MINTEG	0.2386	0.9060	0.1359	0.2813	0.2270	0.9351	0.2549	0.1066	0.0009	0.0091	0.0182	0.1247	0.1340	0.0594
MMAX	0.3794	0.1361	0.3906	0.0021	0.3957	0.0705	0.3455	0.3252	0.1574	0.0633	0.1186	0.2645	0.1608	0.3339
VALR	0.6079	0.3324	0.5813	0.0285	0.3758	0.2162	0.3646	0.2508	0.1167	0.1357	0.0229	0.6185	0.5460	0.4508
VILR	0.6258	0.3877	0.5423	0.1001	0.4023	0.2841	0.3645	0.3084	0.1059	0.0767	0.0462	0.5158	0.4820	0.3367
ZINTEG	0.2345	0.9029	0.1321	0.2850	0.2254	0.9345	0.2535	0.1052	0.0006	0.0107	0.0184	0.1206	0.1296	0.0574
ZMIN	0.3569	0.1314	0.3623	0.0037	0.3840	0.0705	0.3332	0.3193	0.1433	0.0466	0.1238	0.2385	0.1407	0.3115
P3Shank	MHEIGHT	MINTEG	MMAX	MMIN	XHEIGHT	XINTEG	XMAX	XMIN	YHEIGHT	YMAX	YMIN	ZHEIGHT	ZMAX	ZMIN
MINTEG	0.0841	0.9137	0.0516	0.0349	0.0888	0.9030	0.2074	0.0599	0.0319	0.0039	0.0821	0.1056	0.1819	0.0015
MMAX	0.0593	0.1600	0.1289	0.2087	0.5335	0.2113	0.4671	0.1416	0.1493	0.2171	0.0047	0.0978	0.0373	0.1396
VALR	0.3275	0.0078	0.4567	0.2124	0.5410	0.0254	0.3629	0.3277	0.3631	0.3855	0.0800	0.1931	0.1595	0.1067
VILR	0.3720	0.0031	0.4943	0.1838	0.5001	0.0002	0.3187	0.3405	0.3905	0.3847	0.1107	0.2214	0.2051	0.0966
ZINTEG	0.0825	0.9133	0.0502	0.0356	0.0893	0.9030	0.2069	0.0583	0.0303	0.0033	0.0813	0.1026	0.1780	0.0012

ZMIN	0.0555	0.1570	0.1210	0.1965	0.5402	0.2071	0.4838	0.1304	0.1326	0.1916	0.0045	0.0834	0.0290	0.1280
P4Shank	MHEIGHT	MINTEG	MMAX	MMIN	XHEIGHT	XINTEG	XMAX	XMIN	YHEIGHT	YMAX	YMIN	ZHEIGHT	ZMAX	ZMIN
MINTEG	0.5524	0.9203	0.5330	0.0036	0.4054	0.9478	0.3619	0.3810	0.3856	0.5117	0.0631	0.5586	0.5713	0.2284
MMAX	0.5594	0.4863	0.6452	0.0499	0.7230	0.3404	0.7896	0.4641	0.2916	0.4753	0.0115	0.4915	0.4683	0.2639
VALR	0.0679	0.0386	0.1553	0.3037	0.1074	0.0002	0.1111	0.0773	0.2447	0.1645	0.2219	0.1066	0.0563	0.2077
VILR	0.0894	0.0498	0.1736	0.2358	0.1328	0.0023	0.1425	0.0885	0.2631	0.2015	0.1952	0.1376	0.0807	0.2295
ZINTEG	0.5505	0.9200	0.5316	0.0034	0.4053	0.9487	0.3610	0.3822	0.3796	0.5071	0.0602	0.5549	0.5676	0.2268
ZMIN	0.5635	0.4963	0.6510	0.0516	0.7261	0.3510	0.7865	0.4746	0.2833	0.4691	0.0094	0.4919	0.4674	0.2666

Table 30: Individual participant ankle correlations.

Force	Acceleration													
P1Ankle	MHEIGHT	MINTEG	MMAX	MMIN	XHEIGHT	XINTEG	XMAX	XMIN	YHEIGHT	YMAX	YMIN	ZHEIGHT	ZMAX	ZMIN
MINTEG	0.0717	0.8783	0.0894	0.0398	0.0106	0.7569	0.0042	0.0766	0.0987	0.1338	0.0142	0.1299	0.1154	0.0667
MMAX	0.2790	0.0238	0.3430	0.1400	0.4231	0.0233	0.5435	0.1135	0.3199	0.2887	0.1941	0.4247	0.4400	0.1169
VALR	0.1967	0.0140	0.1576	0.0210	0.4066	0.0767	0.4599	0.1484	0.0493	0.0478	0.0251	0.1786	0.1124	0.2146
VILR	0.2103	0.0125	0.1714	0.0178	0.4128	0.0715	0.4581	0.1569	0.0521	0.0514	0.0255	0.1834	0.1168	0.2161
ZINTEG	0.0707	0.8708	0.0883	0.0397	0.0089	0.7591	0.0051	0.0725	0.0936	0.1305	0.0114	0.1192	0.1081	0.0571
ZMIN	0.2572	0.0164	0.3205	0.1425	0.4015	0.0286	0.5381	0.0956	0.2942	0.2708	0.1706	0.3852	0.4071	0.0958
P2Ankle	MHEIGHT	MINTEG	MMAX	MMIN	XHEIGHT	XINTEG	XMAX	XMIN	YHEIGHT	YMAX	YMIN	ZHEIGHT	ZMAX	ZMIN
MINTEG	0.2283	0.9387	0.2017	0.0066	0.2419	0.9650	0.1817	0.2300	0.1225	0.2090	0.0175	0.2349	0.2016	0.1306
MMAX	0.3270	0.1020	0.3083	0.0019	0.2930	0.0866	0.2397	0.2540	0.2746	0.3826	0.0784	0.2704	0.2179	0.1878
VALR	0.3611	0.1721	0.3652	0.0444	0.5071	0.1586	0.5868	0.2726	0.3980	0.6176	0.0817	0.2519	0.1175	0.5576
VILR	0.4140	0.2681	0.4092	0.0278	0.5351	0.2573	0.5659	0.3323	0.3045	0.5305	0.0397	0.3440	0.2103	0.4840
ZINTEG	0.2256	0.9391	0.1986	0.0077	0.2369	0.9662	0.1760	0.2277	0.1185	0.2034	0.0165	0.2345	0.2021	0.1283
ZMIN	0.3217	0.1038	0.3002	0.0004	0.2728	0.0895	0.2125	0.2496	0.2468	0.3451	0.0697	0.2768	0.2259	0.1842
P3Ankle	MHEIGHT	MINTEG	MMAX	MMIN	XHEIGHT	XINTEG	XMAX	XMIN	YHEIGHT	YMAX	YMIN	ZHEIGHT	ZMAX	ZMIN
MINTEG	0.3507	0.9778	0.2818	0.1144	0.0211	0.9844	0.0310	0.0053	0.1760	0.4843	0.0616	0.0000	0.0607	0.0987
MMAX	0.0309	0.1805	0.0485	0.0012	0.1505	0.2366	0.0812	0.1942	0.0133	0.0009	0.0277	0.1787	0.2100	0.0083
VALR	0.2697	0.0073	0.3027	0.0133	0.3159	0.0234	0.2243	0.3114	0.1118	0.1427	0.0036	0.2025	0.4729	0.0242
VILR	0.3705	0.0018	0.4243	0.0148	0.3555	0.0003	0.2594	0.3395	0.1765	0.2427	0.0024	0.1627	0.4892	0.0598
ZINTEG	0.3471	0.9773	0.2798	0.1120	0.0208	0.9843	0.0306	0.0052	0.1736	0.4812	0.0625	0.0001	0.0587	0.1014
ZMIN	0.0250	0.1823	0.0453	0.0038	0.1514	0.2372	0.0807	0.1974	0.0095	0.0003	0.0232	0.1517	0.1952	0.0035
P4Ankle	MHEIGHT	MINTEG	MMAX	MMIN	XHEIGHT	XINTEG	XMAX	XMIN	YHEIGHT	YMAX	YMIN	ZHEIGHT	ZMAX	ZMIN
MINTEG	0.1981	0.8952	0.1874	0.0090	0.0090	0.9143	0.0436	0.0134	0.3860	0.2168	0.4118	0.6660	0.6208	0.3133
MMAX	0.2007	0.1852	0.2981	0.0147	0.1112	0.1266	0.1542	0.0215	0.2947	0.2297	0.2147	0.5177	0.5724	0.1078
VALR	0.0309	0.0200	0.1220	0.0981	0.2034	0.0013	0.2365	0.0734	0.0023	0.0126	0.0028	0.1024	0.1026	0.0359
VILR	0.0475	0.0209	0.1426	0.0779	0.1888	0.0009	0.2301	0.0591	0.0140	0.0378	0.0004	0.1229	0.1219	0.0450
ZINTEG	0.1953	0.8931	0.1853	0.0086	0.0090	0.9147	0.0438	0.0135	0.3821	0.2124	0.4117	0.6621	0.6178	0.3100
ZMIN	0.1988	0.1930	0.2985	0.0160	0.1153	0.1358	0.1618	0.0212	0.2908	0.2195	0.2214	0.5191	0.5743	0.1077

Table 31: All Participants combined at each location: Part 1.

Force	Acceleration										
Thigh	MHEIGHT	MINTEG	MINTEGMASS	MMAX	MMAXMASS	MMIN	XHEIGHT	XINTEG	XINTEGMASS	XMAX	XMAXMASS
MINTEG	0.0237	0.8272	0.8487	0.0173	0.0309	0.0039	0.0000	0.7759	0.8339	0.0003	0.0000
MMAX	0.3907	0.0336	0.0586	0.4273	0.5769	0.0242	0.3282	0.0001	0.0014	0.2590	0.2871
VALR	0.0960	0.0524	0.0622	0.1442	0.1772	0.0714	0.2012	0.0040	0.0073	0.1805	0.1687
VILR	0.0975	0.0949	0.1089	0.1399	0.1776	0.0575	0.1763	0.0226	0.0310	0.1536	0.1450
ZINTEG	0.0226	0.8255	0.8473	0.0163	0.0298	0.0041	0.0000	0.7757	0.8338	0.0005	0.0000
ZMIN	0.3839	0.0335	0.0586	0.4204	0.5694	0.0242	0.3246	0.0000	0.0016	0.2564	0.2852
Shank	MHEIGHT	MINTEG	MINTEGMASS	MMAX	MMAXMASS	MMIN	XHEIGHT	XINTEG	XINTEGMASS	XMAX	XMAXMASS
MINTEG	0.1390	0.9010	0.9041	0.1106	0.1288	0.0230	0.0248	0.8880	0.8993	0.0059	0.0094
MMAX	0.2597	0.0261	0.0461	0.3428	0.4536	0.0978	0.5000	0.0013	0.0057	0.5392	0.5927
VALR	0.2668	0.0556	0.0632	0.3478	0.3488	0.0915	0.2390	0.0148	0.0172	0.2139	0.2112
VILR	0.2839	0.0975	0.1077	0.3460	0.3529	0.0539	0.2362	0.0441	0.0482	0.2052	0.2056
ZINTEG	0.1359	0.8999	0.9033	0.1077	0.1262	0.0234	0.0242	0.8884	0.8997	0.0057	0.0092
ZMIN	0.2543	0.0265	0.0469	0.3350	0.4465	0.0944	0.4992	0.0017	0.0064	0.5386	0.5924
Ankle	MHEIGHT	MINTEG	MINTEGMASS	MMAX	MMAXMASS	MMIN	XHEIGHT	XINTEG	XINTEGMASS	XMAX	XMAXMASS
MINTEG	0.2097	0.9317	0.9463	0.1786	0.2070	0.0186	0.0327	0.9464	0.9602	0.0340	0.0367
MMAX	0.1185	0.0045	0.0118	0.1567	0.2664	0.0160	0.1888	0.0001	0.0007	0.2295	0.2549
VALR	0.1910	0.0369	0.0432	0.2405	0.2821	0.0156	0.2871	0.0150	0.0181	0.3009	0.2898
VILR	0.2297	0.0807	0.0899	0.2780	0.3272	0.0113	0.2830	0.0478	0.0531	0.2908	0.2820

ZINTEG	0.2071	0.9304	0.9452	0.1765	0.2051	0.0183	0.0318	0.9467	0.9606	0.0332	0.0360
ZMIN	0.1126	0.0046	0.0121	0.1520	0.2612	0.0182	0.1854	0.0001	0.0009	0.2273	0.2533

Table 32: All Participants combined at each location: Part 2.

Force	Acceleration									
Thigh	XMIN	XMINMASS	YHEIGHT	YMAX	YMAXMASS	YMIN	ZHEIGHT	ZMAX	ZMAXMASS	ZMIN
MINTEG	0.0011	0.0082	0.0426	0.0145	0.0201	0.0672	0.0084	0.0152	0.0261	0.0012
MMAX	0.2584	0.4241	0.4551	0.4736	0.5156	0.2176	0.4864	0.2963	0.4131	0.4929
VALR	0.1348	0.1809	0.1575	0.1292	0.1269	0.1110	0.1788	0.0815	0.1056	0.2264
VILR	0.1228	0.1727	0.1529	0.1182	0.1198	0.1167	0.1702	0.0802	0.1072	0.2106
ZINTEG	0.0008	0.0075	0.0409	0.0137	0.0193	0.0652	0.0076	0.0142	0.0249	0.0009
ZMIN	0.2553	0.4203	0.4452	0.4628	0.5057	0.2133	0.4717	0.2847	0.3996	0.4819
Shank	XMIN	XMINMASS	YHEIGHT	YMAX	YMAXMASS	YMIN	ZHEIGHT	ZMAX	ZMAXMASS	ZMIN
MINTEG	0.0632	0.0914	0.0650	0.0428	0.0531	0.0401	0.1373	0.1529	0.1654	0.0533
MMAX	0.1565	0.2992	0.2426	0.3210	0.3760	0.0329	0.3258	0.2561	0.3012	0.2835
VALR	0.1285	0.1669	0.2019	0.2506	0.2506	0.0345	0.3062	0.2409	0.2347	0.2661
VILR	0.1364	0.1807	0.2129	0.2348	0.2392	0.0515	0.3035	0.2491	0.2456	0.2441
ZINTEG	0.0620	0.0903	0.0626	0.0406	0.0508	0.0394	0.1335	0.1492	0.1619	0.0512
ZMIN	0.1560	0.2994	0.2295	0.3034	0.3584	0.0313	0.3137	0.2464	0.2917	0.2731
Ankle	XMIN	XMINMASS	YHEIGHT	YMAX	YMAXMASS	YMIN	ZHEIGHT	ZMAX	ZMAXMASS	ZMIN
MINTEG	0.0162	0.0284	0.1297	0.2028	0.2444	0.0085	0.1139	0.1433	0.1579	0.0045
MMAX	0.0657	0.1521	0.1252	0.0815	0.1377	0.1017	0.3337	0.3472	0.4167	0.0665
VALR	0.1403	0.1846	0.0891	0.1204	0.1516	0.0131	0.1304	0.1129	0.1248	0.0575
VILR	0.1438	0.1928	0.0929	0.1407	0.1798	0.0075	0.1564	0.1499	0.1641	0.0466
ZINTEG	0.0157	0.0279	0.1271	0.1997	0.2411	0.0080	0.1109	0.1411	0.1558	0.0038
ZMIN	0.0631	0.1489	0.1168	0.0741	0.1282	0.0981	0.3244	0.3419	0.4123	0.0600

Appendix B. Logarithmic Correlations

Logarithmically modelling the vertical force and axial acceleration of all participants and for the cohort from the generalised models.

Table 33: Participant-modelled logarithmic results.

Results of Logarithmic Modelling							
Participant	Location	Correlation		R^2		$RMSE\ (N)$	
		Force	Acceleration	Linear	Log	Linear	Log
P4	Thigh	ZMIN	XMAX	0.17	0.12	879.9	903.7
		ZMIN	XMIN	0.52	0.43	672.5	726.6
		ZMIN	XHEIGHT	0.36	0.31	774.7	804.9
	Shank	ZMIN	XMAX	0.79	0.59	445.5	619.3
		ZMIN	XMIN	0.47	0.44	699.0	722.8
		ZMIN	XHEIGHT	0.73	0.62	504.6	593.9
	Ankle	ZMIN	XMAX	0.17	0.22	884.6	857.2
		ZMIN	XMIN	0.02	0.04	957.2	947.4
		ZMIN	XHEIGHT	0.12	0.16	908.5	889.7
P3	Thigh	ZMIN	XMAX	0.33	0.40	500.6	471.6
		ZMIN	XMIN	0.58	0.57	397.7	400.2
		ZMIN	XHEIGHT	0.52	0.55	422.2	411.2
	Shank	ZMIN	XMAX	0.48	0.56	431.6	397.3
		ZMIN	XMIN	0.13	0.14	560.2	556.1
		ZMIN	XHEIGHT	0.54	0.52	407.3	416.9
	Ankle	ZMIN	XMAX	0.09	0.08	582.5	585.2
		ZMIN	XMIN	0.21	0.23	540.6	535.0
		ZMIN	XHEIGHT	0.16	0.20	557.5	545.2
P2	Thigh	ZMIN	XMAX	0.21	0.15	463.4	479.1
		ZMIN	XMIN	0.21	0.23	461.6	455.6
		ZMIN	XHEIGHT	0.25	0.25	451.0	449.7
	Shank	ZMIN	XMAX	0.33	0.30	415.4	426.5
		ZMIN	XMIN	0.32	0.33	419.7	415.9
		ZMIN	XHEIGHT	0.38	0.38	399.3	401.0
	Ankle	ZMIN	XMAX	0.21	0.19	451.4	458.4
		ZMIN	XMIN	0.25	0.27	440.7	434.2
		ZMIN	XHEIGHT	0.27	0.29	433.8	430.1
P1	Thigh	ZMIN	XMAX	0.22	0.24	449.0	443.1
		ZMIN	XMIN	0.23	0.23	445.5	446.3
		ZMIN	XHEIGHT	0.33	0.33	414.6	415.3
	Shank	ZMIN	XMAX	0.49	0.52	356.2	345.7
		ZMIN	XMIN	0.01	0.02	497.3	492.7
		ZMIN	XHEIGHT	0.35	0.30	402.4	417.4
	Ankle	ZMIN	XMAX	0.54	0.55	341.3	337.4
		ZMIN	XMIN	0.11	0.12	476.1	471.8
		ZMIN	XHEIGHT	0.42	0.36	384.9	402.5

Table 34: Cohort-modelled logarithmic results.

Results of Logarithmic Cohort Modelling									
Participant	Location	Correlation		R^2			RMSE (N)		
		Force	Acceleration	Linear	Log	Adjusted Log	Linear	Log	Adjusted Log
1	Thigh	ZMIN	XMAXMASS	0.29	0.16	0.12	601	650	665
		ZMIN	XMINMASS	0.42	0.36	0.01	541	567	708
		ZMIN	XHEIGHT	0.32	0.29	0.40	584	600	551
	Shank	ZMIN	XMAXMASS	0.59	0.39	0.29	449	552	593
		ZMIN	XMINMASS	0.30	0.27	0.00	589	602	702
		ZMIN	XHEIGHT	0.50	0.41	0.42	498	539	537
	Ankle	ZMIN	XMAXMASS	0.26	0.16	0.13	611	647	662
		ZMIN	XMINMASS	0.16	0.17	0.00	651	646	707
		ZMIN	XHEIGHT	0.19	0.20	0.31	637	635	589
2	Thigh	ZMIN	XMAXMASS	0.29	0.16	0.19	601	650	638
		ZMIN	XMINMASS	0.42	0.36	0.41	541	567	546
		ZMIN	XHEIGHT	0.32	0.29	0.41	584	600	543
	Shank	ZMIN	XMAXMASS	0.59	0.39	0.40	449	552	544
		ZMIN	XMINMASS	0.30	0.27	0.28	589	602	598
		ZMIN	XHEIGHT	0.50	0.41	0.47	498	539	513
	Ankle	ZMIN	XMAXMASS	0.26	0.16	0.20	611	647	634
		ZMIN	XMINMASS	0.16	0.17	0.25	651	646	611
		ZMIN	XHEIGHT	0.19	0.20	0.32	637	635	586
3	Thigh	ZMIN	XMAXMASS	0.29	0.16	0.19	601	650	640
		ZMIN	XMINMASS	0.42	0.36	0.41	541	567	544
		ZMIN	XHEIGHT	0.32	0.29	0.41	584	600	546
	Shank	ZMIN	XMAXMASS	0.59	0.39	0.40	449	552	546
		ZMIN	XMINMASS	0.30	0.27	0.28	589	602	597
		ZMIN	XHEIGHT	0.50	0.41	0.49	498	539	505
	Ankle	ZMIN	XMAXMASS	0.26	0.16	0.19	611	647	636
		ZMIN	XMINMASS	0.16	0.17	0.25	651	646	611
		ZMIN	XHEIGHT	0.19	0.20	0.31	637	635	587
4	Thigh	ZMIN	XMAXMASS	0.29	0.16	0.24	601	650	619
		ZMIN	XMINMASS	0.42	0.36	0.23	541	567	623
		ZMIN	XHEIGHT	0.32	0.29	0.41	584	600	546
	Shank	ZMIN	XMAXMASS	0.59	0.39	0.44	449	552	528
		ZMIN	XMINMASS	0.30	0.27	0.21	589	602	627
		ZMIN	XHEIGHT	0.50	0.41	0.52	498	539	489
	Ankle	ZMIN	XMAXMASS	0.26	0.16	0.26	611	647	611
		ZMIN	XMINMASS	0.16	0.17	0.19	651	646	636
		ZMIN	XHEIGHT	0.19	0.20	0.31	637	635	589